EVALUATION OF DESIGN PARAMETERS OF NEAR EMBANKMENT UNDERGROUND TUNNEL STRUCTURE

ASKER RAJIN RAHMAN

MASTER OF SCIENCE IN CIVIL ENGINEERING (STRUCTURAL)

DEPARTMENT OF CIVIL ENGINEERING
BANGLADESH UNIVERSITY OF ENGINEERING AND TECHNOLOGY
DHAKA, BANGLADESH
MARCH, 2018

EVALUATION OF DESIGN PARAMETERS OF NEAR EMBANKMENT UNDERGROUND TUNNEL STRUCTURE

ASKER RAJIN RAHMAN

(Student No: 0412042356 P)

A thesis Submitted to The Department of Civil Engineering of Bangladesh University of Engineering and Technology in partial fulfillment of the requirement for the degree of

MASTER OF SCIENCE IN CIVIL ENGINEERING (STRUCTURAL)

Department of Civil Engineering

Bangladesh University of Engineering and Technology

Dhaka, Bangladesh

March, 2018

CERTIFICATION OF APPROVAL

The thesis titled "Evaluation of Design Parameters of Near Embankment Underground Tunnel Structure", submitted by Asker Rajin Rahman, Roll No. 0412042356 P, Session April/2012, has been accepted as satisfactory in partial fulfillment of the requirement for the degree of **Master of Science in Civil Engineering (Structural)** on 28th March, 2018.

Dr. Raquib Ahsan
Professor
Department of CE, BUET, Dhaka

Chairman
(Supervisor)

28.3.18

Dr. Ahsanul Kabir
Professor and Head
Department of CE, BUET, Dhaka

Member
(Ex-Officio)

Dr. Mohammad Al Amin Siddique
Associate Professor
Department of CE, BUET, Dhaka

Member

Dr. Khondaker Sakil Ahmed PE, MASCE
Associate Professor
Department of Civil Engineering, MIST, Dhaka

Member
(External)

DECLARATION

It is hereby declared that this thesis work or any part of it has not been submitted elsewhere for the award of any degree or diploma.

(Asker Rajin Rahman)

Signature of the Candidate

ACKNOWLEDGEMENTS

First of all, the author would like to express his gratefulness to the almighty Allah the creator of universe. Without the rahmat of Allah the author couldn’t have finished the degree.

The author acknowledges his deepest gratitude to his supervisor Dr. Raquib Ahsan, Professor, Department of Civil Engineering, BUET for providing an interesting idea for the thesis and encouraging to work with it. His cordial supervision, valuable suggestion and expertise contributed greatly to this thesis.

The author is also grateful to Dr. Mehedi Ahmed Ansary, Professor, Department of Civil Engineering, BUET for his valuable suggestions during the period of this study. The author also acknowledges the valuable comments of Dr. Ahsanul Kabir, Professor and Head, Department of CE, BUET, Dr. Mohammad Al Amin Siddique, Professor, Department of CE, BUET and Dr. Khondaker Sakil Ahmed P Eng, Associate Professor (Instr. UB), Dept. of Civil Engg., MIST, Dhaka, who were the members of the board of Examiners.

The author would like to thank his parents for their encouragement and inspiration.

The author is truly grateful to his wife for her continuous support and inspiration. He appreciates and admires her patience and encouragement throughout his study.

The author would like to express his sincere gratitude and appreciation to his all colleagues and friends for their help, support and inspiration.

Asker Rajin Rahman
March 2018

ABSTRACT

Now-a-days, traffic congestion is a major problem in many cities. Due to excessive pressure on overland roadways, underground subway or roadway is regarded as an alternative solution to accommodate this huge traffic. For this reason, construction of a suitable underground tunnel is a good alternative. Because the urban tunnel construction is normally carried out in difficult and crowded city areas, one of major design and construction challenges lies in minimizing the induced ground movement, as it poses potential threats to nearby buildings and utilities along the tunnel alignment. Most of the previous works were done to study the impact of the tunnel excavation on adjacent buildings which is of major interest for tunneling construction in urban areas, due to the high interaction between tunneling and existing structures. In context of the previous studies, present study aims at investigating the design parameters (such as thickness, position) of an underground tunnel which is constructed in such a zone where a residential area is being developed far away from the business center, for example, near any river embankment, where new land is being developed using sand filling taken from the dredged materials from the bed of the rivers. The response of the nearby structures (displacement, bending moment, shear force) will not only be dependent on the construction sequence of the tunnel, but also will be dependent on the change in water level near the embankment as these embankments are subjected to a certain water head difference due to difference in water levels on both sides of the embankment causing seepage of water through the embankment and generating uplift forces in adjacent structures. Such phenomena may also induce lateral displacements to nearby tunnels, buildings and if overlooked, can cause severe structural damage at their base. In this particular study, a simple 2D plain strain model has been developed in PLAXIS-2D. Various scenarios have been simulated by construction of tunnel and varying the water level on one side of the embankment. The behavior of both nearby tunnel and building has been observed in terms of generated maximum displacement, bending moment and shear force. Simulated results show both increase and decrease in the parameters mentioned above for varying thickness of tunnel, vertical distance of center of tunnel from existing ground level, distance between tunnel center and center of structure and varying water head difference on both sides of the embankment. Model results in this research, incorporating some of these variations showed that a tunnel away from the embankment, just below the center of the road or any heavily loaded building, having lining thickness of 0.380m at 6.5m below ground level is adequate considering economy of tunneling and vertical displacements generated in nearby structures.

Table of Contents

List of Figures

List of Tables

ALUATION OF DESIGN PARAMETERS OF NEAR EMBANKMENT UNDERGROUND TUNNEL STRUCTURE

ASKER RAJIN RAHMAN

MASTER OF SCIENCE IN CIVIL ENGINEERING (STRUCTURAL)

DEPARTMENT OF CIVIL ENGINEERING
BANGLADESH UNIVERSITY OF ENGINEERING AND TECHNOLOGY
DHAKA, BANGLADESH

MARCH, 2018

EVALUATION OF DESIGN PARAMETERS OF NEAR EMBANKMENT UNDERGROUND TUNNEL STRUCTURE

ASKER RAJIN RAHMAN

(Student No: 0412042356 P)

A thesis Submitted to The Department of Civil Engineering of Bangladesh University of Engineering and Technology in partial fulfillment of the requirement for the degree of

MASTER OF SCIENCE IN CIVIL ENGINEERING (STRUCTURAL)

Department of Civil Engineering

Bangladesh University of Engineering and Technology

Dhaka, Bangladesh

March, 2018

CERTIFICATION OF APPROVAL

The thesis titled "Evaluation of Design Parameters of Near Embankment Underground Tunnel Structure", submitted by Asker Rajin Rahman, Roll No. 0412042356 P, Session April/2012, has been accepted as satisfactory in partial fulfillment of the requirement for the degree of **Master of Science in Civil Engineering (Structural)** on 28th March, 2018.

Dr. Raquib Ahsan
Professor
Department of CE, BUET, Dhaka

Chairman
(Supervisor)

28.3.18

Dr. Ahsanul Kabir
Professor and Head
Department of CE, BUET, Dhaka

Member
(Ex-Officio)

Dr. Mohammad Al Amin Siddique
Associate Professor
Department of CE, BUET, Dhaka

Member

Dr. Khondaker Sakil Ahmed PE, MASCE
Associate Professor
Department of Civil Engineering, MIST, Dhaka

Member
(External)

DECLARATION

It is hereby declared that this thesis work or any part of it has not been submitted elsewhere for the award of any degree or diploma.

ARRahman

____

(Asker Rajin Rahman)

Signature of the Candidate

ACKNOWLEDGEMENTS

First of all, the author would like to express his gratefulness to the almighty Allah the creator of universe. Without the rahmat of Allah the author couldn't have finished the degree.

The author acknowledges his deepest gratitude to his supervisor Dr. Raquib Ahsan, Professor, Department of Civil Engineering, BUET for providing an interesting idea for the thesis and encouraging to work with it. His cordial supervision, valuable suggestion and expertise contributed greatly to this thesis.

The author is also grateful to Dr. Mehedi Ahmed Ansary, Professor, Department of Civil Engineering, BUET for his valuable suggestions during the period of this study. The author also acknowledges the valuable comments of Dr. Ahsanul Kabir, Professor and Head, Department of CE, BUET, Dr. Mohammad Al Amin Siddique, Professor, Department of CE, BUET and Dr. Khondaker Sakil Ahmed P Eng, Associate Professor (Instr. UB), Dept. of Civil Engg., MIST, Dhaka, who were the members of the board of Examiners.

The author would like to thank his parents for their encouragement and inspiration.

The author is truly grateful to his wife for her continuous support and inspiration. He appreciates and admires her patience and encouragement throughout his study.

The author would like to express his sincere gratitude and appreciation to his all colleagues and friends for their help, support and inspiration.

Asker Rajin Rahman
March 2018

ABSTRACT

Now-a-days, traffic congestion is a major problem in many cities. Due to excessive pressure on overland roadways, underground subway or roadway is regarded as an alternative solution to accommodate this huge traffic. For this reason, construction of a suitable underground tunnel is a good alternative. Because the urban tunnel construction is normally carried out in difficult and crowded city areas, one of major design and construction challenges lies in minimizing the induced ground movement, as it poses potential threats to nearby buildings and utilities along the tunnel alignment. Most of the previous works were done to study the impact of the tunnel excavation on adjacent buildings which is of major interest for tunneling construction in urban areas, due to the high interaction between tunneling and existing structures. In context of the previous studies, present study aims at investigating the design parameters (such as thickness, position) of an underground tunnel which is constructed in such a zone where a residential area is being developed far away from the business center, for example, near any river embankment, where new land is being developed using sand filling taken from the dredged materials from the bed of the rivers. The response of the nearby structures (displacement, bending moment, shear force) will not only be dependent on the construction sequence of the tunnel, but also will be dependent on the change in water level near the embankment as these embankments are subjected to a certain water head difference due to difference in water levels on both sides of the embankment causing seepage of water through the embankment and generating uplift forces in adjacent structures. Such phenomena may also induce lateral displacements to nearby tunnels, buildings and if overlooked, can cause severe structural damage at their base. In this particular study, a simple 2D plain strain model has been developed in PLAXIS-2D. Various scenarios have been simulated by construction of tunnel and varying the water level on one side of the embankment. The behavior of both nearby tunnel and building has been observed in terms of generated maximum displacement, bending moment and shear force. Simulated results show both increase and decrease in the parameters mentioned above for varying thickness of tunnel, vertical distance of center of tunnel from existing ground level, distance between tunnel center and center of structure and varying water head difference on both sides of the embankment. Model results in this research, incorporating some of these variations showed that a tunnel away from the embankment, just below the center of the road or any heavily loaded building, having lining thickness of 0.380m at 6.5m below ground level is adequate considering economy of tunneling and vertical displacements generated in nearby structures.

Table of Contents

List of Figures

List of Tables

Chapter 1

INTRODUCTION

1.1 General

Bangladesh is a riverine country. It is criss-crossed by hundreds of rivers. To protect the country side from flood waters, embankments are constructed along many of these rivers. To match with the population growth, many residential areas are now being developed on sides of these river embankments. These factors in turn creating mass traffic problems and necessitating new road ways and alternate mode of transport facilities. However, due to lack of available space and excessive pressure on overland roadways, underground subway or roadway is regarded as an alternative solution to accommodate this huge traffic. For this reason, construction of a suitable underground tunnel is a good alternative. Many works currently are undertaken in different parts of the world in the field of tunneling, are related to the construction and extension of underground network in big overpopulated cities. Because the urban tunnel construction is normally carried out in difficult and crowded city areas, one of major design and construction challenges lies in minimizing the induced ground movement, as it poses potential threats to nearby buildings and utilities along the tunnel alignment. Most of the previous works were conducted to study the impact of the tunnel excavation on adjacent buildings which is of major interest for tunneling construction in urban areas, due to the high interaction between tunneling and existing structures. Some researchers have also applied 2D numerical models for the analysis of tunnels under static conditions. In many of the previous studies, the impact of drilling urban tunnels on adjacent structures has been extensively studied using FE analysis and field monitoring measurements.

The present study aims at investigating the design parameters of an underground tunnel which is constructed in such a zone where a residential area is being developed far away from the business center, for example, near any river embankment, where new land is being developed using sand filling taken from the dredged materials from the bed of the rivers. The response of the nearby structures (bending moment, shear force) will not only be dependent on the construction sequence of the tunnel, but also will be dependent on the change in water level near the embankment. In context of the previous studies, this study aims mainly at joint response of the tunnel construction and change in water level near the embankment to other nearby structures.

1.2 Objectives and Scope of Work

This study mainly deals with the behavior/response of near embankment structures due to tunnel construction and change in water head difference on both sides of the embankment. Specific objectives of the present research may be stated as follows:

1. To study the response of nearby road and building structures in terms of base deformation (along with the tunnel itself) due to the generated deformation.
2. To analyze the response of the tunnel and nearby structures due to change in water level on the other side of the embankment.
3. To identify suitable position for the tunnel construction by changing various variables such as depth of tunnel construction, distance of tunnel from embankment and other nearby structures.

1.3 Methodology of Present Study

In this research, a finite element model is developed using PLAXIS-2D. The model includes a typical soil profile, an embankment, a tunnel (constructed by a TBM), nearby structures (such as road, building etc.). Appropriate boundary and load conditions then are applied on the boundary and structures to simulate a practical situation.

The following steps are adopted:

1. Deformation of the nearby structures due to tunnel construction (along with the tunnel itself) are analyzed.
2. Response of the nearby structures (along with the tunnel itself) are analyzed in terms of bending moment and shear force.
3. Repetition of steps 1 and 2 for several cases varying the parameters such as thickness of tunnel lining, depth of tunnel construction, distance of tunnel from nearby structures, change in water level near the embankment.
4. Analyzing all the results and following a tunnel design manual, most suitable thickness and position of the tunnel is selected.

Finally, analyzing all the cases, some conclusions and recommendations are made considering economy of tunnel design and safety of nearby structures.

1.4 Organization of the Thesis

For a better understanding of this research work, this thesis report is organized in several chapters.

Chapter 1, *Introduction*, containing some general introduction, specific objectives and methodology of this study and information regarding organization of chapters of this report.

Chapter 2, *Literature Review*, containing brief description on some of the previous works related to this study are presented in this chapter.

Chapter 3, *Development of Soil-Structure Interaction Model,* containing the data, detail steps of developing the soil-structure interaction model generated in this research.

Chapter 4, *Validation of Model*, incorporating the validation procedure of the developed PLAXIS-2D model.

Chapter 5, *Model Results and Discussion,* describing the results of all the simulated models are presented in full for each of the simulation cases.

Chapter 6, *Conclusions and Summary of Suggestions*, containing some conclusions and recommendations which are made based on the simulated model results.

Chapter 7, *References*, all the references mentioned in this report are listed in this chapter.

Chapter 2

LITERATURE REVIEW

2.1 Introduction

Many works have been done in the past to study the behavior of soil-structure interaction under specific cases such as tunneling induced ground movement, construction of foundation of a building, soil excavation and land filling supported by structural measures etc. In this chapter, literature review of some of the such related works are presented.

2.2 Structure-Soil-Structure interaction

Investigations of soil–structure interaction have shown that the response of a structure supported on flexible soil may differ significantly from the response of the same structure when supported on a rigid base (Chopra and Gutierre, 1974). Besides when there is more than one structure in the medium, because of interference of the structural responses through the soil, the soil–structure problem evolves to a cross-interaction problem between multiple structures.

Soil-structure studies the influence of the presence of adjacent structures to the others further through the interaction effect of the sub-soil under disturbances. It is an interdisciplinary field of endeavor, which lies at the intersection of soil and structural mechanics, soil and structural dynamics, earthquake engineering, geophysics and geomechanics, material science, computational and numerical methods, and diverse other technical disciplines.

Numerical method greatly developed because of the rapid progress of computers. This method of calculation is considered one of the most effective tools for the study of soil-structure interaction. Thus, a great deal of publications based on it have spring up from 1980 up to the present. Finite element method (FEM), an efficient common computing method widely used in civil engineering, discretizes a continuum into a series of elements with limited sizes to compute for the mechanics of the continuum. FEM can simulate the mechanics of soil and structures better than other methods, deal with complicated geometry and applied load, and determine non-linear phenomena. To date, there are many general-purpose programs developed by commercial corporations for research in the engineering field. Specifically, FEM is used frequently in the study of soil-structure interaction, and has produced some notable achievements. In considering the radiation damping of semi-infinite space, the scale of the soil should be large enough. This requirement demands a serious consumption of time and the internal memory of a computer to have full FEM. Laing (1974), Lysmer et al. (1975), and Aydinoglu and Cakiroglu (1977) employed the FEM under plane strain conditions to study the cross-interaction of two or more foundations or structures subjected to vertically propagating harmonic SV-waves. To model the half-plane properly, Laing used consistent boundaries, Lysmer et al. employed viscous bound- aries, and Aydinoglu and Cakiroglu relied on the discrete soil stiffness matrix procedure. A number of previous works have been based on circular or semi-cylindrical foundations and superstructures simulated by lumped mass with a single degree of freedom or cylindrical mass blocks. Thus, Roesset and Gonzalez in (1977 and 1978), and Solari et al. (1980) employed the FEM in conjunction with consistent boundaries to study the 3D problem of two squares, their rigid foundations resting on a linear-elastic layer under vertically propagating S-waves. Roesset and Gonzalez considered embedded foundations, whereas Solari et al. focused on surface foundations. In most practical engineering applications, depending on the soil conditions and the structural type, the foundations are partially or totally embedded in the ground and the effects of the surrounding soil greatly alter their static and dynamic response. As with the single foundation case, when the effect of the embedment is included in the multiple foundations case, analytical difficulties and enormous numerical calculations limit the analysis of foundations of relatively simple geometry. Yahyai et al. (2008) used the ANSYS5.4 program to simulate two steel moment frames with concrete shear walls on three types of soil, such as soft clay, sandy gravel, and compacted sandy gravel. Yahyai et al.'s study is one of the works in the study of SSSI that subtly models superstructures. FEM requires the use of special transmitting boundaries or infinite elements, which may lead to inaccuracy. In addition, FEM also necessitates a rigid bedrock at a relatively shallow depth. The model of soil and structures via FEM is still very large, and although it introduces transmitting boundaries, it still requires relatively much internal computer memory and time. The development level of hardware and software has restricted the application of FEM in the study of SSSI.

The boundary element method (BEM), a new numerical method developed after FEM, only discretizes the boundary of the definition domain. It is different from the discretization of total continuum and uses functions satisfying the governing equation to approximate boundary conditions. The BEM is more advantageous than the FEM because it requires only a surface discretization and satisfies automatically the radiation condition without any need for using special complicated non-reflecting boundaries as required by FEM (Manolis and Beskos, 1988 and Beskos, 1993). This explains why the BEM is frequently used by engineers to analyze SSI and why the some publications on SSSI use BEM or its variations as their computational tool. In their pioneering work, Wong and Luco (1977 and 1986) extended the boundary integral question approach, which they had presented previously for isolated foundations to the case of multiple rigid foundations of different shapes resting on an elastic or viscoelastic half-space and subjected to external forces They found that the choice of discretization of the foundations has a significant effect on the calculated impedance functions for extremely small separations. They also determined that the extensive numerical results presented by

Sato et al. in 1983 and Yoshida et al. in 1984, in the case of vanishing small separation between the foundations are erroneous.

Owing to the respective disadvantages of FEM and BEM, the coupling method of FEM and BEM (FEM–BEM) was developed in the field of SSSI in the 1990s. This method shows the advantages of both FEM and BEM. Generally in a general way, FEM is used for simulation of superstructures, foundations and near-field soil, whereas BEM is applied for far-field soil.

2.3 Numerical Simulation of the Mechanical Response of the Tunnels

In this study Houari et al. (2011), the case of a shallow tunnel was studied, and in this case there were various arrivals of ground caused by digging, tending to be propagated towards the surface, where they resulted in settlements and horizontal displacements on the surface affecting the behavior of existing works. Horizontal displacements tend to follow the face, by changing direction with advance, but few work treated the calculation of these displacements by empirical methods. Acceptable ranges of settlements on the surface for tunnels were observed going from 25 to 40 mm for sand and from 40 to 65 mm for clay (Dolzhenko, 2002). In addition, *in situ* measurements showed that the settlements observed on the surface represent only part of the vertical displacements in the underground. Chapeau (1991) noticed a delay and a damping between settlements of the surface and the in depth movements. This phenomenon becomes more significant as the height of cover increases. For shallow tunnels, damping is so weak that an error in the procedure of construction can involve a rupture in the block of the cover. Because of the recent developments in these works, the need for modeling towards a keener demand as regards the forecast of movements induced in the ground was accentuated, whereas the former applications of the numerical models were rather concentrated on the local response of the work (convergence of the walls of the gallery, effort taken again by the structure of supporting). However, many research was devoted during the last years to the development of models of calculation allowing better taking in account the characteristics of the behavior of the ground in the analysis of the phenomenon of ground-structure interaction suitable for the tunneling in soft soil, mainly with an aim of obtaining forecasts of the settlements caused on the surface by the construction of shallow tunnels. The numerical methods, by their flexibility, have proved to be effective for the study of these movements. They are employed in a quasi-systematic way and impose a good knowledge of displacements of the ground and efforts applied, making it possible to validate the choices carried out or to compare different methods of digging (Dias, 1999). However, the application of these methods to modeling of tunnels is delicate because of the three dimensional aspect of the behavior of the ground around the coal face and the complexity of requests induced in the soil by work (Atwa et al., 2001). The use of a two dimensional model compared to a

3D model proved more advantageous from the points of view that the 2D model is less expensive in computing times, the interpretation of the results is easier and the model of behavior is more complex. Nevertheless, the 3D model remains most suitable since it takes into account the complete aspects of the problem. Considering the complexity of the movements resulting from tunneling, it appears necessary for the determination of these movements to have a reliable computational tool for the numerical simulation of this extremely delicate behavior.

In this study, a sandy ground was modeled which consisted of only one layer, where a tunnel was built. It was a case studied in recent work (Liu, 1997; Kasper and Meschke, 2006; Augarde et al., 1997 and Bloodworth, 2002). The geometry used is that of the model of reference of Liu (1997). The characteristics of the model were drawn from the literature, and they were modified one by one in order to see the behavior of the ground in response to each modification. Initial objective was to evaluate the movements (vertical and horizontal) generated by the construction of a tunnel by the technique of the shield.

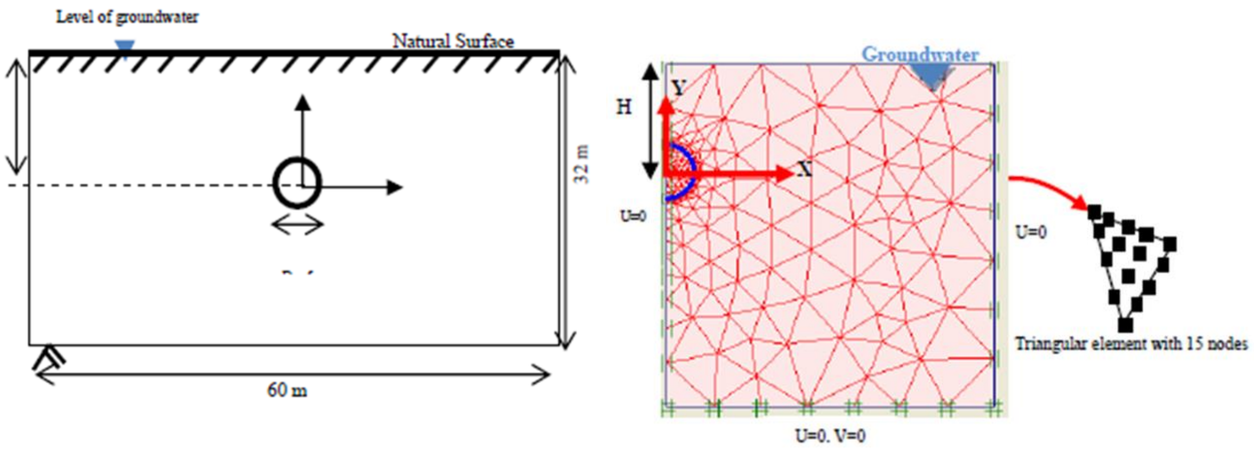

Figure 2.1 Geometry model and finite element mesh (After N. El Houari, 2011)

After the construction of the tunnel, it was noted that a movement of ground occurred at the level of natural surface, as well as at the level of the excavation (in clay). The finite element mesh clearly showed the existence of a trough caused by the construction of the tunnel. It was noted also a certain shortening of the lining of the tunnel that is due to the various phases of constructions such as the digging, the filling of the annular vacuum, the installation of supporting etc. However, the following points were noted:

- The ground located below the foundation raft remained practically undisturbed.
- The ground located on the surface tended to converge towards the center of the basin.

Also, according to the observations of Ollier (1997), the ground on the surface generally rocks towards the center of the basin. He bound this phenomenon to the various phases of tunneling with the tunnel boring.

The methodology which were applied to the construction of a shallow tunnel gave movements of ground, qualitatively comparable with those drawn from literature. Parametric study was of a great utility, since it enabled to study the influence of the geometrical and geotechnical parameters on the behavior of the ground. The geometrical parameters depth and diameter of the tunnel seemed to have an outstanding influence on the behavior of the ground. Also, the coefficient of grounds at rest affects the movements in the ground, emphasizing the need for a good determination of this parameter. Maximum settlement on the surface decreases with the depth of the tunnel. As for horizontal displacements, they are pushed back towards the outside of the tunnel and reach their maxima at the level of the kidneys of the tunnel. The increase in the angle of friction decreases the intensity of the movements; however, results were reversed owing to the fact that PLAXIS uses the formula of Jacky in calculations. Each modified parameter presents an influence on the behavior of the ground caused by the construction of tunnels. However, the ground behaves differently from one parameter to the other. In urban sites, tunneling presents more concern considering the complexity of the phenomenon of ground-structure interaction. Being always in the context of parametric study, this study was extended to investigate the incidence of tunneling on settlements on the surface in the presence of a building. These settlements are of increased amplitude, more particularly, at the level of the tunnel axis. It was also noted that the presence of another tunnel influences the amplitude of settlement.

2.4 Effect of Basement Raft Loading on Existing Urban Tunnel in Soil

Tunnels are the vital elements for the everyday life of the people especially in heavily crowded urban areas. In an urban environment, due to lack of space, a lot of underground constructions such as metro tunnel and building with 2 to 3 basements are increasing. The tunnelling induced ground settlement is the major problem in tunnelling activities in urban areas. These settlements can damage the overlying structures and should be reduced to an acceptable value. Peck (1969) developed a method to determine surface settlement and lining stresses induced by tunnelling based on field measurements and empirical data. Analytical and empirical solutions of similar problems were also developed by several researchers to calculate the surface settlements and lining stresses. As of today well established design guidelines are available to evaluate the displacement of adjacent structures/foundations due to tunnel excavation, which are typically verified using proper monitoring system in practice. On the other hand, the impacts of deep excavation, foundation construction and foundation loading on existing tunnels have not yet been examined sufficiently. Influence of pile foundation construction and loading on existing tunnel was studied by few researchers (Benton and Phillips, 1991; Arunkumar and Ayothiraman, 2010). Although there are few studies reported on influence of pile loading on exiting tunnels, not enough attention have been given to understand the interaction of basement raft foundation with the existing urban tunnels (Sesharao, 2014). There exists a great gap, thus giving scope to focus the research on this problem thus the results of 3D FE analyses on effect of raft excavation and loading on existing tunnel were analysed. Before the analyses, the proposed numerical modelling procedure was verified by comparing the reported case studies as discussed below.

Settlement trough due to tunnelling has been validated using PLAXIS 2D for the Barcelona subway Network Extension Tunnel. Soil was predominately red and brown clay with sand and gravel (Cu=30-150 kPa). The depth of tunnel axis was 10.0 m and diameter of the tunnel was 8.0 m with percentage volume loss of 0.8%. The predicted and measured settlement trough is given in **Figure 2.2**. It was found that the surface settlement profile obtained from the finite element was shallow and wide compared to the measured data and the closed form analytical solution given by Loganathan and Poulos (1998) shown in **Figure 2.2**. Maximum settlement of the trough ranges from 21.4 mm to 25.6 mm, which are comparable.

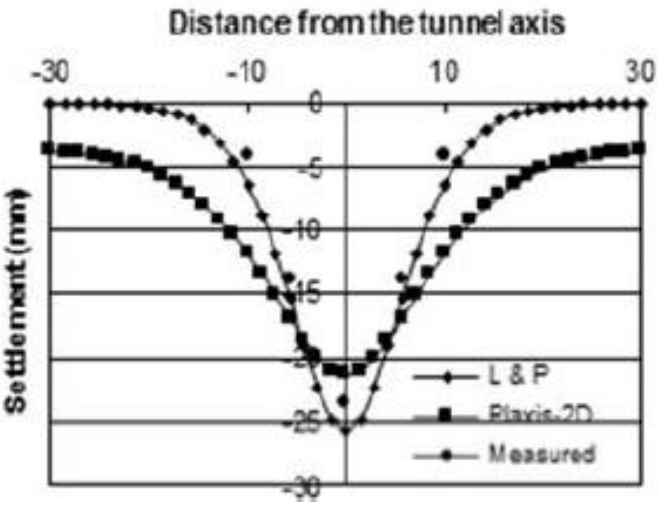

Figure 2.2 Predicted and observed settlement trough (After Sumeet Mahajan, 2016)

Based on the results obtained, it was concluded that the variation of displacement is significant with respect to various stages of construction. It was observed that vertical displacement of tunnel is more prominent compared to its horizontal movement. The tunnel liner was found to move towards the raft foundation while excavation and then away from it as a result of loading. This is due to the heaving effect of soil as a result of release of stress as excavation is made. Further due to loading of raft foundation, the opposite effect was made.

2.5 Geotechnical Modelling of a Deep Tunnel Excavation in the Boom Clay Formation

In this research, a simulation of an undrained tunnel excavation in the Boom Clay (BC) formation was presented, with the use of the PLAXIS 2D 2011 finite element program, in plane strain conditions. The response of the BC material was modelled with the Hardening Soil (HS) model. The aim was to investigate the individual effect and the level of influence of particular HS model input parameters on selected numerical results, by means of a mechanical sensitivity analysis. To this purpose, 22 numerical simulations were performed, where the values of the input parameters were individually varied to an upper and a lower bound, for values of the dilatancy angle (Ψ) equal to 0° and 1°. The numerical outcomes of two analyses (one with Ψ = 0° and one with Ψ = 1°), where the values of the model input parameters were equal to the mean of the ranges used, served as a basis for comparison with the results of all other simulations. This set of parameters was referred to as mean data. The varied HS model input parameters were the reference secant modulus (E_{50}^{ref}), the reference un-/reloading modulus (E_{ur}^{ref}), the rate of the level of stress dependency of stiffness (*m*), the effective friction angle (Ø') and the effective cohesion (c').

The examined numerical results concerned the thickness of the fully Plastic Zone (PZ) around the excavation, the width of the shear Hardening Zone (HZ), and the extent of the hydromechanical disturbance or the extent of the Disturbed Zone (DZ = PZ + HZ). Furthermore, the influence of the varied HS model input parameters on the resulting axial liner forces (*N*) and the generated pore water pressures (*u*) at the tunnel sidewall was examined.

It was found that the extent of the PZ is influenced by the magnitude of the elastoplastic shear stiffness of the material, which controls the amount of deviatoric strains (γ_s) at failure. The latter was significant as all analyses were performed by applying a constant amount of the tunnel contraction (i.e. the amount of imposed strains was kept constant). In such case, a larger shear stiffness in the elastoplastic domain entailed failure of the soil elements at lower level of (γ_s). Consequently, a larger amount of *q* was redistributed from the fully plastified soil elements to their surroundings, as a larger portion of the prescribed γ_s needed to be applied after failure, until the completion of the simulation. Thus, the extent of the PZ increased for an increase in the elasto-plastic shear stiffness of the material. The thickness of the PZ was found to increase for a rise in the values of E_{50}^{ref} and *m*. On the other hand, an increase in the values of Ø' and c' was found to induce a smaller extent of the PZ. The un-/reloading modulus was found not to influence the extent of the PZ. The thickness of the HZ was found to be influenced by both the elastoplastic and the elastic shear stiffness of the material. A rise in the first induced a smaller extent of the HZ as a lower amount of *q* was redistributed from stiffer stress points, of which the ESP lay on the shear hardening locus, to their surroundings. On the contrary, an increase in the elastic shear stiffness caused the ESP of the stress points which were

situated in the elastic domain to yield at a smaller amount of γ_s, leading to a larger extent of the HZ. The thickness of the HZ was found to increase for a rise in the values of E_{ur}^{ref} and m. A rise in E_{50}^{ref} , Ø' and c' led to a reduction in the extent of the HZ. The thickness of the DZ, which was derived by adding the width of the PZ and the HZ, increased for a rise in the values of E_{ur}^{ref} and m, whereas it reduced for an increase in the magnitudes of E_{50}^{ref} , Ø' and c'. The pore water pressures next to the sidewall of the tunnel were found to be affected by the generated negative excess pore water pressures (u_{excess}). The produced "u" reduced for an increase in the values of E_{50}^{ref} ,m, Ø' and c', whereas they increased slightly for a rise in the magnitude of E_{ur}^{ref} .
The hoop forces in the tunnel liner were found to be mainly influenced by the magnitude of the total radial stresses (σ_r) acting on the periphery of the excavation, which resulted from adding the generated radial effective stresses (σ_r') and "u". For the simulations where $\Psi=0°$ was used, the value of N was found to reduce for an increase in the values of all varied model input parameters. This reduction was larger for the analyses where $\Psi=1°$ was used, owing to the generation of more negative u_{excess} and therefore, to the generation of less compressive "u" acting on the liner. Aside from the different magnitudes of *N* and *u*, the thickness of the PZ, the HZ and the DZ was found to remain constant for $\Psi=0°$ and $\Psi=1°$. Finally, the varied model input parameters which affect the investigated numerical results the most, were identified. It was found that the thickness of the PZ is mainly influenced by E_{50}^{ref} . The extent of the HZ and the DZ were mostly affected by $E_{ur}^{ref.}$ The magnitudes of *N* and *u* were predominantly influenced by Ø'.

2.6 Structural Design of Tunnel Lining (FHWA-NHI-09-010, Road Tunnel Manual)

Tunnel linings are structural systems installed after excavation to provide ground support, to maintain the tunnel opening, to limit the inflow of ground water, to support appurtenances and to provide a base for the final finished exposed surface of the tunnel. Tunnel linings can be used for initial stabilization of the excavation, permanent ground support or a combination of both. The materials for tunnel linings can be are cast-in-place concrete lining, precast segmental concrete lining, steel plate linings and shotcrete lining (also a cast-in-place lining).
Cast-in-place concrete linings are generally installed some time after the initial ground support. Cast-in-place concrete linings are used in both soft ground and hard rock tunnels and can be constructed of either reinforced or plain concrete. Cast-in-place concrete linings can take on any geometric shape, with the shape being determined by the use, mining method and ground conditions.
In this article, AASHTO Load and Resistance factor Design (LRFD) is taken into account for design of tunnel lining. LRFD is a design philosophy that takes into account the variability in the prediction

of loads and the variability in the behavior of structural elements. It is an extension of the load factor design methodology that has been in use for a number of years.

The AASHTO provisions do not address plain concrete. The following design procedures are followed for structural plain concrete.

The moment capacity on the compression face of the lining can be calculated as follows:

$\varphi M_{nC} = \varphi\ 0.85\ f_c'\ S$

Where,

M_{nC} = The nominal resistance of the compression face of the concrete

φ = 0.55 for plain concrete

f_c' = 28 day compressive strength of the concrete

S = The section modulus of the lining section based on the gross uncracked section

The moment capacity on the tension face of the lining can be calculated as follows:

$\varphi M_{nT} = \varphi 5(f_c')^{1/2}\ S$

Where,

M_{nT} = The nominal resistance of the tension face of the concrete

φ = 0.55 for plain concrete

f_c' = 28 day compressive strength of the concrete

S = The section modulus of the lining section

The compressive strength of the lining can be calculated as follows:

$\varphi P_C = \varphi 0.6 f_c' A$

Where

P_C = The nominal resistance of lining in compression

φ = 0.55 for plain concrete

f_c' = 28 day compressive strength of the concrete

A = The cross sectional area of the lining section

Check the compression face as follows:

$Q_A/\varphi P_C + Q_M/\varphi M_{nC} \leq 1$

Where,

Q_A = The axial load force effect modified by the appropriate factors

Q_M = The moment force effect modified by the appropriate factors

The tension strength of the lining can be calculated as follows:

$\varphi P_T = 5\varphi (f_c')^{1/2}$

Where,

P_T = The nominal resistance of lining in tension

φ = 0.55 for plain concrete

f_c' = 28 day compressive strength of the concrete

The tension face can be checked as follows:

$Q_M/S - Q_A/A \leq \varphi P_T$

Where the values of the variables are described above.

Then the shear strength of the lining is calculated as follows:

$\varphi V_n = \varphi 1.33(f_c')^{1/2}\, b_w h$

Where,

V_n = The nominal resistance of lining in shear

φ = 0.55 for plain concrete

f_c' = 28 day compressive strength of the concrete

b_w = the length if tunnel lining under design

h = the design thickness of the tunnel lining

This design method is adapted for LRFD from the provisions for structural plain concrete from the American Concrete Institute's Building Requirements for Structural Concrete (ACI 318).

Chapter 3

DEVELOPMENT OF SOIL-STRUCTURE INTERACTION MODEL

3.1 Introduction

Most of the civil engineering structures involve some type of structural element with direct contact with ground. When the external forces, such as earthquakes or any means of ground movement act on these systems, neither the structural displacements nor the ground displacements, are independent of each other. The process in which the response of the soil influences the motion of the structure and the motion of the structure influences the response of the soil is termed as soil-structure interaction (SSI). Considering soil-structure interaction makes a structure more flexible. Investigations of soil–structure interaction have shown that the dynamic response of a structure supported on flexible soil may differ significantly from the response of the same structure when supported on a rigid base (Chopra AK, 1974) , which describes the importance of a soil-structure interaction model.

Soil-structure problems are very difficult to understand and depends largely on the prevailing site conditions. Creation of physical models and simulations using them are very time consuming. However, this complex phenomenon can be easily simulated and understand numerically with the help of finite element models. Finite element models has been proved to be very useful in dealing with such problems in a very short time.

PLAXIS has many versions depending its uses and applicability on different soil-structure interaction problems. The Professional Version which is used in this research, PLAXIS-2D Version 8, is a finite element package which is capable of handling soil-structure interaction phenomenon with much accuracy/efficiently. It is intended for the two-dimensional analysis of deformation and stability in geotechnical engineering. Geotechnical applications require advanced constitutive models for the simulation of the non-linear, time dependent and anisotropic behavior of soils and/or rock. In addition, since soil is a multi-phase material, special procedures are required to deal with hydrostatic and non-hydrostatic pore pressures in the soil. Although the modeling of the soil itself is an important issue, many tunnel projects involve the modeling of structures and the interaction between the structures and the soil. PLAXIS-2D is equipped with features to deal with various aspects of complex geotechnical structures. Real situations may be modeled either by a plane strain or an axisymmetric model. The program uses a convenient graphical user interface that enables users to quickly generate a geometry model and finite element mesh based on a representative vertical cross-section of the situation at hand.

As mentioned earlier, for this research, the soil-structure interaction model was developed using PLAXIS-2D. The modelling steps involved several steps such as generation of model boundaries, selection of finite elements, generation of finite element mesh, generation of pore water pressures and inital stress, generation of load conditions etc. The sequential steps that were followed while development of the model are described in the following sections.

3.2 Features of PLAXIS-2D

PLAXIS Version 8, which has been used in this research as a modeling tolls, has several special features like the extensions involve new modelling options, calculation facilities, output features and a general improved 'user friendliness' and consistency. It as an extended package, including static elastoplastic deformation, advanced soil models, consolidation, updated mesh and steady-state groundwater flow. Some special features of PLAXIS-2D used in this research are described below.

Graphical input of geometry models: The input of soil layers, structures, construction stages, loads and boundary conditions is based on convenient CAD drawing procedures, which allows for a detailed modelling of the geometry cross-section. From this geometry model, a 2D finite element mesh is easily generated.

Automatic mesh generation: PLAXIS allows for automatic generation of unstructured 2D finite element meshes with options for global and local mesh refinement. The 2D mesh generator is a special version of the Triangle generator, which was developed by Sepra.
High-order elements: Quadratic 6-node and 4th order 15-node triangular elements are available to model the deformations and stresses in the soil.

Plates: Special beam elements are used to model the bending of retaining walls, tunnel linings, shells, and other slender structures. The behaviour of these elements is defined using a flexural rigidity, a normal stiffness and an ultimate bending moment. A plastic hinge may develop for elastoplastic plates, as soon as the ultimate moment is mobilised. Plates with interfaces may be used to perform realistic analyses of geotechnical structures.

Interfaces: Joint elements are available to model soil-structure interaction. For example, these elements may be used to simulate the thin zone of intensely shearing material at the contact between a tunnel lining and the surrounding soil. Values of interface friction angle and adhesion are generally not the same as the friction angle and cohesion of the surrounding soil.

Tunnels: The PLAXIS program offers a convenient option to create circular and non-circular tunnels using arcs and lines. Plates and interfaces may be used to model the tunnel lining and the interaction with the surrounding soil. Fully isoparametric elements are used to model the curved boundaries within the mesh. Various methods have been implemented to analyse the deformations that occur as a result of various methods of tunnel construction.

Mohr-Coulomb model: This robust and simple non-linear model is based on soil parameters that are well-known in engineering practice. Not all non-linear features of soil behaviour are included in this model, however. The Mohr-Coulomb model may be used to compute realistic support pressures for tunnel faces, ultimate loads for footings, etc. It may also be used to calculate a safety factor using a 'phi-c reduction' approach.

Advanced soil models: In addition to the Mohr-Coulomb model, PLAXIS offers a variety of advanced soil models. As a general second-order model, an elastoplastic type of hyperbolic model, called the Hardening Soil model, is available. To model accurately the time-dependent and logarithmic compression behaviour of normally consolidated soft soils, a Creep model is available, which is referred to as the Soft Soil Creep model. In addition to these soil models, a special model is available to analyse the anisotropic behaviour of jointed rock.

Steady state pore pressure: Complex pore pressure distributions may be generated on the basis of a combination of phreatic levels or direct input of water pressures. As an alternative, a steady-state groundwater flow calculation can be performed to calculate the pore pressure distribution in problems that involve steady flow or seepage.

Automatic load stepping: The PLAXIS program can be run in an automatic step size and automatic time step selection mode. This avoids the need for users to select suitable load increments for plastic calculations and it guarantees an efficient and robust calculation process.

Staged construction: This powerful PLAXIS feature enables a realistic simulation of construction and excavation processes by activating and deactivating clusters of elements, application of loads, changing of water tables, etc. This procedure allows for a realistic assessment of stresses and displacements as caused, for example, by soil excavation during an underground construction project.

Presentation of results: The PLAXIS postprocessor has enhanced graphical features for displaying computational results. Values of displacements, stresses, strains and structural forces can be obtained from the output tables. Plots and tables can be send to output devices or to the Windows clipboard to export them to other software.

3.3 Limitations of PLAXIS-2D

PLAXIS is a finite element program for soil-structure interaction applications in which soil models are used to simulate the soil and soil-structure interaction behavior. Although a lot of testing and validation have been performed, it cannot be guaranteed that the PLAXIS code is free of errors. Moreover, the simulation of geotechnical problems by means of the finite element method implicitly involves some inevitable numerical and modeling errors. The accuracy at which reality is approximated depends highly on the expertise of the user regarding the modelling of the problem, the understanding of the soil models and their limitations, the selection of model parameters, and the ability to judge the reliability of the computational results. Hence, PLAXIS may only be used by professionals that possess the aforementioned expertise.

Besides, in this research, PLAXIS-2D software package has been used which presumes that modeling done in plain strain condition. Actual 3D conditions may differ with 2D simulations depending on site conditions, loadings, response of model elements due to loading etc.

3.4 Modeling Steps

Modeling in PLAXIS-2D involves several steps. Each of the steps are equally important as one error cumulatively contributes to another. The whole process can be summarized in three steps:

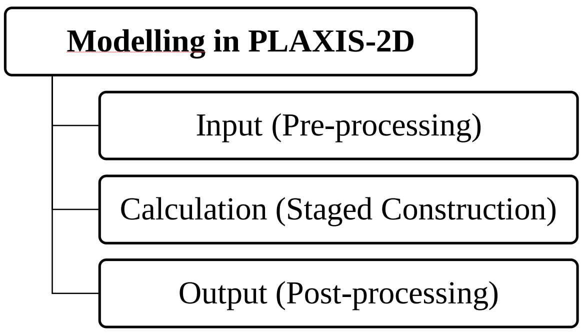

Figure 3.1 Modelling Steps

3.4.1 Input (Pre-processing)

The first stage for developing the soil-structure interaction model in PLAXIS-2D is input or pre-processing. This stage consists of several sub-stages as described below.

Defining the Model Extent

The first step for developing the model was to create a model domain in which the finite element mesh will be generated. At this stage the soil cluster elments, dimensions of each of the soil layers, units of data input and output were defined. Short description of the elements used are given in the following sections.

Soil Elements

In this research, the soil layers are modelled with 15-node triangular elements. The 15-node triangle is the default element. It provides a fourth order interpolation for displacements and the numerical integration involves twelve Gauss points (stress points). The 15-node triangle is a very accurate element that produce high quality stress results for difficult problems, as for example in collapse calculations for incompressible soils . The only drawback of using this element is, it leads to relatively high memory consumption and relatively slow calculation and operation performance.

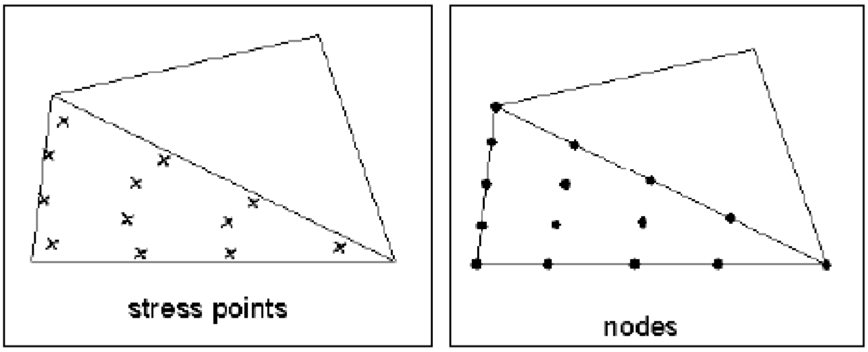

Figure 3.2 Position of nodes and stress points in 15-node triangular soil element (PLAXIS Reference Manual)

Beam elements

Plates in the PLAXIS-2D finite element model are composed of beam elements (line elements) with three degrees of freedom per node: Two translational degrees of freedom (u_x, u_y) and one rotational degrees of freedom (rotation in the x-y plane: φ_z). When 6-node soil elements are employed then each beam element is defined by three nodes whereas 5- node beam elements are used together with the 15-node soil elements (**Figure 3.2**). The beam elements are based on Mindlin's beam theory. This theory allows for beam deflections due to shearing as well as bending. In addition, the element can change length when an axial force is applied. Beam elements can become plastic if a prescribed maximum bending moment or maximum axial force is reached.

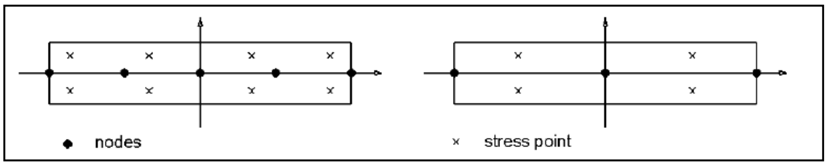

Figure 3.3 Beam Elements(PLAXIS Reference Manual)

Bending moments and axial forces are evaluated from the stresses at the stress points. A 3-node beam element contains two pairs of Gaussian stress points whereas a 5-node beam element contains four pairs of stress points. Within each pair, stress points are located at a distance ½ deq 3 above and below the plate centre-line. **Figure 3.3** shows a single 3-node and 5-node beam element with an indication of the nodes and stress points.

Interface elements

To model the soil-structure behavior more accurately, an interface was used below the structures (plates) and on the sides of the tunnel lining. The interfaces are composed of interface elements. **Figure 3.4** shows how interface elements are connected to soil elements. When using 15-node soil elements, the corresponding interface elements are defined by five pairs of nodes, whereas for 6-node soil elements the corresponding interface elements are defined by three pairs of nodes. In the figure, the interface elements are shown to have a finite thickness, but in the finite element formulation the coordinates of each node pair are identical, which means that the element has a zero thickness. Each interface has assigned to it a 'virtual thickness' which is an imaginary dimension used to define the material properties of the interface. The virtual thickness is calculated as the virtual thickness factor times the average element size. The average element size is determined by the global coarseness setting for the 2D mesh generation. The default value of the virtual thickness factor is 0.1.

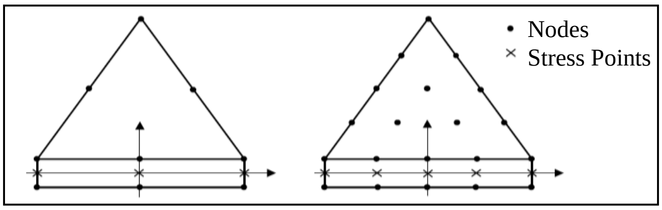

Figure 3.4 Distribution of nodes and stress points in interface elements and their Connecting nodes to soil elements (PLAXIS Reference Manual)

Units of Input and Output Data

In PLAXIS-2D, units of input and output data have to be mentioned at the first stage while defining the model extent. For this research work, units of length, force and time were selected as meter, kN and day respectively.

Soil Model

As mentioned in Chapter 3, different types of soil models are available in PLAXIS-2D. In this research a very commonly used soil model namely, Mohr-Coulomb model was used. In PLAXIS, the Mohr-Coulomb model is one of the most typically used and representative soil model. This model is also known as Linear-Elastic Perfectly-Plastic model which is used as a "first-order" approximation of soil behavior in general. The model involves five parameters, namely Young's modulus, E, Poisson's ratio, ν, the cohesion, c, the friction angle, ϕ, and the dilatancy angle, ψ. The main advantage of this model is, for each layer, a constant average stiffness is specified and due to this constant stiffness, computations tend to be relatively fast and one obtains a first estimate of deformations.
The Mohr-Coulomb yield condition is an extension of Coulomb's friction law to general states of stress. In fact, this condition ensures that Coulomb's friction law is obeyed in any plane within a material element. The full Mohr-Coulomb yield condition consists of six yield functions when formulated in terms of principal stresses (see for instance Smith & Griffith, 1982):

$$f_{1a} = \tfrac{1}{2}(\sigma'_2 - \sigma'_3) + \tfrac{1}{2}(\sigma'_2 + \sigma'_3)\sin\varphi - c\cos\varphi \leq 0$$

$$f_{1b} = \tfrac{1}{2}(\sigma'_3 - \sigma'_2) + \tfrac{1}{2}(\sigma'_3 + \sigma'_2)\sin\varphi - c\cos\varphi \leq 0$$

$$f_{2a} = \tfrac{1}{2}(\sigma'_3 - \sigma'_1) + \tfrac{1}{2}(\sigma'_3 + \sigma'_1)\sin\varphi - c\cos\varphi \leq 0$$

$$f_{2b} = \tfrac{1}{2}(\sigma'_1 - \sigma'_3) + \tfrac{1}{2}(\sigma'_1 + \sigma'_3)\sin\varphi - c\cos\varphi \leq 0$$

$$f_{3a} = \tfrac{1}{2}(\sigma'_1 - \sigma'_2) + \tfrac{1}{2}(\sigma'_1 + \sigma'_2)\sin\varphi - c\cos\varphi \leq 0$$

$$f_{3b} = \tfrac{1}{2}(\sigma'_2 - \sigma'_1) + \tfrac{1}{2}(\sigma'_2 + \sigma'_1)\sin\varphi - c\cos\varphi \leq 0$$

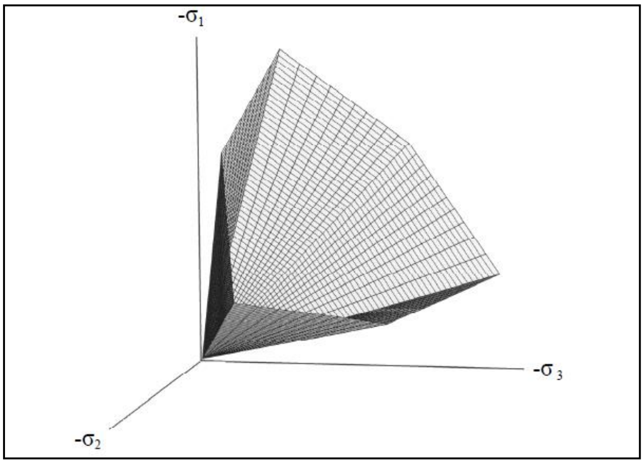

Figure 3.5 Mohr-Coulomb yield surface (PLAXIS Material Models Manual)

The two plastic model parameters appearing in the yield functions are the well-known friction angle ϕ and the cohesion c. These yield functions together represent a hexagonal cone in principal stress space as shown in **Figure 3.5**. In addition to the yield functions, six plastic potential functions are defined for the Mohr-Coulomb model:

$$g_{1a} = \tfrac{1}{2}(\sigma'_2 - \sigma'_3) + \tfrac{1}{2}(\sigma'_2 + \sigma'_3)\sin\psi$$

$$g_{1b} = \tfrac{1}{2}(\sigma'_3 - \sigma'_2) + \tfrac{1}{2}(\sigma'_3 + \sigma'_2)\sin\psi$$

$$g_{2a} = \tfrac{1}{2}(\sigma'_3 - \sigma'_1) + \tfrac{1}{2}(\sigma'_3 + \sigma'_1)\sin\psi$$

$$g_{2b} = \tfrac{1}{2}(\sigma'_1 - \sigma'_3) + \tfrac{1}{2}(\sigma'_1 + \sigma'_3)\sin\psi$$

$$g_{3a} = \tfrac{1}{2}(\sigma'_1 - \sigma'_2) + \tfrac{1}{2}(\sigma'_1 + \sigma'_2)\sin\psi$$

$$g_{3b} = \tfrac{1}{2}(\sigma'_2 - \sigma'_1) + \tfrac{1}{2}(\sigma'_2 + \sigma'_1)\sin\psi$$

The plastic potential functions contain a third plasticity parameter, the dilatancy angle ψ. This parameter is required to model positive plastic volumetric strain increments (dilatancy) as actually observed for dense soils. A discussion of all of the model parameters used in the Mohr-Coulomb model is given at the end of this section. When implementing the Mohr-Coulomb model for general stress states, special treatment is required for the intersection of two yield surfaces. Some programs use a smooth transition from one yield surface to another, i.e. the rounding-off of the corners (see for example Smith & Griffith, 1982). In PLAXIS, however, the exact form of the full Mohr-Coulomb model is implemented, using a sharp transition from one yield surface to another (detailed description of the corner treatment is provided in the literature Koiter, 1960; van Langen & Vermeer, 1990). For $c > 0$, the standard Mohr-Coulomb criterion allows for tension. In fact, allowable tensile stresses increase with cohesion. In reality, soil can sustain none or only very small tensile stresses. This behavior can be included in a PLAXIS analysis by specifying a tension cut-off. In this case, Mohr circles with positive principal stresses are not allowed. The tension cut-off introduces three additional yield functions, defined as:

$$f_4 = \sigma_1' - \sigma_t \leq 0$$

$$f_5 = \sigma_2' - \sigma_t \leq 0$$

$$f_6 = \sigma_3' - \sigma_t \leq 0$$

When this tension cut-off procedure is used, the allowable tensile stress, σ t, is, by default, taken equal to zero. For these three yield functions an associated flow rule is adopted. For stress states within the yield surface, the behavior is elastic and obeys Hooke's law for isotropic linear elasticity. For this model, the input parameters were the plasticity parameters c, ϕ, and ψ, the elastic Young's modulus E and Poisson's ratio ν.

Type of Material

In principle, all model parameters in PLAXIS-2D are meant to represent the effective soil response, i.e. the relation between the stresses and strains associated with the soil skeleton. But presence of pore water pressures affects stresses and strains in soil significantly. PLAXIS-2D uses two types of material behavior- dranined and undrained. In this research drained condition of soil was used to simulate long term behavior of water-soil skeleton.

Interface Strength (R_{inter})

An elastic-plastic model was used to describe the behaviour of interfaces for the modelling of soil-structure interaction. The Coulomb criterion was used to distinguish between elastic behaviour, where small displacements can occur within the interface, and plastic interface behaviour when permanent slip may occur.

For the interface to remain elastic the shear stress τ is given by:

$|\tau| < \sigma_n \tan\phi_i + c_i$

and for plastic behaviour τ is given by:

$|\tau| = \sigma_n \tan\phi_i + c_i$

where ϕ_i and c_i are the friction angle and cohesion (adhesion) of the interface.

The strength properties of interfaces are linked to the strength properties of a soil layer. Eachdata set has an associated strength reduction factor for interfaces (R_{inter}). The interface properties were automatically calculated by PLAXIS-2D from the soil properties in the associated data set and the strength reduction factor by applying the following rules:

$c_i = R_{inter}\ c_{soil}$

$\tan\phi_i = R_{inter} \tan\phi_{soil} \leq \tan\phi_{soil}$

$\psi_i = 0°$ for $R_{inter} < 1$, otherwise $\psi_i = \psi_{soil}$

In general, as in real soil-structure interaction, the interface is weaker and more flexible than the associated soil layer, meaning that the value of R_{inter} should be less than 1. In the absence of detailed information, according to PLAXIS-2D reference manual, the value of R_{inter} was chosen as 2/3.

Input Data of Soil and Structures

For this research, a typical soil profile of Dhaka Soil was used to model the soil layers. The soil profile composed of two types of sand layer upto a depth of top 5 meter, underlaying a 5 meter thick clay layer. Beneath the clay layer, another 10 meter of sand layer was assumed. The SPT values, varying with depth were used for calculating angle of internal friction (Ø) and Modulus of Elasticity (E) with the help of empirical relations found from literature..

Table 3.1 Soil Data

Soil Layer	Depth (m)	SPT (avg)	Undrained Angle of Internal Friction, Ø' (°)	Undrained Coheson, c' (kN/m^2)	Modulus of Elasticity, E (kN/m^2)	Remarks
layer-1	2	11	30	0.1	15990	Cohesionless
layer-2	3	8	28	0.1	13636	Cohesionless
layer-3	5	5	25	35	21000	Cohesive
layer-4	10	11	30	0.1	15990	Cohesionless

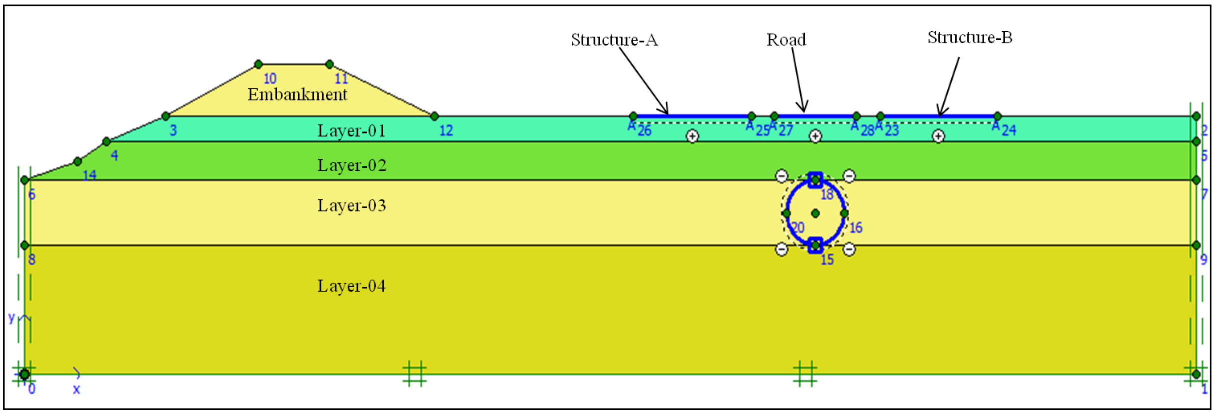

Figure 3.6 Developed 2D model

In this research, for the basic model, two types of structures were assumed to model the soil-structure interaction behavior. One was a raft foundation of 10 sqm. area (2 nos. on both sides of the tunnel), another was a typical road of 7m width, all of which were constructed at the existing ground level. The raft was assumed to have a thickness of 0.61 m (24 inch) whereas the road was assumed to have a thickness of 0.38 m (15 inch), both of them were made with 27579 kN/m^2 (4000 psi) concrete. One of the major elements of the model, the tunnel, was assumed to have a thickness of 0.38 m (15 inch), diameter of 5.0 m and made of high strength shotcrete of 55158 kN/m^2 (8000 psi) strength. The developed model is shown in **Figure 3.6**.

3.4.2 Calculation Stage

At this stage, different load cases were defined with the help of PLAXIS Calculation module. A total number of seven (07) calculation phases were defined for each of the trial cases. The calculation phases were defined so as to simulate the practical loading conditions sequentially. The calculation phases are stated in **Table 3.2** below.

Table 3.2 Calculation Stages

Calculation Phase	Name of the Phase	Description of the Phase
1	Mweight	Total weight of the soil is activated
2	Loading	Loads (UDL) of typical building and road are activated
3	Construction of Tunnel	Construction of Tunnel by TBM
4	Contraction of Tunnel	2% Contraction of Tunnel Lining
5	WL-1	Incorporation of Water Head difference of 2.5m
6	WL-2	Incorporation of Water Head difference of 4.5m
7	WL-3	Incorporation of Water Head difference of 6.5m

Mweight

This is the first calculation phase where only the load of the total soil layers were activated. All other structural loads and stresses due to presence of ground water level were neglected. This was done by the setting the total multiplier of Mweight equal to one.

Loading

The second phase was defined to activate the structural loadings of two buildings having 10.0 sqm area on both sides of the center of the tunnel to be constructed and a typical road of 7.0 m width. An uniformly distributed load (UDL) of 15 kN/m^2 were applied on both of the buildings to simulate the practical situation of a typical residential building. Both the buildings and road were modelled as plate element having an average bending stiffness and normal stiffness, specified according to their thickness and concrete strength. It is to be noted here that the road were separated by a horizontal distance of 2 m from the edge of the buildings.

Construction of Tunnel

At this phase, construction of tunnel by Tunnel Boring Machine (TBM) technique was done by activating the tunnel lining and deactivating the soil inside the tunnel lining.. As mentioned earlier, the lining was assumed to have a concrete strength of 55158 kN/m^2 (8000 psi) and a thickness of 0.38 m (15 inch) for the basic model. Besides, as the tunnel was assumed to be constructed below the ground water level at site, dewatering of the tunnel was done in this phase by making the cluster dry inside the tunnel lining. Water seal around the tunnel was ensured by introducing and activating a separate interface (active interface works as impermeable layer in PLAXIS) around the tunnel.

Contraction of Tunnel

As tunnel lining was assumed to be of 15 inch thick concrete, shrinkage of concrete lining would take place for a certain time. This was simulated at the phase named Contraction of Tunnel where a typical 2% contraction of tunnel lining was assumed.

WL-1

In all the previous phases, ground water level was assumed to be 2.5m below the exsiting ground level on the country side of the embankment. At this phase, first water head difference was specified in the model domain by raising the water level on river side by 2.5m while water level at the country side remaining at previous level (2.5m below existing ground level).

WL-2

This was the next phase after WL-1 phase, imposing a water head difference of 4.5m on the riverside while in the country side it remained same as previous.

WL-3

This was the final stage where highest water level difference was applied in the model. At riverside, the water level was raised to 6.5m above the existing ground water level, while at the countryside it remained same as existing ground water level. This also represents the most vulnerable situation for an embankment just prior to overtopping during the monsoon which causes highest seepage forces to act at the base of the structures at the countryside.

3.4.3 Output of Model

As mentioned earlier, the basic outputs of PLAXIS-2D are deformations, stresses, strains for any point in the soil layer and deformations, bending moments, shear and axial forces for any structure. The details of generated outputs of the models are described separately in **Chapter 6**.

Chapter 4

VALIDATION OF MODEL

4.1 Introduction

Validation of a model represents its applicability of simulating certain practical scenario. In this present study, validation of PLAXIS-2D model of a raft foundation and a tunnel have been done analytically by using Poulos and Davis method and PLAXIS-2D tutorial manual respectively.

4.2 Validation of Raft Foundation by Poulos and Davis's Analytical Method

According to Poulos and Davis (Poulos H.G. and Davis E.H., 1980), a simplified approach to calculate the settlement of a raft can be estimated by the following equation:

$$\rho = 0.947\frac{P}{B}[\frac{1-\nu^2}{E_s}]$$

Where,

ρ = settlement at the base of the raft

P = total load working on the raft

E_s = modulus of elasticity of soil below the raft

ν = Poisson's ratio of the soil below the raft

For the present study, a raft of 0.30 m thickness, 10m width has been considered with a working load of 15 kN/m^2. The soil beneath the raft has been considered as same as that used in the models for which analysis has been done, having an average modulus of elasticity of 16654 kN/m^2 and average Poisson's ratio of 0.30. For these values, the settlement of the raft was calculated both analytically and numerically which is tabulated in **Table 4.1** below.

Table 4.1 Calculated settlement of raft for validation purpose

Settlement of raft by analytical method of Poulos and Davis (m)	*Settlement of raft by numerical method using PLAXIS-2D (m)*
0.014	0.016

It is observed from **Table 4.1** that the settlement of raft calculated by PLAXIS-2D is in well agreement with that of calculated by Poulos and Davis's simplified method which implies that PLAXIS-2D can be used with sufficient accuracy in simulating behavior of a raft.

Figure 4.1 and **Figure 4.2** represents the model used and deformed mesh of the model for validation purpose.

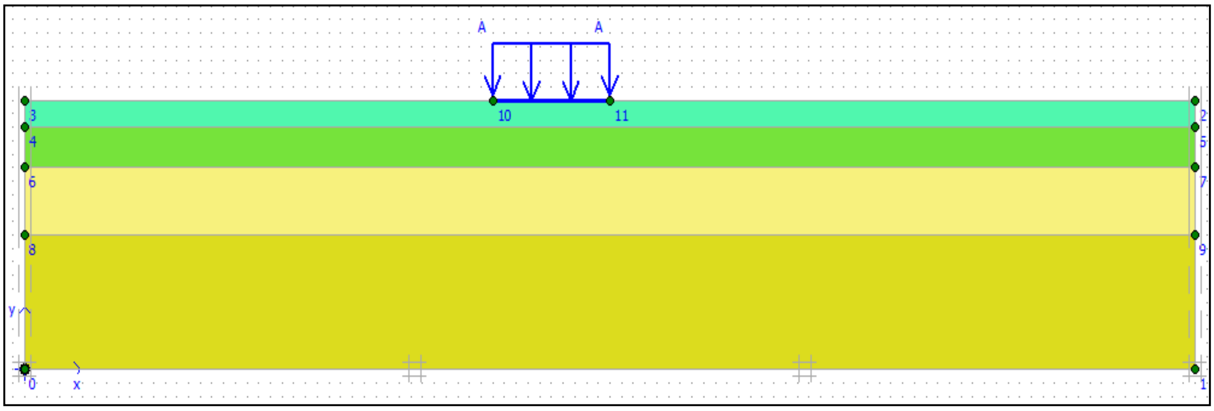

Figure 4.1 Developed 2D Raft model used for validation purpose

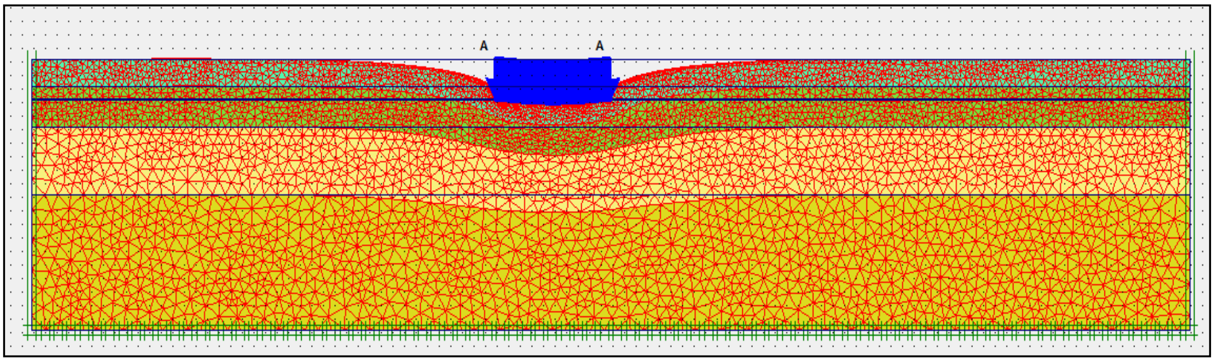

Figure 4.2 Deformed Mesh of the developed 2D Raft model used for validation purpose

4.3 Validation of Tunnel

In this research, validation of the tunnel model is done following two steps. First, in which the model developed in PLAXIS-2D tutorial manual is developed. Secondly, the same steps were employed for a previously developed model from literature (Shabna and Sankar, 2016) which was compared with analytical results. Both are described in the following sections.

4.3.1 Developing a 2D model using PLAXIS-2D Tutorial Manual

In this article, a simple representative tunnel model has been used which is present in detail in Section 8 (Settlements Due To Tunnel Construction) of PLAXIS-2D tutorial manual.

The tunnel considered in this section has a diameter of 5.0 m and is located at an average depth of 20 m. The soil profile indicates four distinct layers: The upper 13 m consists of soft clay type soil with stiffness that increases approximately linearly with depth. Under the clay layer there is a 2.0 m thick fine sand layer. This layer is used as a foundation layer for old wooden piles on which traditional brickwork houses were built. The pile foundation of such a building is modelled next to the tunnel. Displacements of these piles may cause damage to the building, which is highly undesirable. Below the sand layer there is a 5.0 m thick deep loamy clay layer. This is one of the layers in which the tunnel is constructed. The other part of the tunnel is constructed in the deep sand layer, which consists of dense sand and some gravel. This layer is very stiff. As a result only 5.0 m of this layer is included in the finite element model; the deeper part is considered to be fully rigid and modelled by appropriate boundary conditions. The pore pressure distribution is hydrostatic. The phreatic level is located 3 m below the ground surface (at a level of y = 0 m). Since the situation is more or less symmetric, only one half (the right half) is taken into account in the plane strain model. From the centre of the tunnel the model extends for 30 m in horizontal direction. The 15-node element is adopted for this model.

Table 4.2 Material Properties of the soil for Validation of Tunnel

Parameter	Name	Clay	Sand	Dp. Clay	Dp.sand	Unit
Material model	*Model*	MC	MC	MC	MC	-
Material beh.	*Type*	Drained	drained	Drained	drained	-
Soil unit weight above phreatic level	γ_{unsat}	15	16.5	16	17	kN/m^3
Soil unit weight below phreatic level	γ_{sat}	18	20	18.5	21	kN/m^3
H. permeability	k_x	$1{\cdot}10^{-4}$	1.0	$1{\cdot}10^{-2}$	0.5	m/day
V. permeability	k_y	$1{\cdot}10^{-4}$	1.0	$1{\cdot}10^{-2}$	0.5	m/day
Young's modulus	E_{ref}	1000	80000	10000	120000	kN/m^2
Increase *E*	E_{incr}	650	-	-	-	kN/m^3
Reference level	y_{ref}	0.0	-	-	-	m
Poisson's ratio	ν	0.33	0.3	0.33	0.3	-
Cohesion	c_{ref}	5.5	1.0	4.0	1.0	kN/m^2
Friction angle	φ	24	31	25	33	°
Dilatancy angle	ψ	0.0	1.0	0.0	3.0	°
Interface strength	R_{inter}	rigid	rigid	0.7	0.7	-

Table 4.3 Material Properties of the plates for Validation of Tunnel

Parameter	Name	Lining	Pile toe	Building	Unit
Type of behaviour	*Type*	Elastic	Elastic	Elastic	
Normal stiffness	*EA*	$1.4{\cdot}10^7$	$2{\cdot}10^6$	$1{\cdot}10^{10}$	kN/m
Flexural rigidity	*EI*	$1.43{\cdot}10^5$	$8{\cdot}10^3$	$1{\cdot}10^{10}$	kNm^2/m
Equivalent thickness	*d*	0.35	0.219	3.464	m
Weight	*w*	8.4	2.0	25	kN/m/m
Poisson's ratio	ν	0.15	0.2	0.0	-

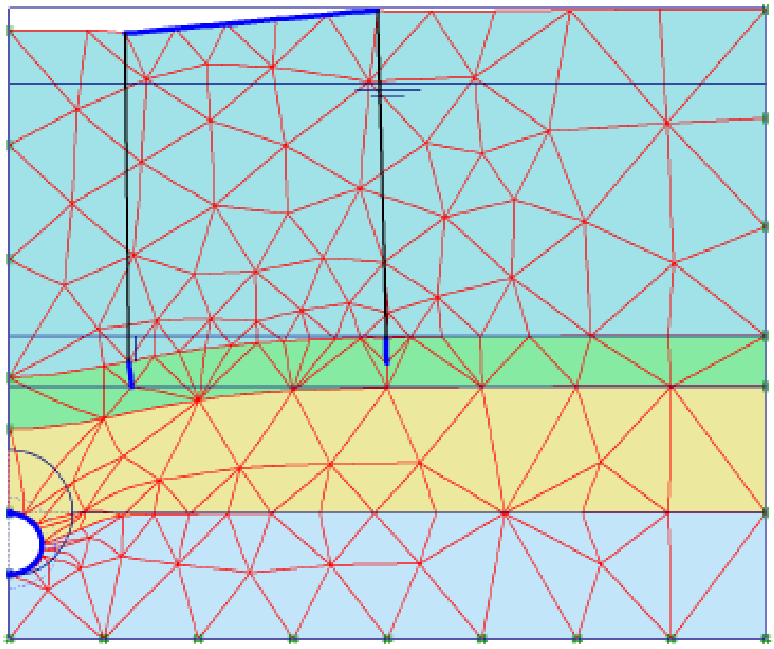

Figure 4.3 Deformed Mesh of the developed 2D Tunnel model used for validation purpose

The model was developed following the steps described in the PLAXIS-2D tutorial manual. Three calculation steps were defined to simulate a practical condition. At the first stage, the soil layers were activated. In the second stage, the tunnel lining was activated and the soil clusters inside the tunnel were deactivated. Finally at the third stage, some contraction of the tunnel lining was specified to simulate the shrinkage of tunnel lining.

4.3.2 Validation of Tunnel Model using Analytical Results

Following the steps described in the previous article, another model was developed and validated comprising a shallow tunnel in a soft clay formation (Shabna and Sankar, 2016). The typical geometry of the model has been shown in **Figure 4.4**.

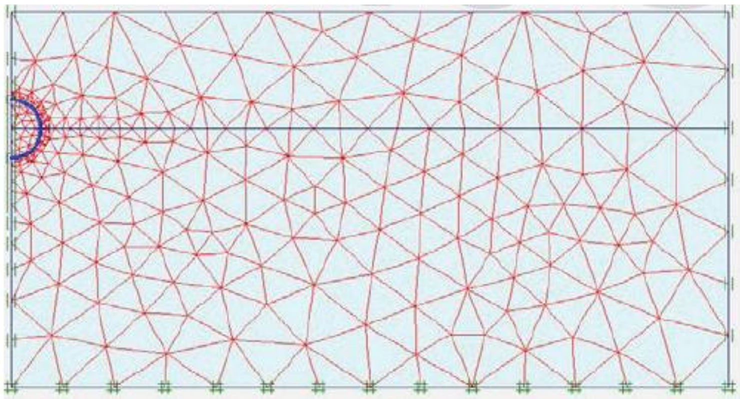

Figure 4.4 Generated Mesh of the developed 2D Tunnel model used for validation purpose

Results obtained from the developed model were compared with analytical calculations which showed that obtained results matched well with the analytical results (**Table 4.4**).

Table 4.4 Comparison of Results for Validation of Tunnel

Constraint	**Numerical Calculation**	**Analytical Calculation**
Maximum effective stress: $\sigma' = \sigma - u_w$	348.85 kPa	346.48 kPa

As the obtained model results are close to that of the analytical results, the tunnel modelling steps are taken to be satisfactory and validated and the same steps were followed for the present study.

Chapter 5

MODEL RESULTS AND DISCUSSION

5.1 Introduction

For this research, a total number of 09 (nine) cases were modeled and simulated, incorporating change in thickness of tunnel lining, varying horizontal position of center of tunnel, varying vertical position of center of tunnel. All these simulated cases (models) are tabulated in **Table 5.1**.

Table 5.1 Simulated Models

Sl. No.	*Simulated Case*	*Notation of Simulated Cases*	*Thickness of Center of Tunnel (m)*	*Horizontal Position of Center of Tunnel (m)*	*Vertical Position of Center of Tunnel (m)*	*Remarks*
01	Case-00 (Basic Case)	C	0.38	67.5	12.5	15" Tunnel Lining
02	Case-01	C1	0.46	67.5	12.5	18" Tunnel Lining
03	Case-02	C2	0.51	67.5	12.5	20" Tunnel Lining
04	Case-03	R1	0.38	72.0	12.5	Tunnel Center at +4.5m Right
05	Case-04	R2	0.38	78.0	12.5	Tunnel Center at +10.5m Right
06	Case-05	L1	0.38	63.0	12.5	Tunnel Center at -4.5m Left
07	Case-06	L2	0.38	57.0	12.5	Tunnel Center at -10.5m Left
08	Case-07	U1	0.38	67.5	13.5	Tunnel Center at +1.0m Upwards
09	Case-08	D1	0.38	67.5	11.5	Tunnel Center at +1.0m Downwards

In the table above, the variation of each of the models from the Basic Case (C), are tabulated in the right most column. Results of each of these simulated models were compared with the Basic model (C). The final results including comparison with Basic model (C) and analysis of each of the models separately are done and presented in the sections below.

5.2 Effect of Tunnel Thickness

To study the behavior of the building and road at their base due to changing the thickness of tunnel lining, three cases were considered (**Table 5.1**). One, the Basic model (C), in which the thickness of tunnel lining was considered to be of 0.38 m. For the second (C1) and third case (C2), the thickness of tunnel lining was assumed to be of 0.46 m and 0.51 m respectively.

To study the behavior of the building and road, the generated maximum displacement, was considered. It is note worthy to mention here that in all simulated models, two structures - A and B were similar. For this reason only structure-B was considered for the analysis.

Results indicate that maximum displacement at the base of the road and building, both increases with increased thickness of tunnel lining, mainly due to increase in self weight of the tunnel causing it to settle down. Two phases are considered. One, the construction of tunnel, another is 2% contraction of tunnel lining. It is noted that during the construction of tunnel stage, the maximum deformation is less than the contraction phase because of generation of uplift forces during construction of tunnel by TBM while in the contraction of tunnel stage, the maximum total deformation is greater because of increased overburden pressure of soil and shrinkage of tunnel lining causing larger settlement.

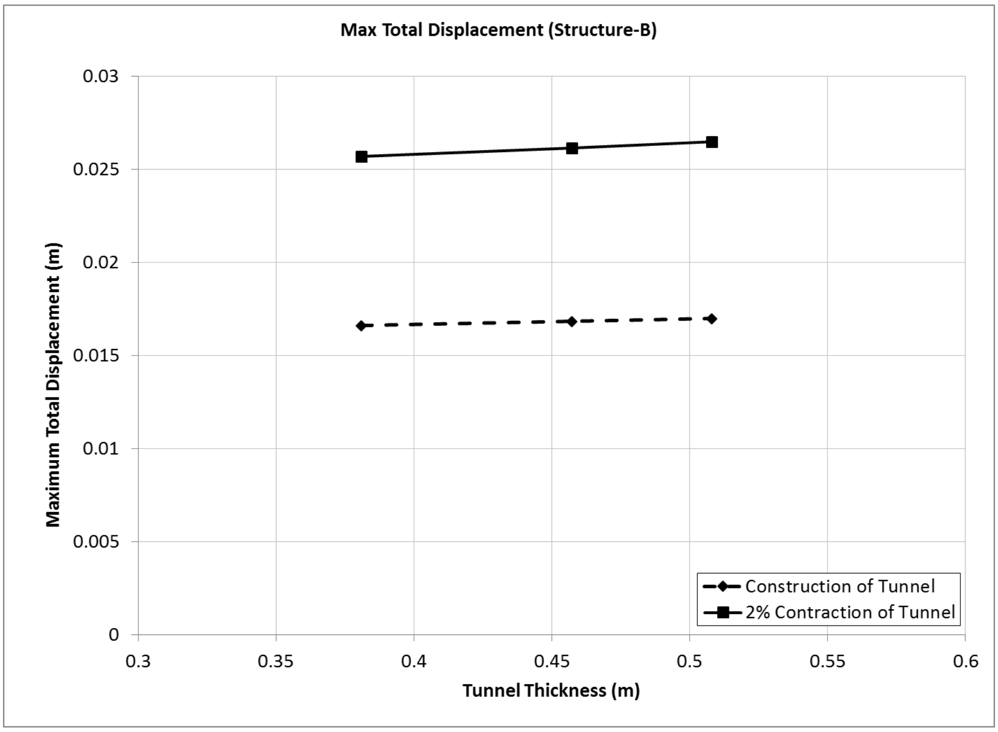

Figure 5.1 Maximum Total Displacement of at the Base of Structure-B

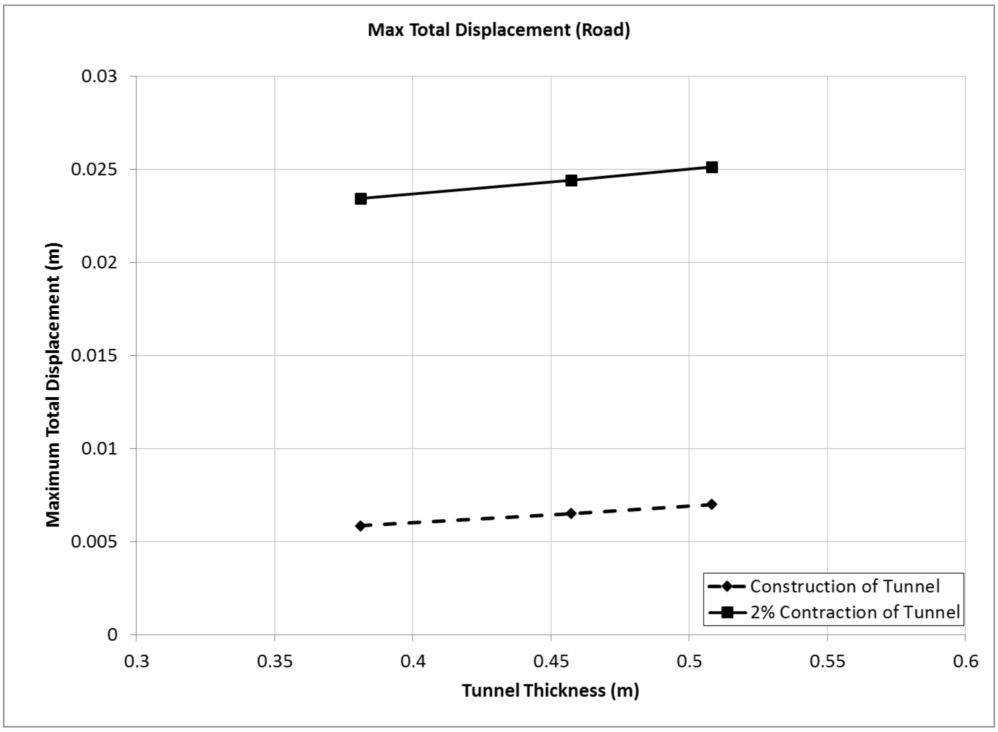

Figure 5.2 Maximum Total Displacement of at the Base of Road

For better understanding, total displacement along the length of the base of Structure-B is plotted in **Figure 5.4** and **Figure 5.5** for construction of tunnel and contraction of tunnel phase respectively. From the plots it is observed that at the end of construction of tunnel phase, maximum displacement occurs near the center of Structure-B (at the center of UDL) for all the three cases. Displacement is less at the left corner due to generation of uplifting pressure by the TBM and at the right corner because of away from the tunnel. Whereas, at the end of contraction phase of tunnel, displacement is maximum at the left most corner due to shrinkage of tunnel lining near that point (closest to tunnel). Similarly, displacement along the base of the road is also plotted in **Figure 5.6** and **Figure 5.7**. It is also observed from the plots that for the same reason mentioned above, increased tunnel thickness generates increased displacements on the road just above the tunnel.

The differential settlement between two corner points of Structure-B are also analyzed (**Figure 5.8**). It is observed that besides increasing displacement, increased tunnel thickness also increases the differential settlement of Structure-B.

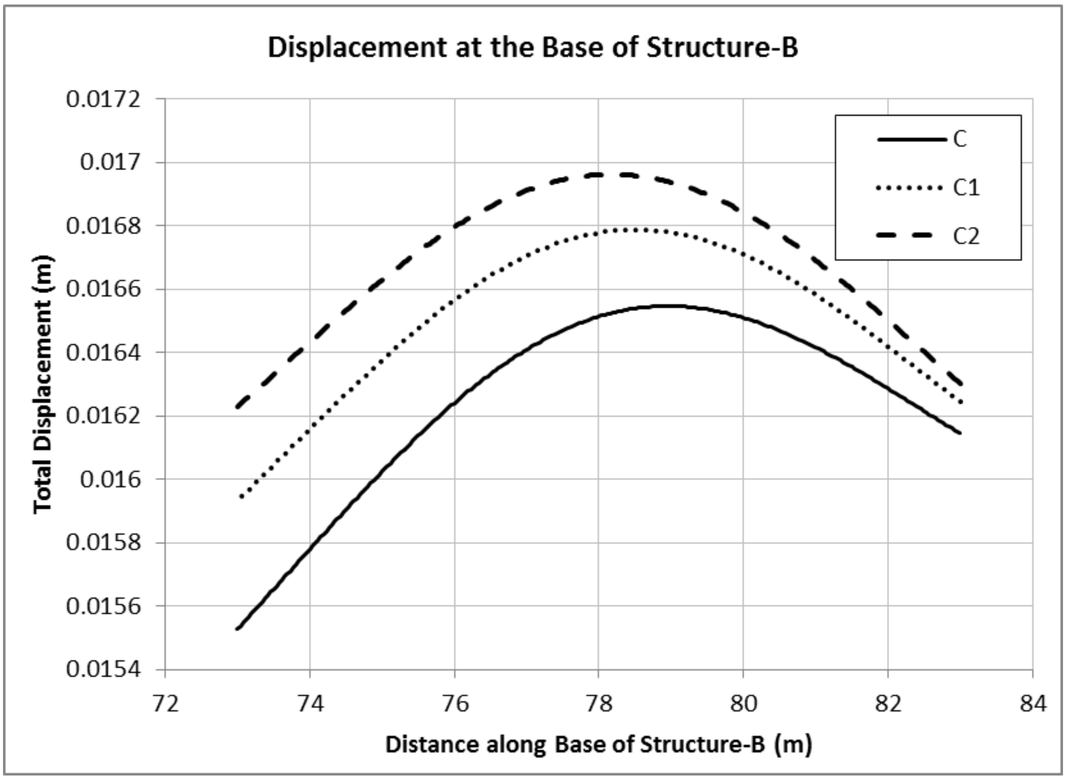

Figure 5.4 Total Displacement at the Base of Structure-B at the end of Construction of Tunnel

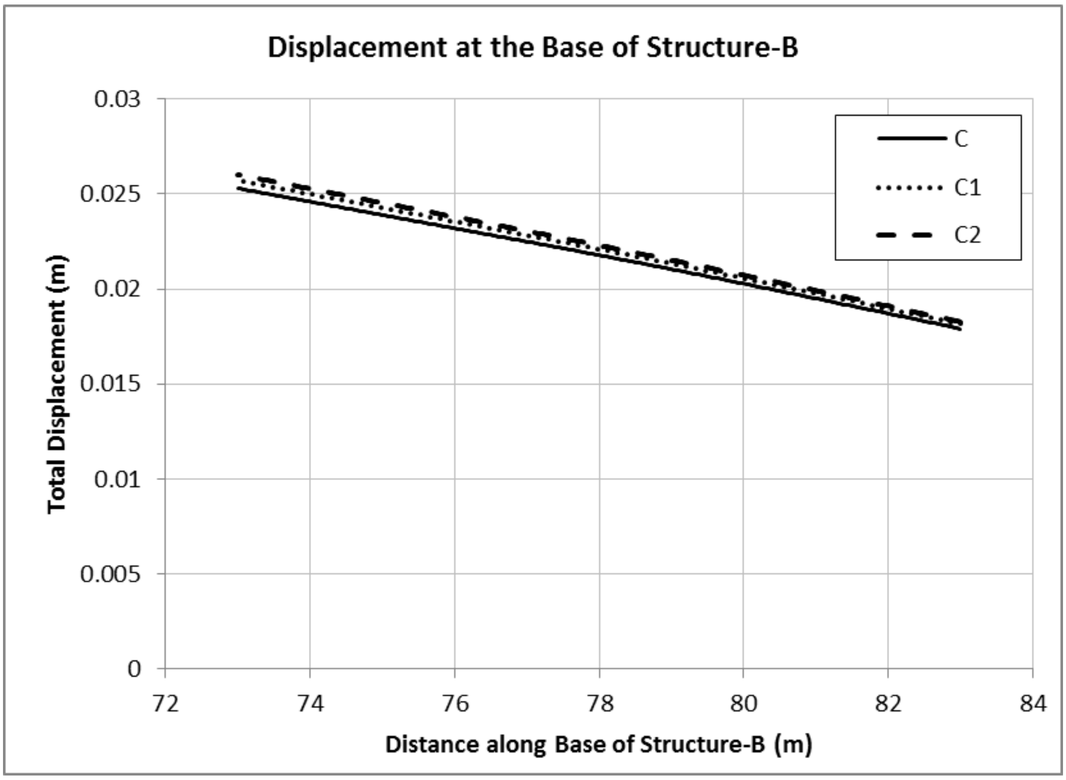

Figure 5.5 Total Displacement at the Base of Structure-B at the end of Contraction of Tunnel

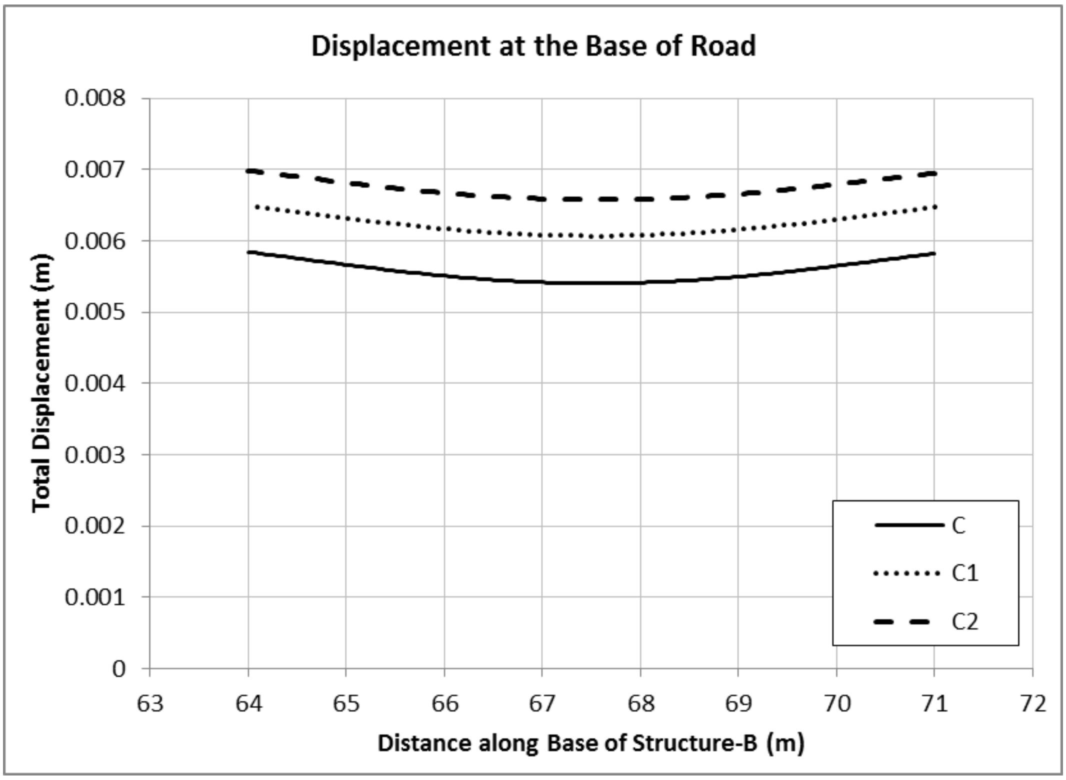

Figure 5.6 Maximum Displacement at the Base Road at the end of Construction of Tunnel

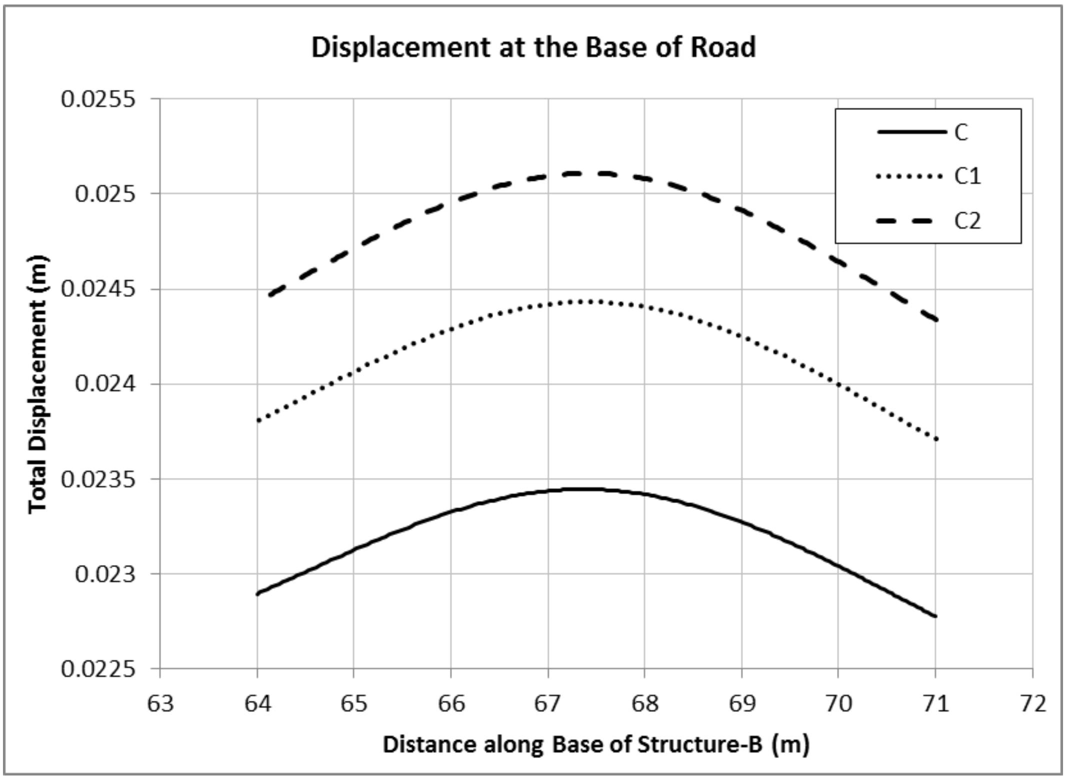

Figure 5.7 Maximum Displacement at the Base Road at the end of Contraction of Tunnel

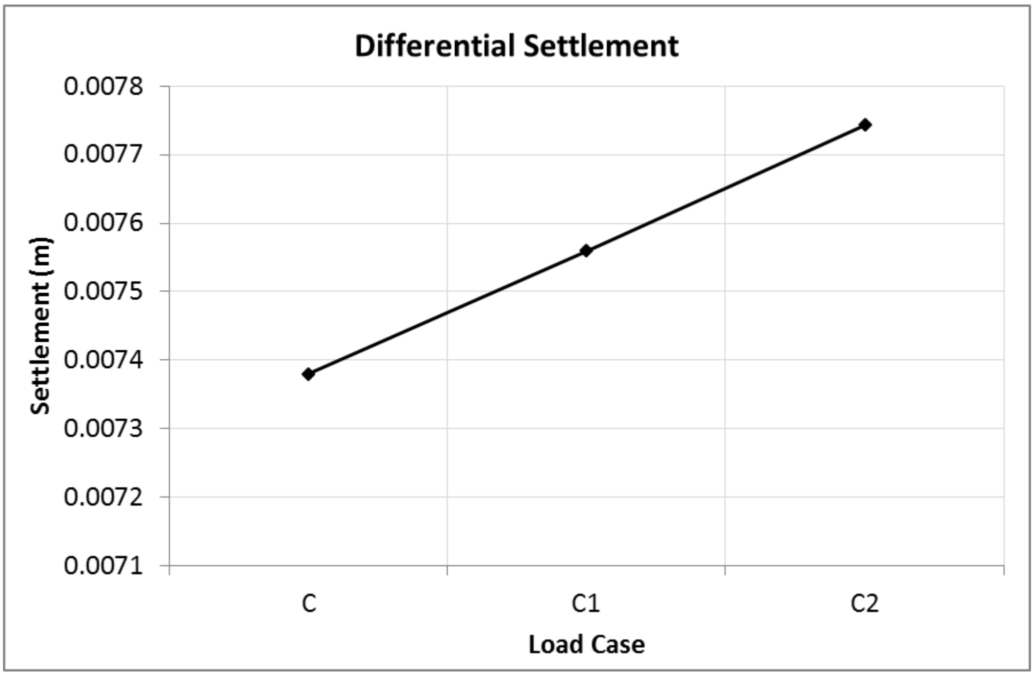

Figure 5.8 Differential Settlement at the Base of Structure-B at the end of Contraction of Tunnel

Increased thickness of tunnel lining also has its effects on the lining itself. At the end of contraction stage of tunnel, the maximum displacement of tunnel increases with increased thickness of tunnel lining due to increase in self weight of the tunnel (**Figure 5.9**).

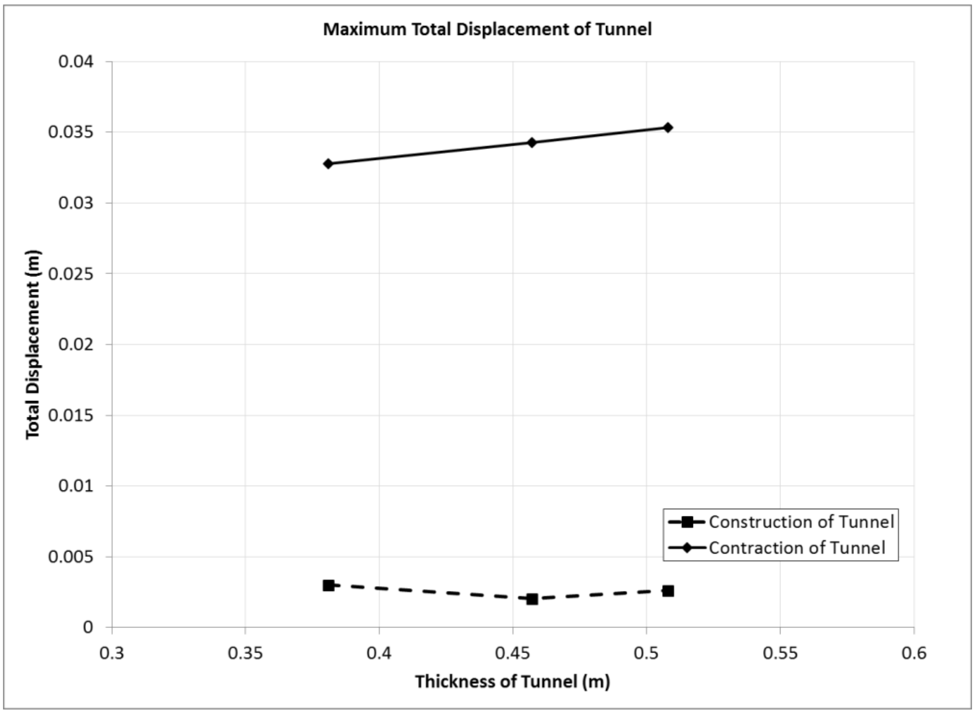

Figure 5.9 Maximum Total Displacement of Tunnel

In **Figure 5.10** and **Figure 5.11**, the maximum bending moment and maximum shear force acting on the tunnel lining are plotted. The plot clearly shows that both the increased displacement of tunnel causes increase in bending moment and shear force to increase with larger thickness of the tunnel lining.

The maximum bending moment and maximum shear force can also be plotted for different tunnel lining thicknesses (**Figure 5.12**). This figure clearly shows a specific linear rising trend (with minor scattering at the starting of loading stage due to imbalanced forces in the initial calculation stage) of shear force with bending moment for different thickness of tunnel lining.

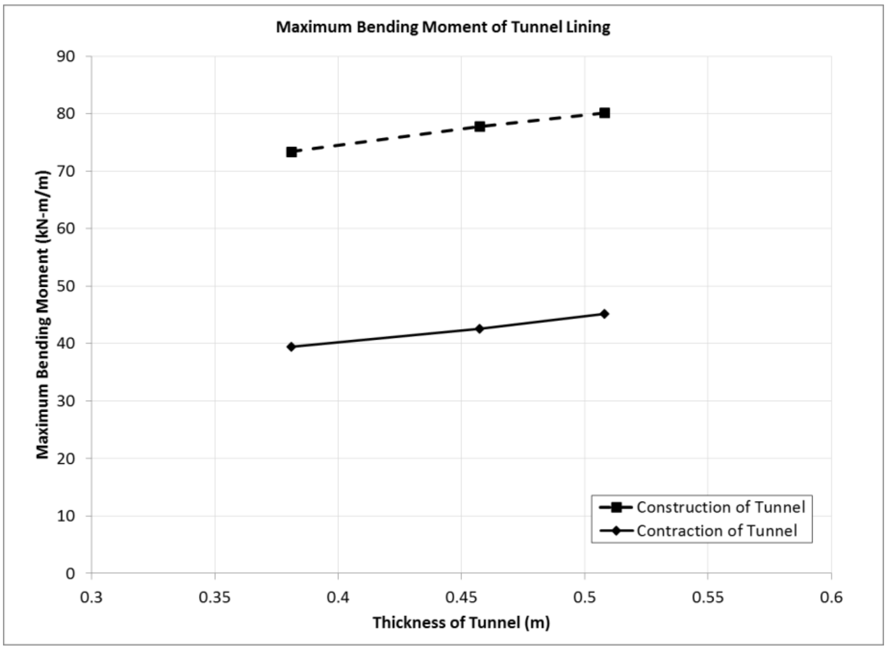

Figure 5.10 Maximum Bending Moment of Tunnel Lining

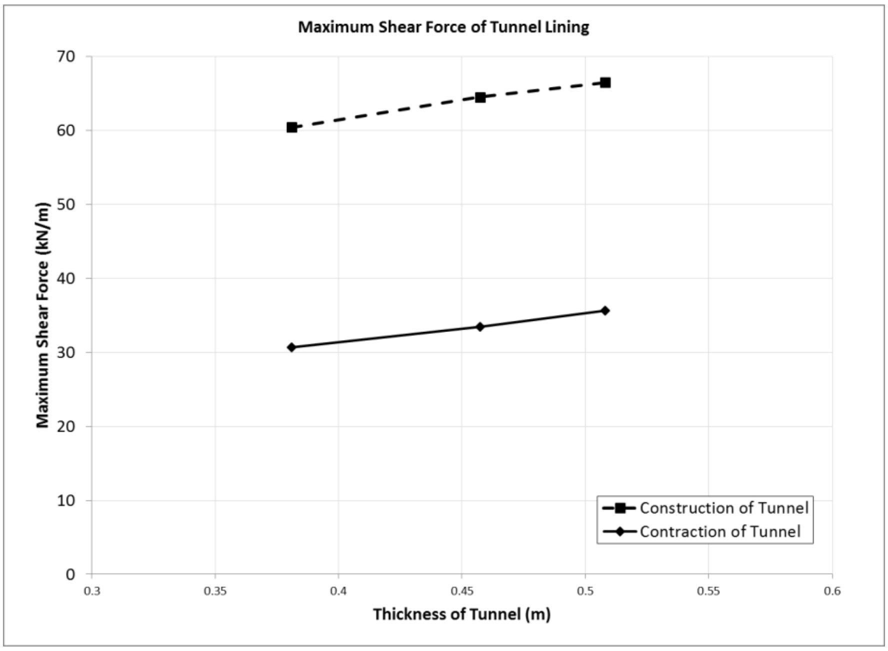

Figure 5.11 Maximum Shear Force of Tunnel Lining

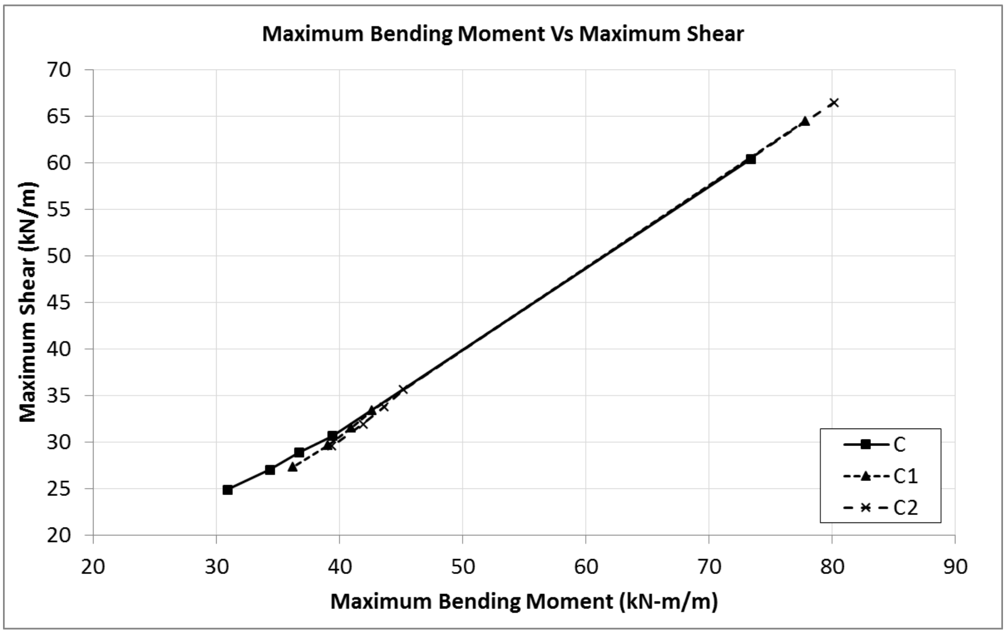

Figure 5.12 Maximum Bending Moment Vs Shear Force of Tunnel Lining for different tunnel thickness

5.3 Effect of Horizontal Position of Tunnel

In this article, the maximum total displacement, maximum bending moment and maximum shear force at the base of structure-B and road are analyzed for different horizontal positions of the tunnel. Besides the maximum values, four different points, two at the base of the road (one at middle, another at corner) and two at the base of the structure-B (one at middle, another at corner), are also taken for analysis. Locations of these points are shown in **Figure 5.13**. Different horizontal positions of the tunnel are named as Case-03 (R1), Case-04 (R2), Case-05 (L1) and Case-06 (L2), details of which are tabulated in **Table 5.1**.

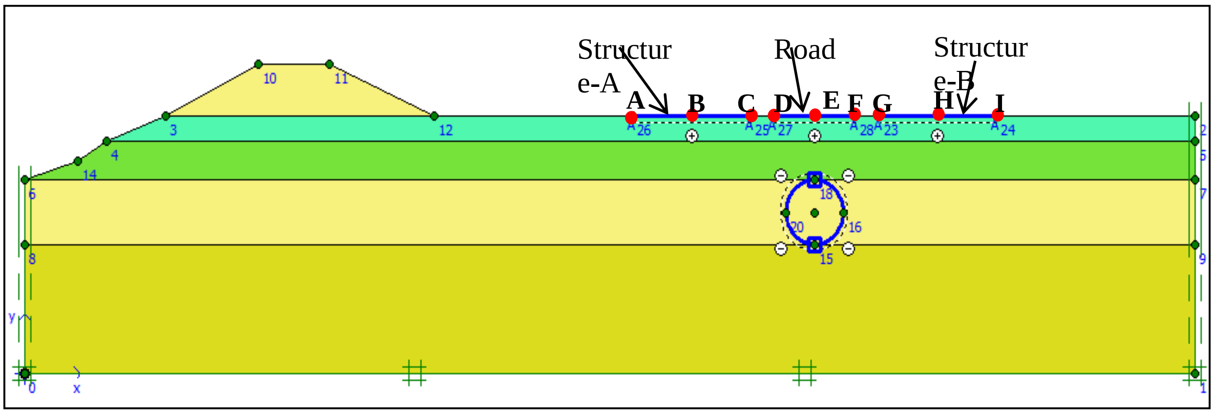

Figure 5.13 Different Points for Analysis

The maximum total displacement of the structure-B and road against horizontal position of the tunnel are plotted in **Figure 5.14** and **Figure 5.15** respectively. Results show that as the tunnel is shifted towards the center of structure-B, the maximum total displacement (downward) at the base of the structure decreases in the construction phase of the tunnel as during construction of the tunnel by TBM method, uplift forces are generated which tend to decrease near the center of the structure-B due to increase of downward loading (UDL). Whereas, in the contraction phase of the tunnel, the maximum total displacement at the base of the structure-B increases as the tunnel is shifted towards the center of structure-B. Besides, at a zone of 5 to 10 m near Structure-B (R1), the rate of increase of displacement is observed to be significantly higher (**Figure 5.14**).

The maximum total displacement at the base of the road, however, follows a different trend (**Figure 5.15**). It tends to decrease near the center of the road in the construction phase of the tunnel due to generation of uplifting forces by TBM and there is a small zone near the center of the road near which the displacement is maximum in the contraction phase of the tunnel.

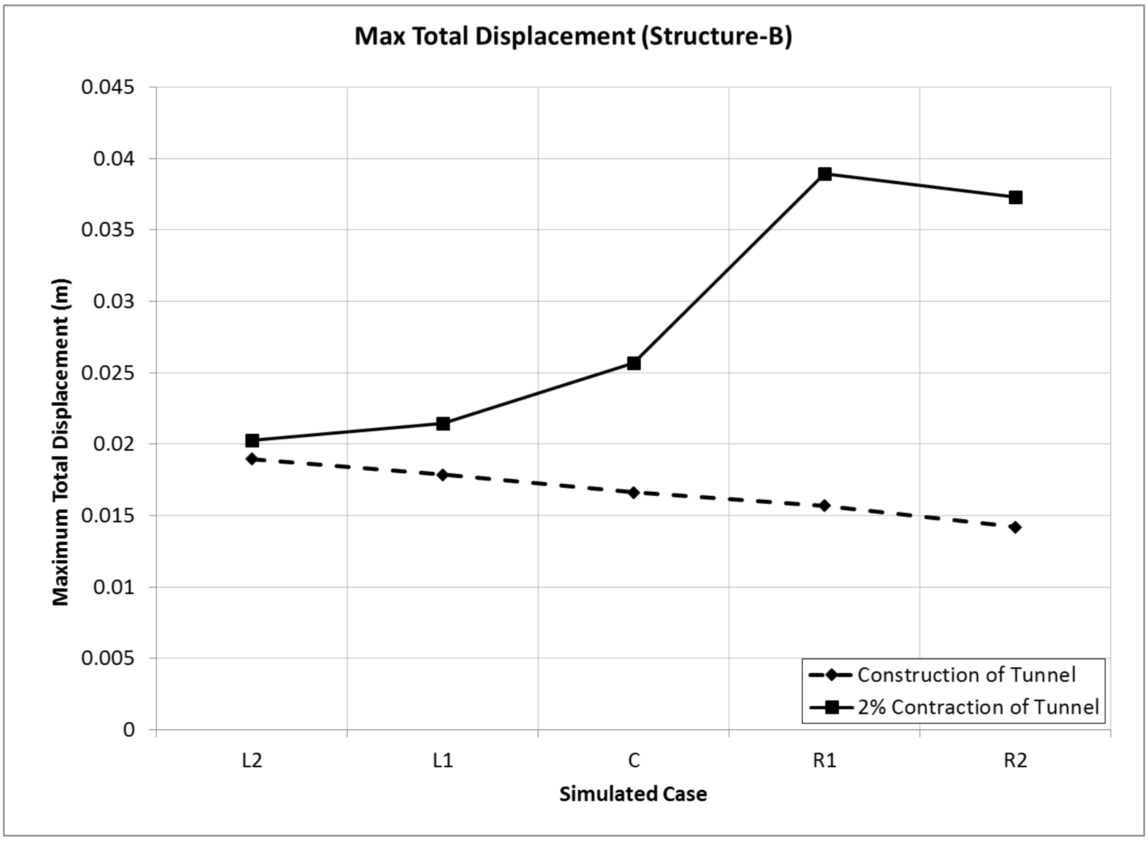

Figure 5.14 Maximum Total Displacement at the Base of Structure-B

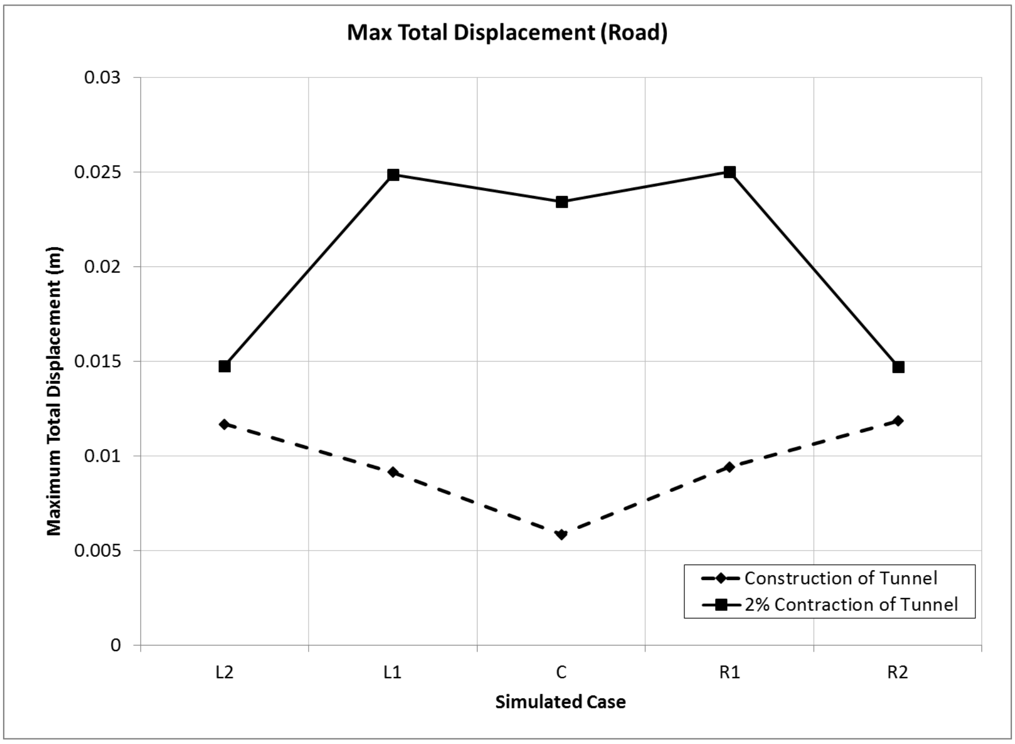

Figure 5.15 Maximum Total Displacement at the Base of Road

The differential settlement between two corner points of Structure-B is also plotted for different horizontal position of tunnel (**Figure 5.16**). It is noted that for R1, when the tunnel is constructed just between the road and Structure-B, the differential settlement of Structure-B is maximum. For L1, it is not same as R1, because tunnel was constructed near to Structure-B at position R1.

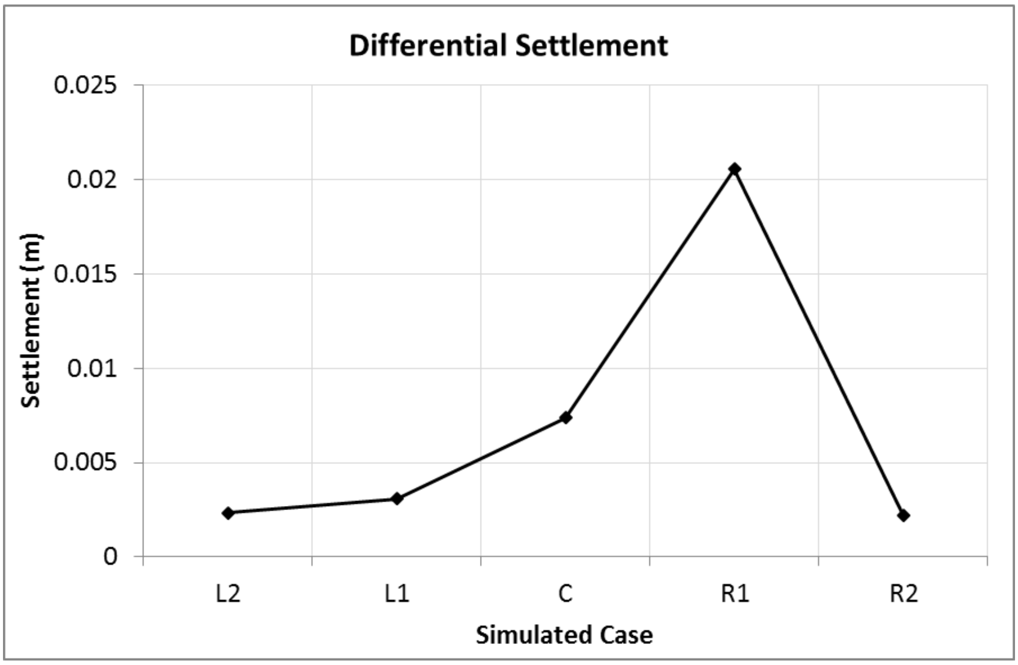

Figure 5.16 Differential Settlement at the Base of Structure-B due to change in horizontal position of tunnel

As mentioned earlier, in addition to the maximum values of displacement, bending moment and shear forces, four additional points- point E, F, G, H were also taken for analysis. These points are shown in **Figure 5.13**.

The total displacement at corner of the structure-B, denoted by Point-G, is plotted in **Figure 5.17**. Results show that as the center of the tunnel is constructed near to Point-G, the total displacement increases in the contraction of tunnel phase where downward vertical displacement occurs due to shrinkage of tunnel lining. Besides, at a distance of 1.0 meter within point-G (R1), the increase in displacement is observed to be much higher.

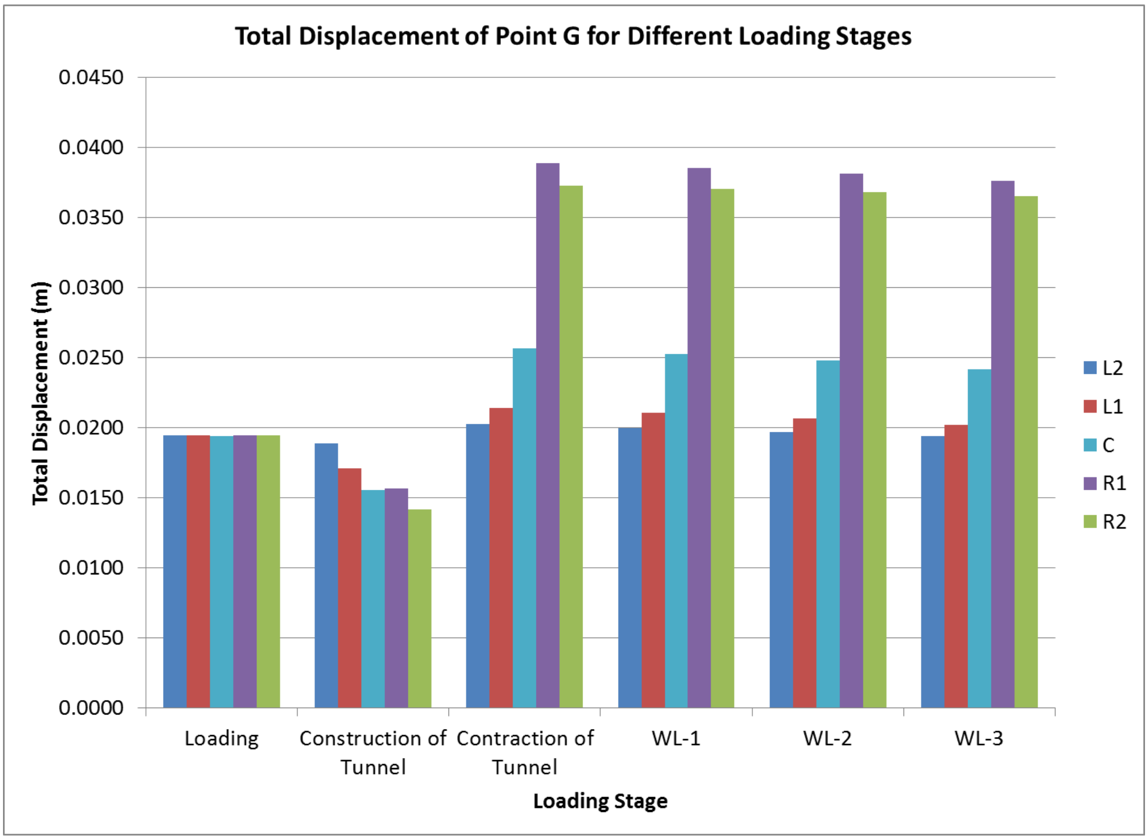

Figure 5.17 Total Displacement at Corner of Structure-B, Point-G

It is also observed that the total displacement of point-G decreases when tunnel is shifted towards point-G in the construction of tunnel phase due to generation of uplift forces by TBM. Similarly, total displacement at center of the structure-B, Point-H, is plotted in **Figure 5.18**. Results show that the total displacement of Point-H decreases in the construction phase and increases in the contraction phase of the tunnel when the tunnel is constructed near the center of the structure-B (R1 and R2).

The total displacement of at center of the road, Point-E, was also plotted along with distance of center of tunnel (**Figure 5.19**). Results showed decrease in total displacement of Point-E in the construction phase of the tunnel where uplift forces are being generated by TBM, which reduces the downward forces near the center of the road whereas opposite trend is observed in the contraction phase due to coincidence of center of road with center of tunnel in the same vertical line.

Similar trend was also observed for Point-F, at corner of the road (**Figure 5.20**).

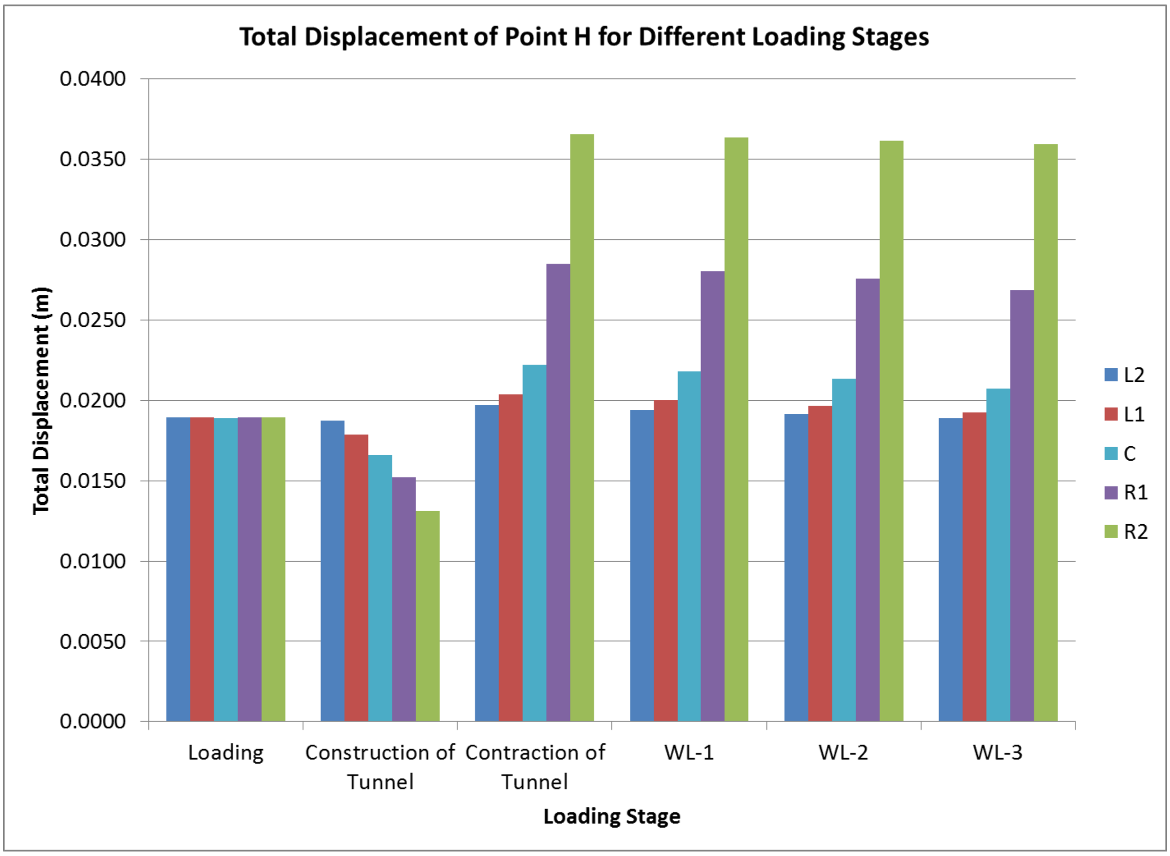

Figure 5.18 Total Displacement at Center of Structure-B, Point-H

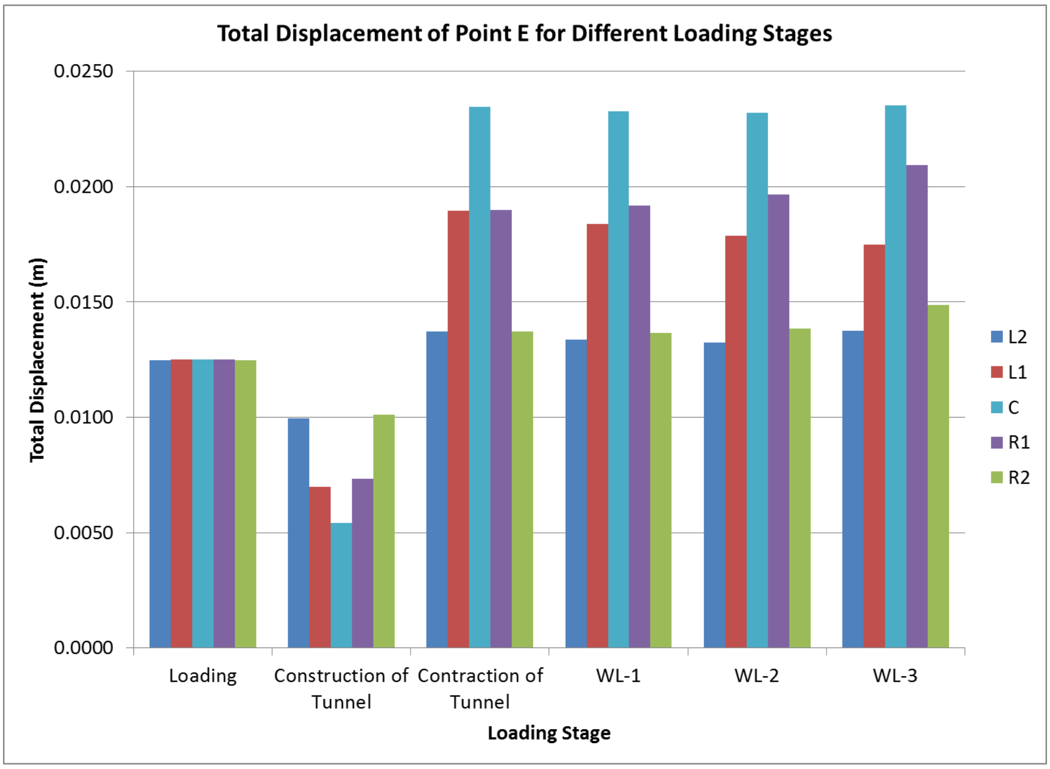

Figure 5.19 Total Displacement at Center of Road, Point-E

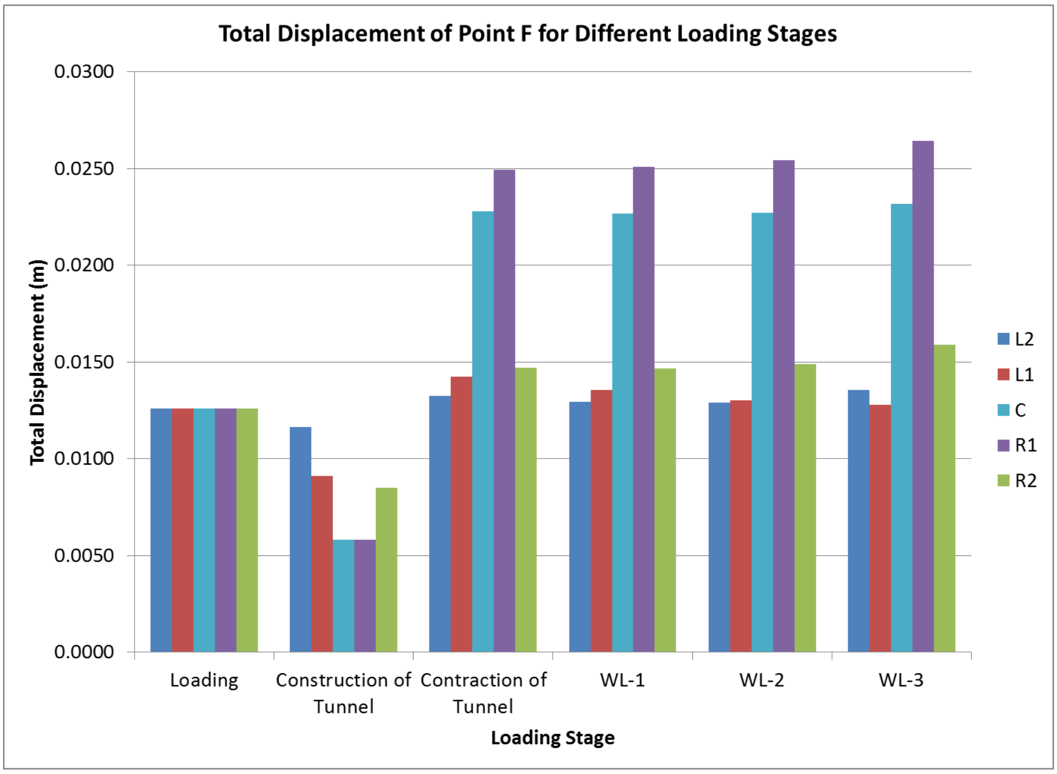

Figure 5.20 Total Displacement at Corner of Road, Point-F

The effect of change in horizontal position of tunnel has also its effects on the vertical displacement, bending moment and shear force of the tunnel itself. **Figure 5.21**, **Figure 5.22** and **Figure 5.23** represent the maximum vertical displacement, bending moment and shear force generated on the tunnel due to change in its horizontal position. Due to increase in over burden pressure above the tunnel, result showed increase in vertical displacement, bending moment and shear force for Cases-R1, R2, L1 and L2. The rate of increase is higher nearer to the Structure-B (R2).

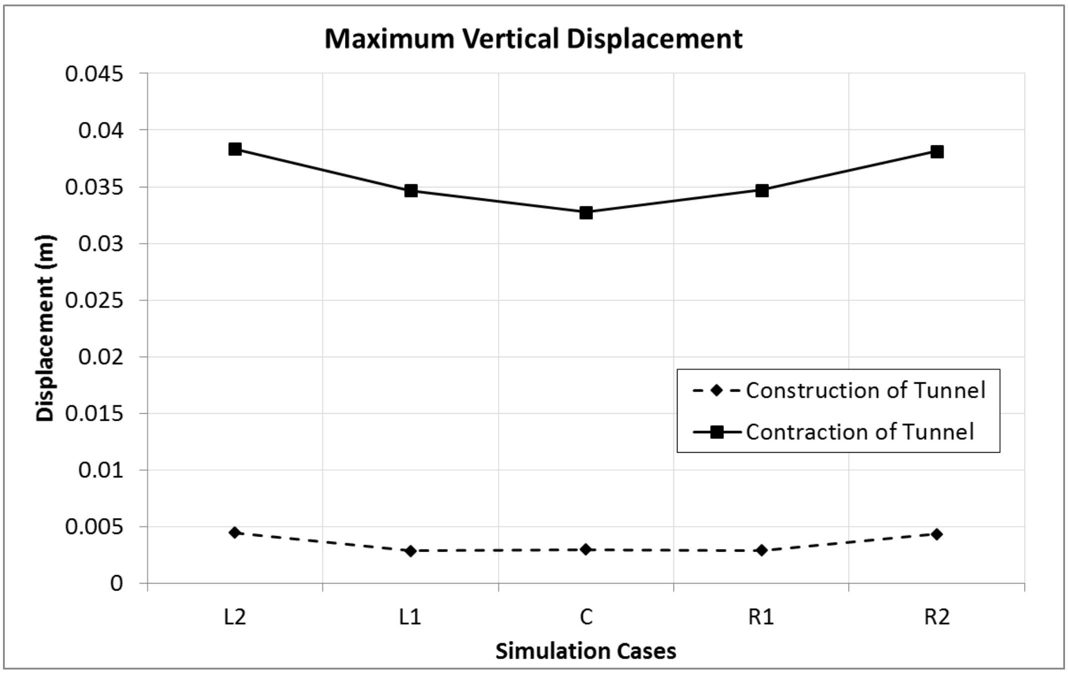

Figure 5.21 Maximum Vertical Displacement of Tunnel due to change in horizontal position of Tunnel

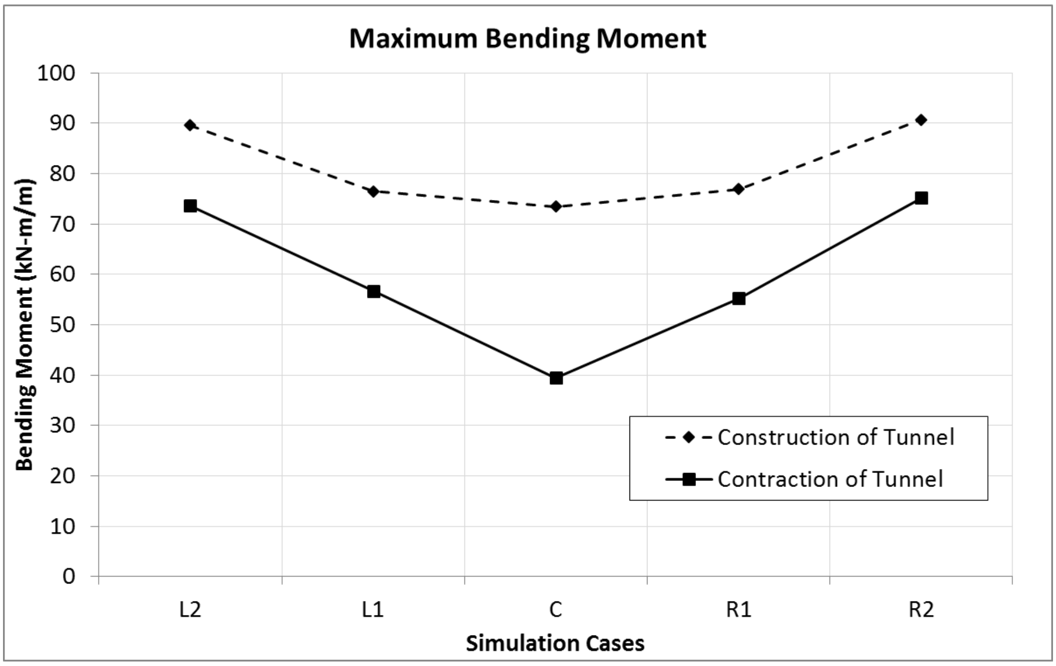

Figure 5.22 Maximum Bending Moment of Tunnel due to change in horizontal position of Tunnel

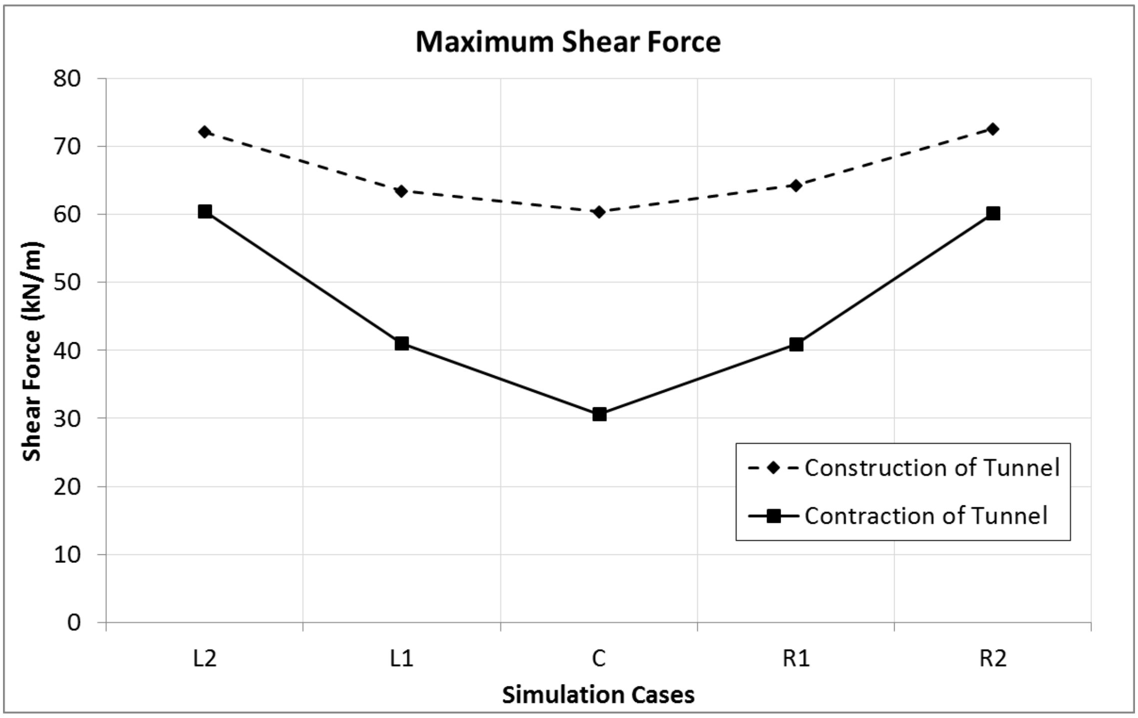

Figure 5.23 Maximum Shear Force of Tunnel due to change in horizontal position of Tunnel

As previous, the maximum shear force is plotted against maximum bending moment in **Figure 5.24** which shows significant scattering with no fixed trend.

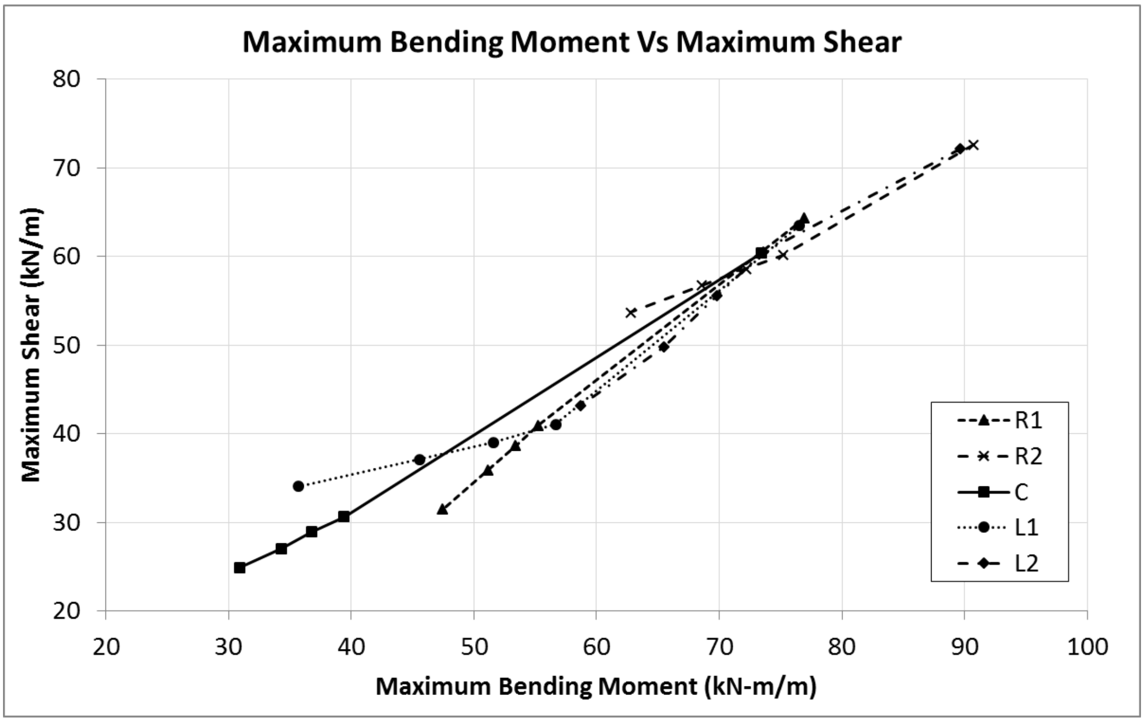

Figure 5.24 Maximum Bending Moment Vs Shear Force of Tunnel Lining for different horizontal position of tunnel

5.4 Effect of Vertical Position of Tunnel

In addition to changing horizontal position of tunnel center, vertical position of it was also changed. In this article results of three cases namely C, U1 and D1 are discussed where center of the tunnel was 1 meter above and below respectively for U1 and D1 than the center of tunnel in the case C. **Figure 5.25** shows the change in maximum displacement of structure-B for the three cases. It is observed from the figure that in the contraction phase of the tunnel, maximum displacement of structure-B increases due to increasing overburden pressure of soil when the tunnel constructed downwards. In the construction phase the displacement remains more or less constant because of generation of less amount of uplift forces by TBM as compared to increase in overburden pressure by soil downwards.

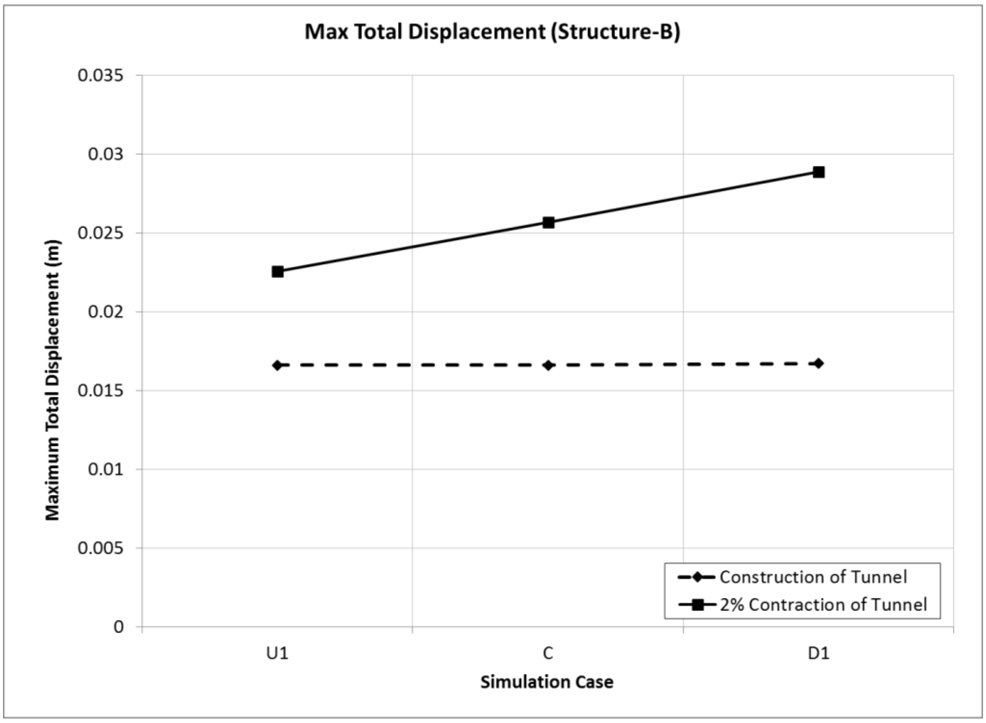

Figure 5.25 Maximum Total Displacement of Structure-B due to change in vertical position of center of Tunnel

Similarly, maximum total displacement at the base of the road is plotted in **Figure 5.26**.

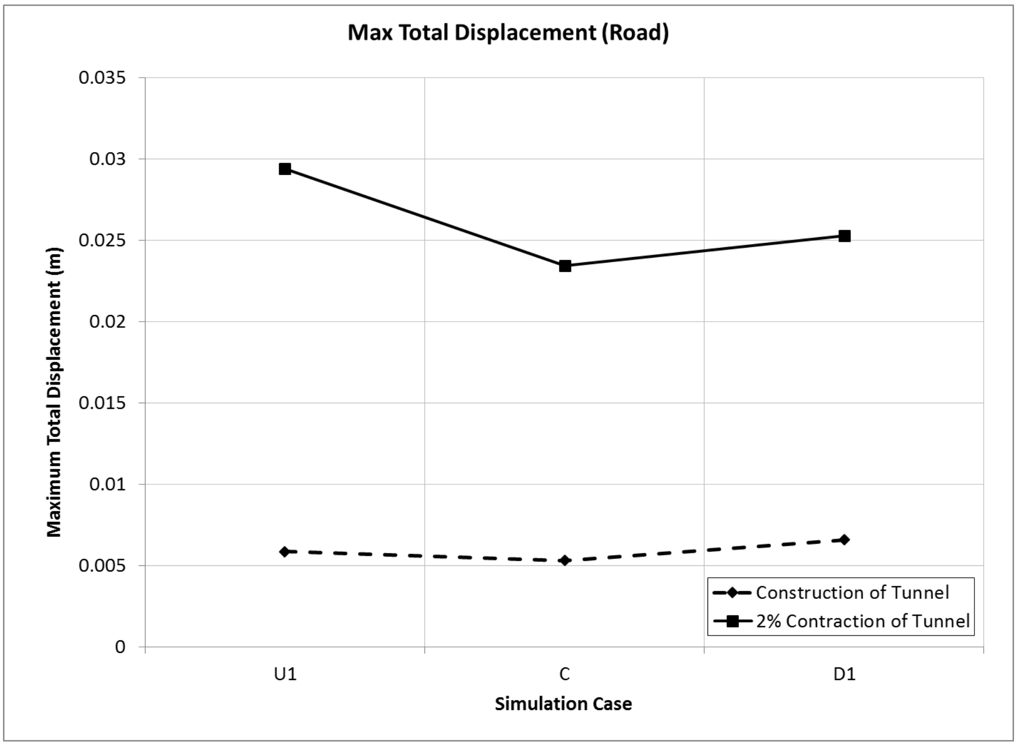

Figure 5.26 Maximum Total Displacement of Road due to change in vertical position of center of Tunnel

The differential settlement of two corners at the base of Structure-B is plotted in **Figure 5.27** which shows significant increase for the three cases mentioned in **Table 5.1**.

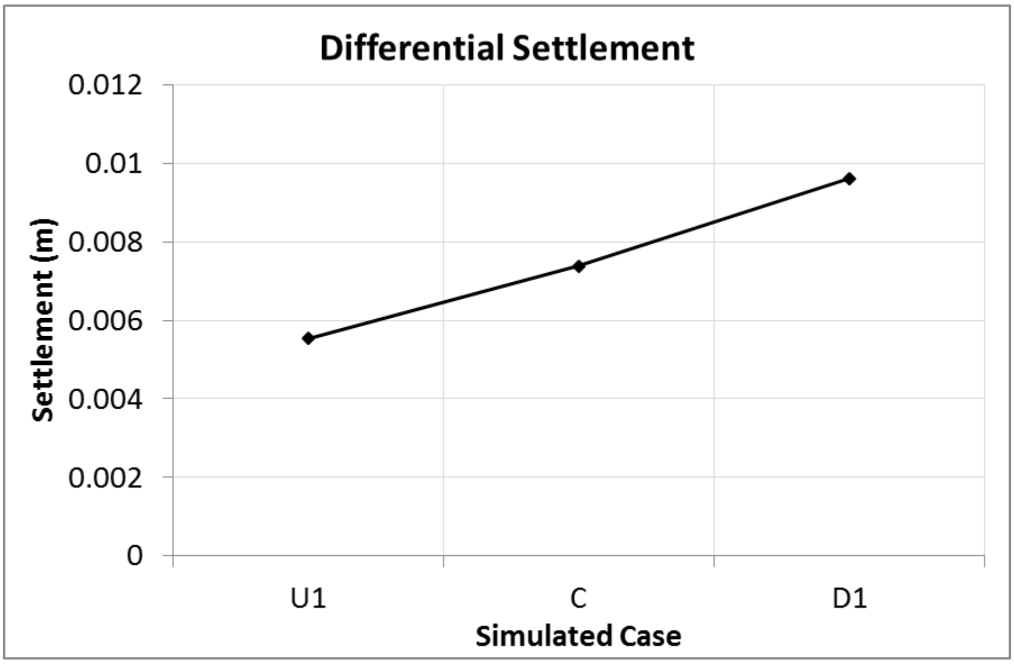

Figure 5.27 Differential Settlement at the Base of Structure-B due to change in vertical position of tunnel

As mentioned earlier, Points-G, H at the base of structure-B and Points-E, F at the base of the road are also analyzed to study the effect of change in vertical position of center of tunnel.

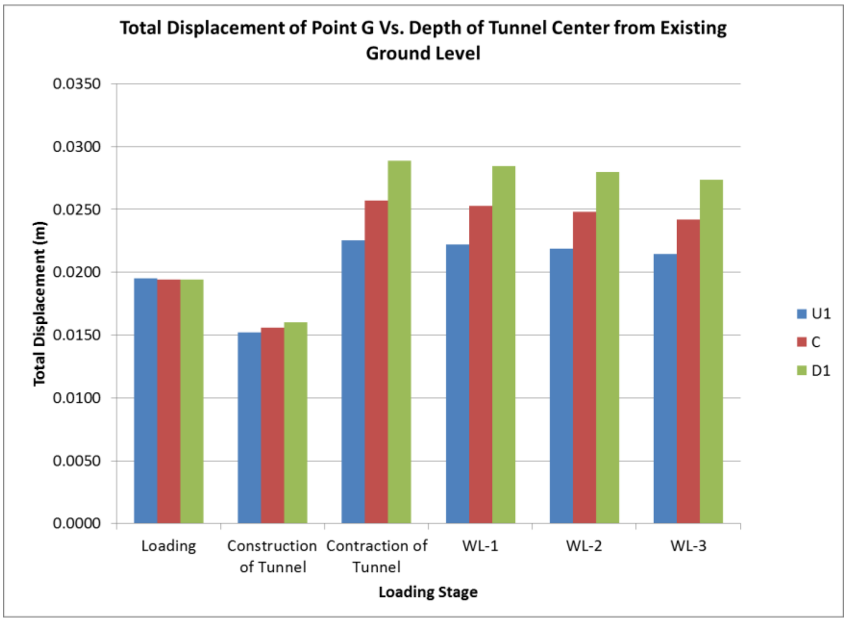

Figure 5.28 Total Displacement of Point-G at the base of Structure-B due to change in vertical position of center of Tunnel

It is evident from **Figure 5.28** that in all the cases, the total displacement at Point-G increases with increase in depth of tunnel due to increase in overburden pressure of soil. Same pattern is also observed for Point-H, at center of structure-B with less displacement as expected (**Figure 5.29**).

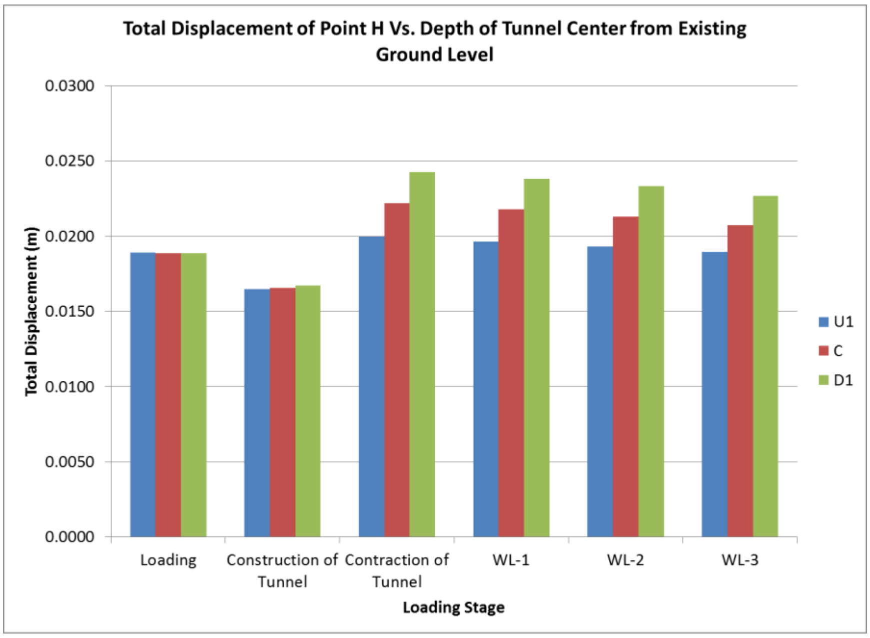

Figure 5.29 Total Displacement of Point-H at the base of Structure-B due to change in vertical position of center of Tunnel

Similarly, **Figure 5.30** and **Figure 5.31** represent total displacement of Point-E and Point-F at the center and corner of the base of road respectively. For both points it is noted that when the center of the tunnel is 6.5m below the ground level (U1), the displacement is maximum in the final contraction stage of the tunnel. When the depth is increased to 8.5m below ground level (D1), displacement of both of the points increases due to considerable increase of overburden pressure of soil above the tunnel.

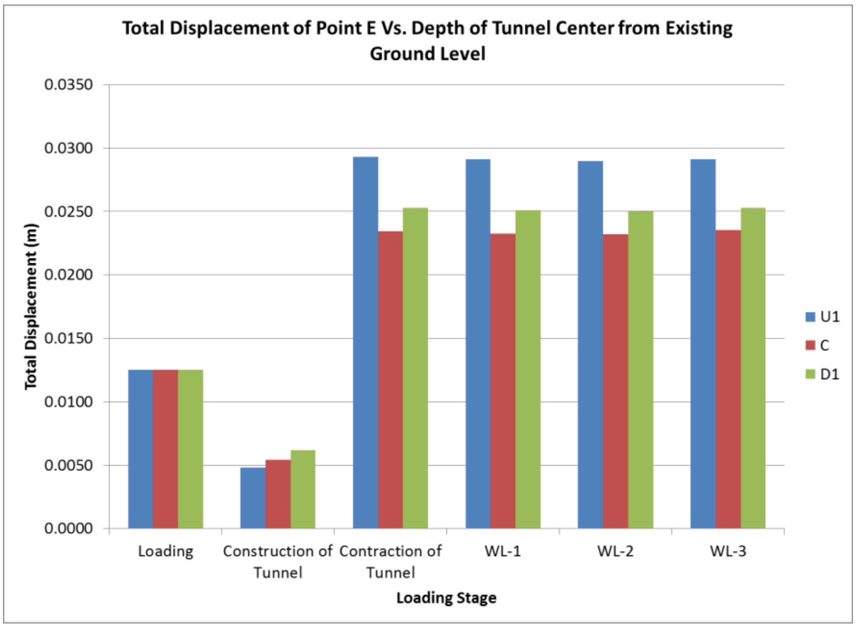

Figure 5.30 Total Displacement of Point-E at the base of Road due to change in vertical position of center of Tunnel

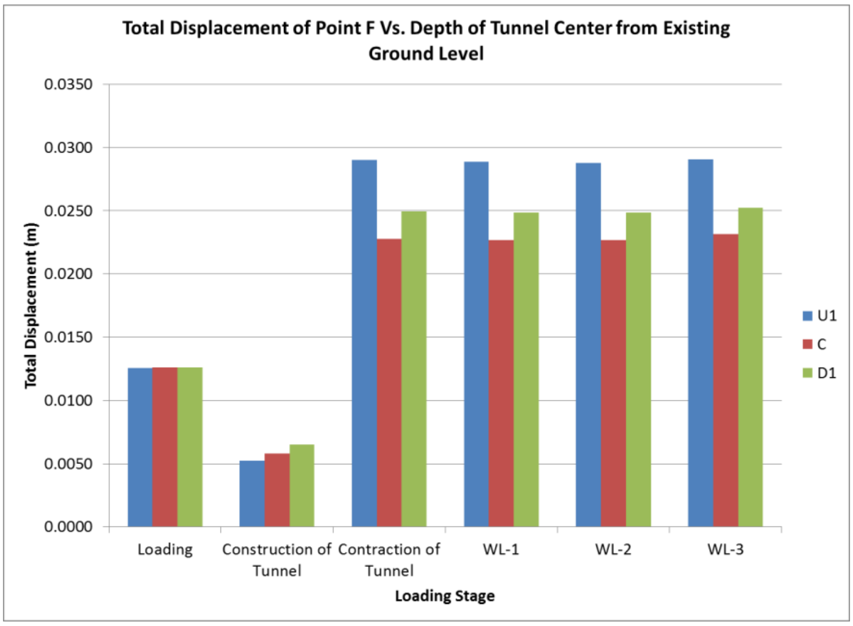

Figure 5.31 Total Displacement of Point-F at the base of Road due to change in vertical position of center of Tunnel

The maximum displacement, bending moment and shear force of the tunnel are also plotted in **Figure 5.32**, **Figure 5.33** and **Figure 5.34** below which shows increase in bending moment and shear force at increase in depth of tunnel.

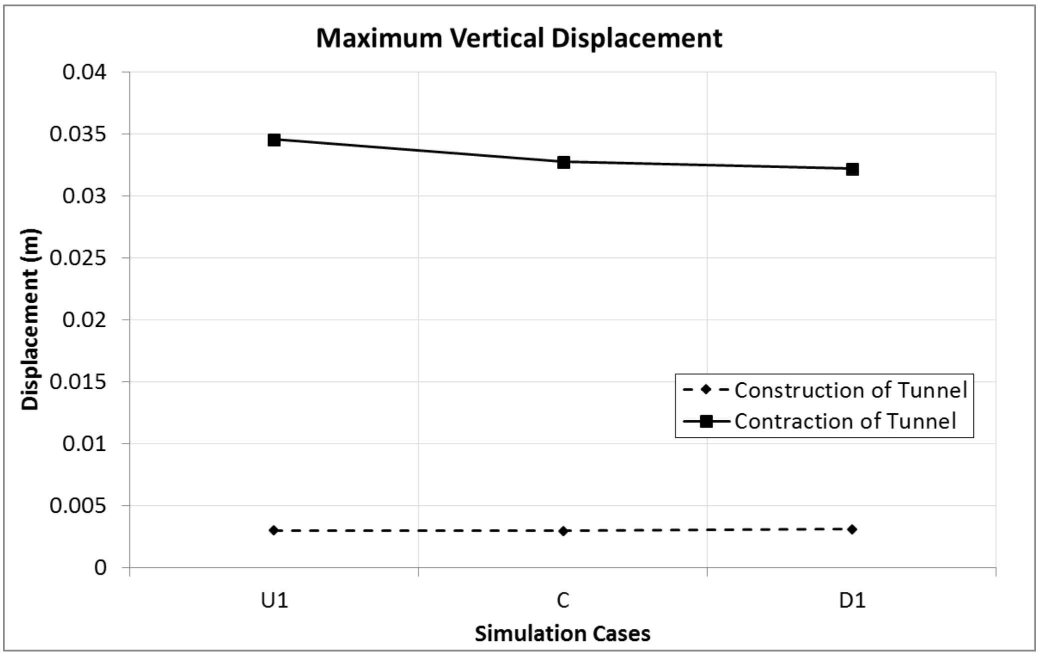

Figure 5.32 Maximum Vertical Displacement of Tunnel due to change in vertical position of Tunnel

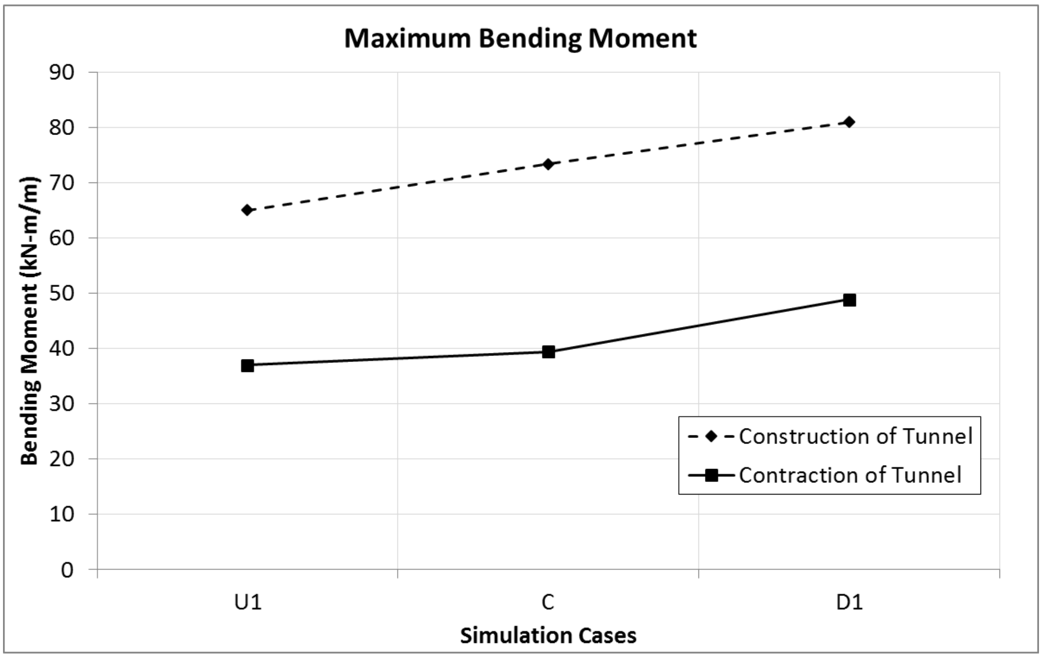

Figure 5.33 Maximum Bending Moment of Tunnel due to change in vertical position of Tunnel

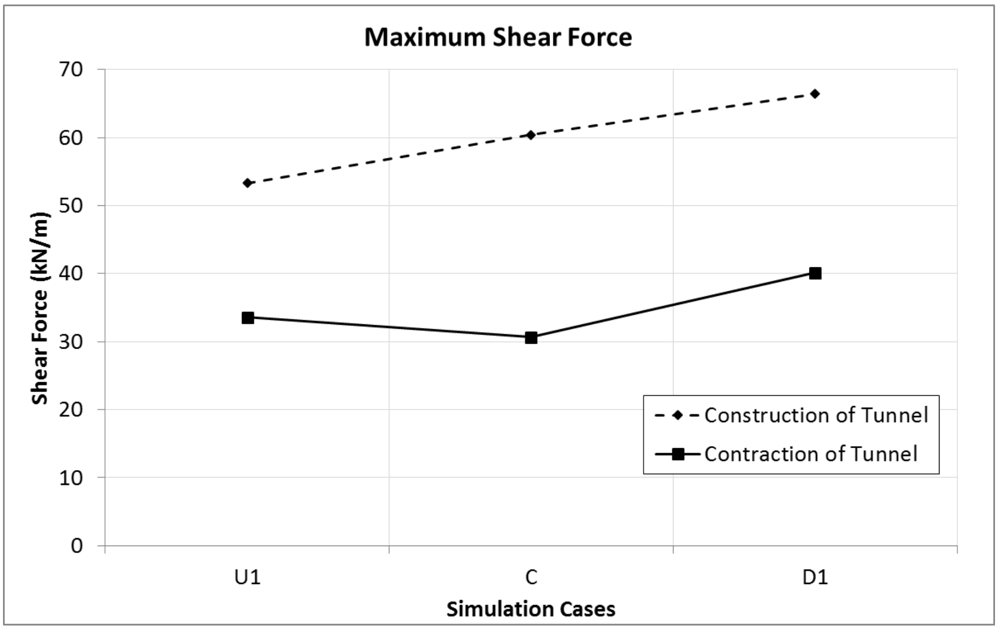

Figure 5.34 Maximum Shear Force of Tunnel due to change in vertical position of Tunnel

As previous, the bending moment and shear force can be plotted in a generalized figure as shown in **Figure 5.35**.

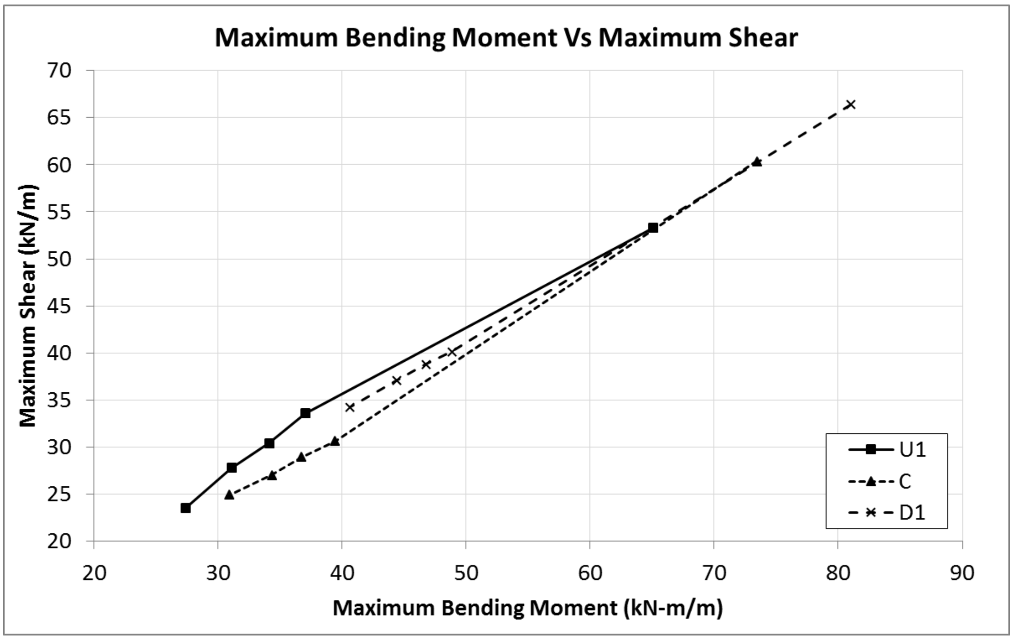

Figure 5.35 Maximum Bending Moment Vs Shear Force of Tunnel Lining for different vertical position of tunnel

5.5 Effect of Change in Water Level

In all the previous articles, the water level on both sides of the embankment was kept same as the ground water level present in the country side. As mentioned earlier in **Table 3.2**, three water level conditions were simulated to study the effect of generation of water level head difference on points-E, F, G, H.

Figure 5.36 and **Figure 5.37** represent the increment of uplifting force of Point-E and F respectively at the base of the road due to change in water level for various cases. It is observed that highest increment of more than 10% is observed for Case-03(R1) where the center of the tunnel was +4.5m away from point-E, at the center of the road. It is also noted that for point-E, the increment is significantly higher when the water level head difference is increased from 4.5 to 6.5m for WL-3 as compared to 2.5m to 4.5m for WL-2 (both R1 and R2).

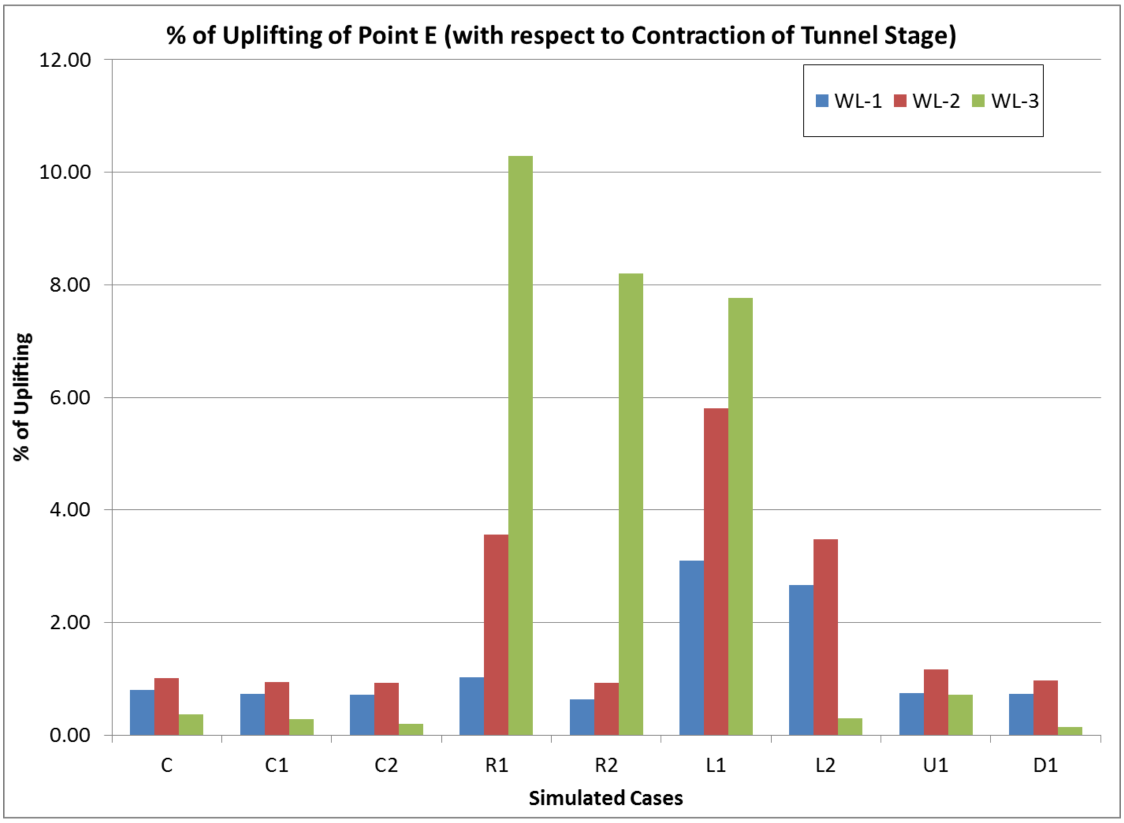

Figure 5.36 Increment of Uplifting Force of Point-E at the base of Road due to change in Water Level for various cases

Besides changing the horizontal position of tunnel, thickness of tunnel has little effect for in generation of uplifting forces (C, C1, C2). As increased tunnel thickness increases the self weight of tunnel, resulting less uplift pressure. Furthermore, when the tunnel is moved towards downward direction, uplifting force at point-E decreases as water head difference decreases in that particular direction (U1, C, D1).

Obviously for point-F, at the corner of the road, the increment is less as the center of the tunnel is +7.0m away. Besides, as point-F is closer to the tunnel, shrinkage of tunnel lining increases downward displacement of point-F, reducing the uplifting force.

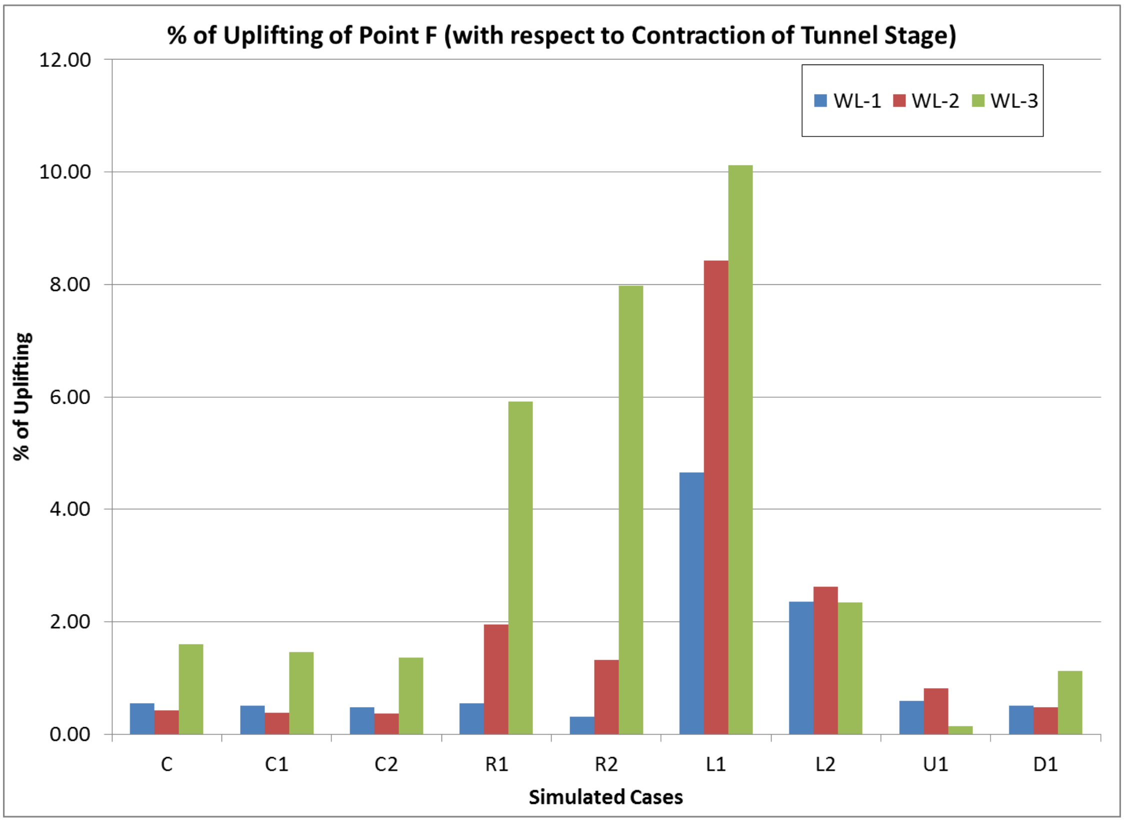

Figure 5.37 Increment of Uplifting Force of Point-F at the base of Road due to change in Water Level for various cases

The increment of displacement of point-G, at the corner of the base of the building, is presented in **Figure 5.38**. It is observed that due to high overburden pressure of the building, the displacement increment is always below 6% for all the cases. Negligible change in observed for changing of thickness of tunnel lining (C, C1, C2). Besides, the increment for all three water level conditions decrease when the tunnel is shifted towards center of the building (near Point-G), as total load of the building acts at its center. In all cases, WL-3 condition generates highest uplifting forces due to largest head difference on both sides of the embankment.

Similarly, the increment of displacement of point-F, at the corner of the building is also plotted in **Figure 5.39** which shows similar type of behavior like point-E, but higher in magnitude as lesser load acting at the corner of the building than that of its center.

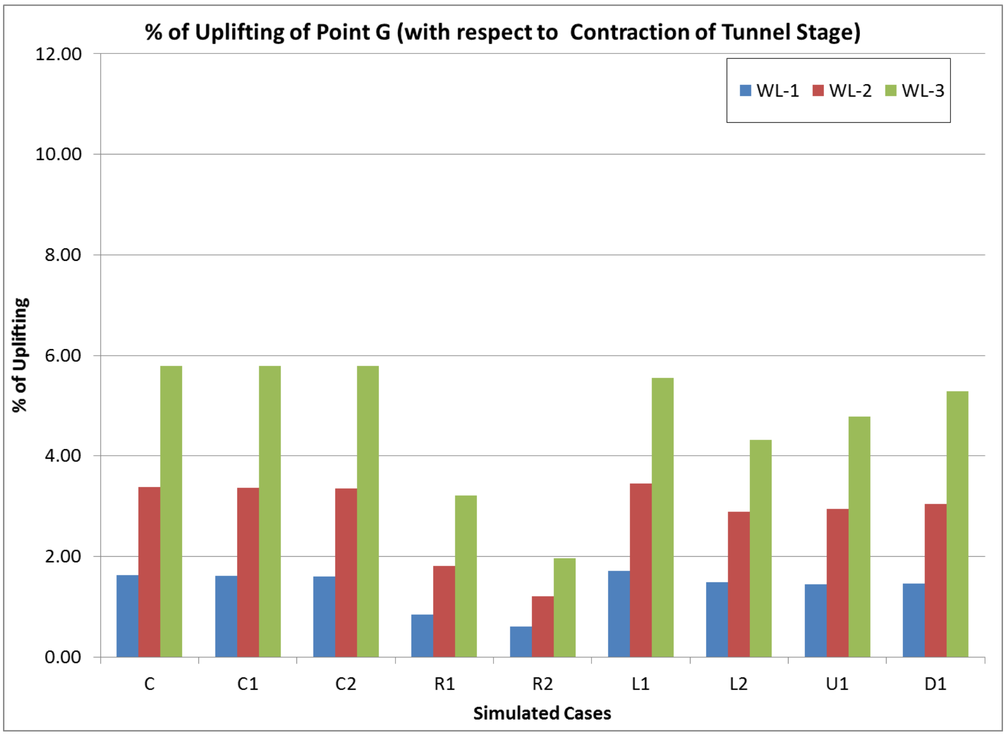

Figure 5.38 Increment of Uplifting Force of Point-G at the base of Building due to change in Water Level for various cases

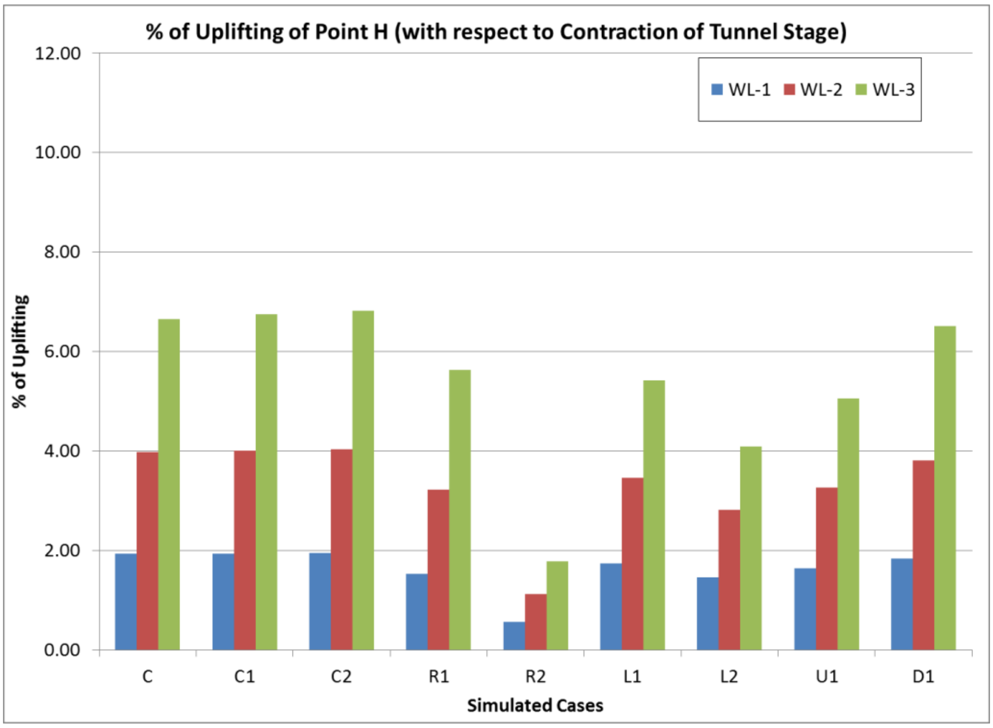

Figure 5.39 Increment of Uplifting Force of Point-H at the base of Building due to change in Water Level for various cases

The change in water level has also its effects on the tunnel. The variation of maximum vertical displacement of the tunnel due to change in water level are plotted in **Figure 5.40**, **Figure 5.41** and **Figure 5.42** below.

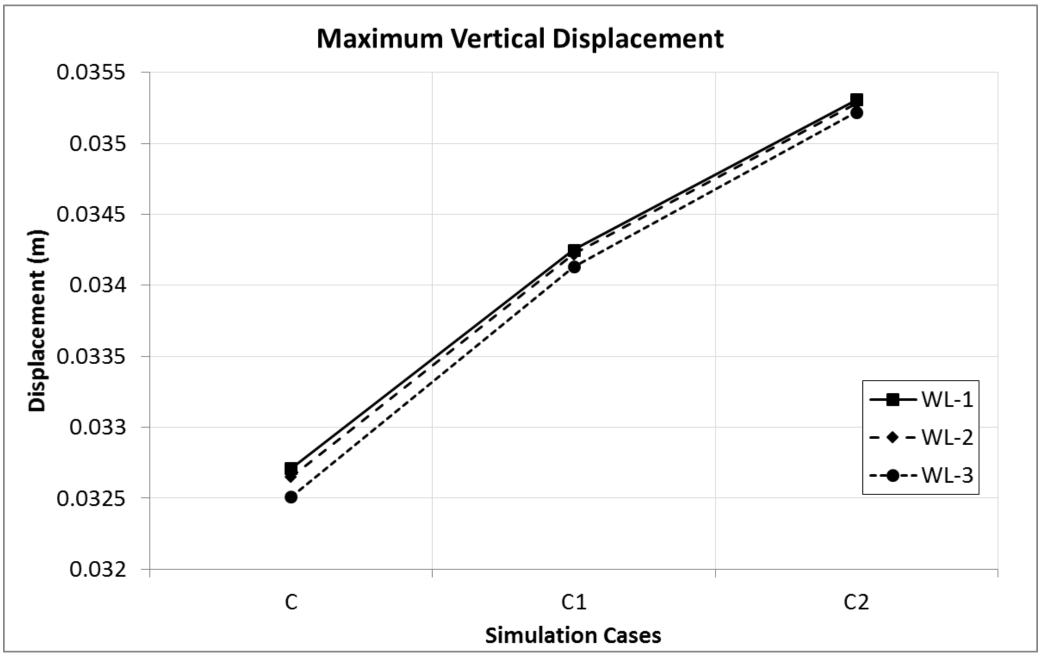

Figure 5.40 Maximum Vertical Displacement of Tunnel due to change in water level for different tunnel thickness

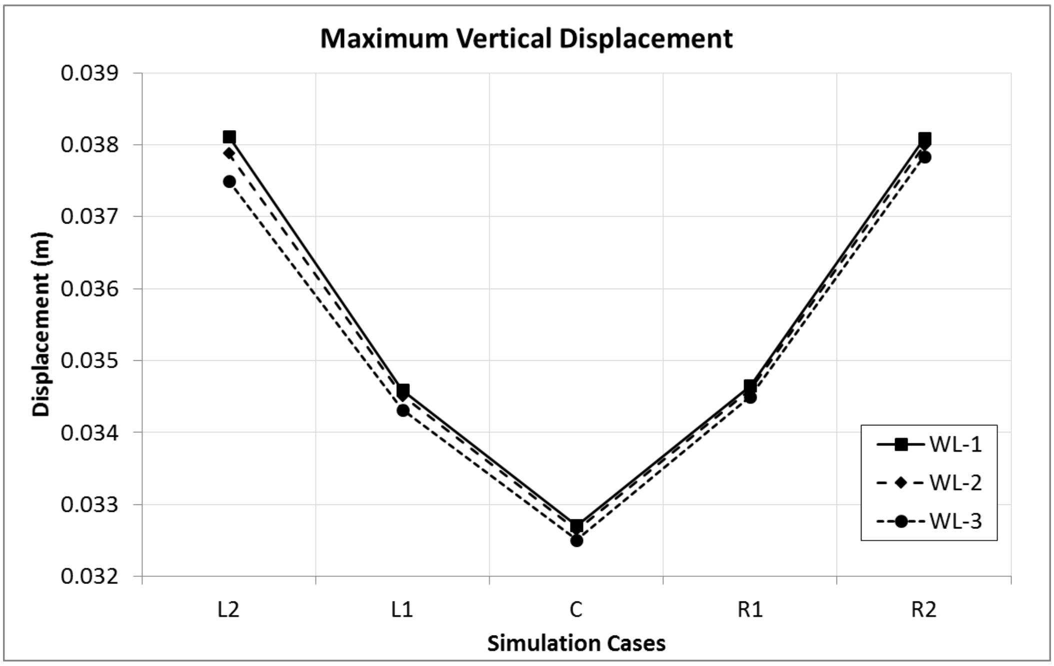

Figure 5.41 Maximum Vertical Displacement of Tunnel due to change in water level for different horizontal position of tunnel

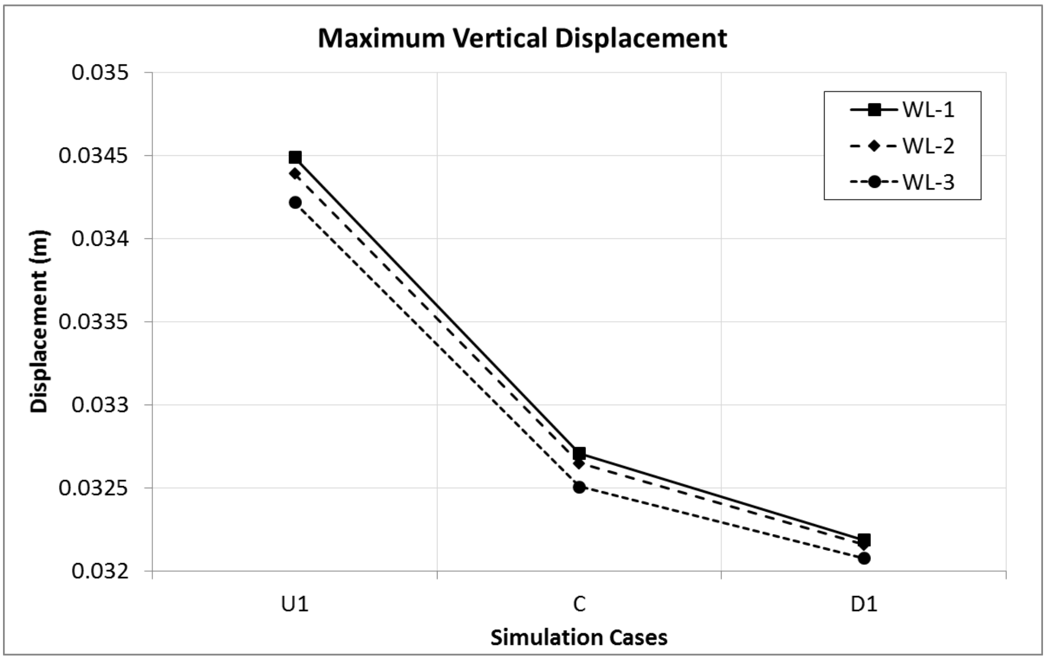

Figure 5.42 Maximum Vertical Displacement of Tunnel due to change in water level for different vertical position of tunnel

It is clear from **Figure 5.40** that increase in thickness increases self weight of the tunnel which results in increase in vertical displacement of tunnel. Besides constructing the tunnel near the heavily loaded structures (Structure-A and Structure-B in either ways) increases the vertical displacement of the tunnel which in reflected in **Figure 5.41**. Moreover, increasing depth of tunnel causes increase in overburden pressure above the tunnel which reduces the effects of uplifting pressure created by increasing the water head difference (**Figure 5.42**). In all the cases above, it is noted that WL-3 generates highest uplifting force for which displacement is less than WL-1 and WL-2 condition.

5.6 Selection of Best Suitable Tunnel Lining & Position of Tunnel

In this article, the main concern has been provided in selecting the best suitable tunnel lining in terms of thickness of the lining. In selecting the most suitable lining thickness, the structural design guidelines of FHWA-NHI-09-010, Road Tunnel Manual, described in **Article 2.6** has been followed. The required thickness of tunnel are calculated using the equations presented in **Article 2.6**. which are tabulated in **Table 5.2**.

Table 5.2 Selection of Tunnel Thickness

Simulation Case	Notation of Simulated Cases	Required Thickness (m)		Thickness Provided (m)	Remarks
		Compression	*Tension*		
Case-00	C	0.094	0.247	0.380	Moment
		0.010	-		Compressive Strength
		0.178	-		Shear Strength
Case-01	C1	0.097	0.257	0.460	Moment
		0.010	-		Compressive Strength
		0.194	-		Shear Strength
Case-02	C2	0.100	0.265	0.510	Moment
		0.010	-		Compressive Strength
		0.208	-		Shear Strength

It is observed from **Table 5.2** that the maximum required thickness of the tunnel lining is 0.247m, 0.257m and 0.265m for Case-00 (C), Case-01 (C1) and Case-02 (C2) respectively. For each of the cases the provided thickness is greater than the required.

Observing the results described on **Article 5.2**, it is also found that least displacement of 0.026m is generated on the nearby structures for a tunnel lining thickness of 0.380m which is also found to be adequate in resisting developed tension and compression in the lining (**Table 5.2**).

Considering the horizontal position of the tunnel, it is found from the results described in **Article 5.3** and **Article 5.4** that two different positions of the tunnel, one below middle of the road, another below center of Structure-B, both below 6.5m from ground level, are found most suitable for tunnel construction. Any position in between the road and the Structure-B, creates asymmetry which increases the displacement (>0.025m) in nearby structures.

The two finally selected positions of tunnel, one just below center of road (Case-00, C) and another just below center of structure-B (Case-04, R2), are again analyzed for a 0.5m thick tunnel lining, having a diameter of 6.0m. The new simulated cases are named as C-mod and R2-mod respectively. The response of tunnel is presented in **Figure 5.43** to **Figure 5.45**. Due to increase in self weight of the tunnel. results show minor changes (small increase in the same ratio of increase in thickness and diameter) in maximum vertical displacement, maximum bending moment and maximum shear force of tunnel lining.

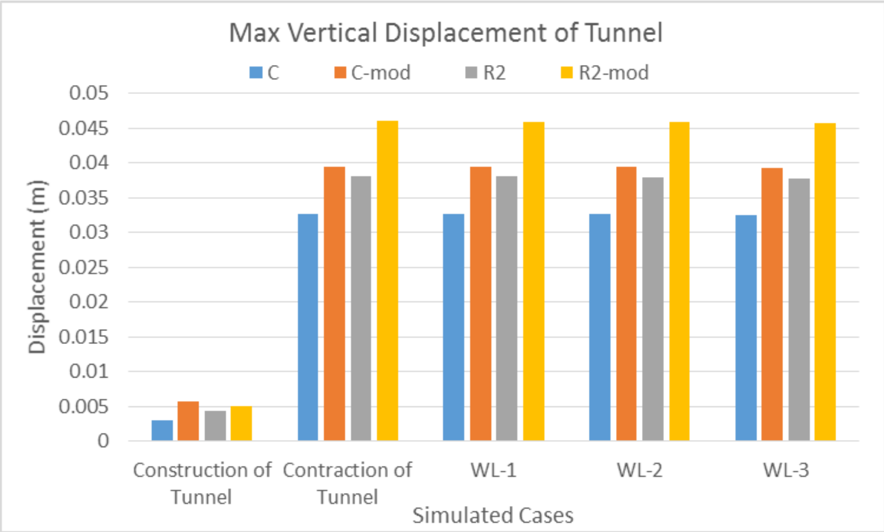

Figure 5.43 Maximum Vertical Displacement of Tunnel for cases C, C-mod, R2 and R2-mod

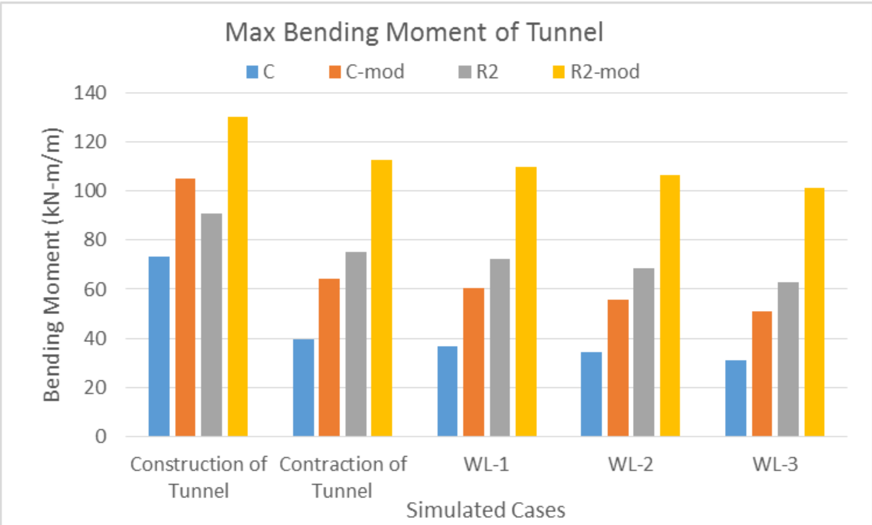

Figure 5.44 Maximum Bending Moment of Tunnel for cases C, C-mod, R2 and R2-mod

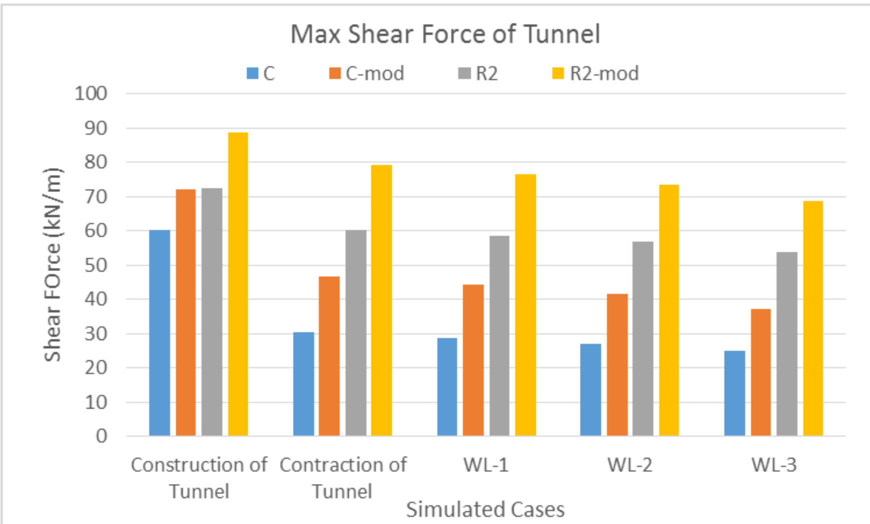

Figure 5.45 Maximum Shear Force of Tunnel for cases C, C-mod, R2 and R2-mod

The differential settlement of Structure-B is also analyzed and presented in **Figure 5.46,** which also shows settlement of same order for the corresponding simulated cases.

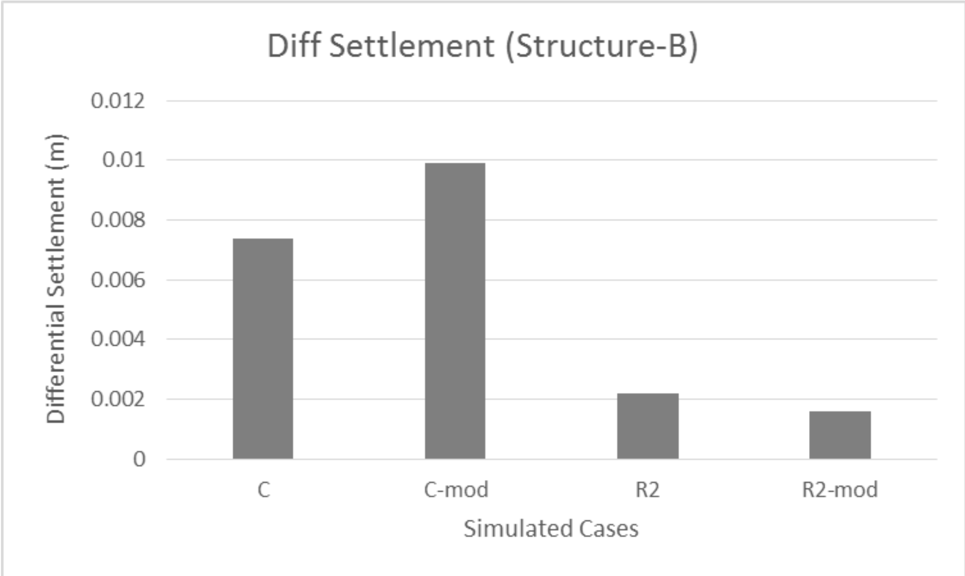

Figure 5.46 Differential Settlement of Structure-B for cases C, C-mod, R2 and R2-mod

Furthermore, maximum displacement of Structure-B and road are also analyzed and compared (**Figure 5.47** to **Figure 5.50**). The maximum displacement of structure-B and road also showed similar type of result, minor decrease in construction of tunnel stage due to generation of uplifting force by TBM and minor increase in contraction of tunnel stage due to contraction of tunnel lining.

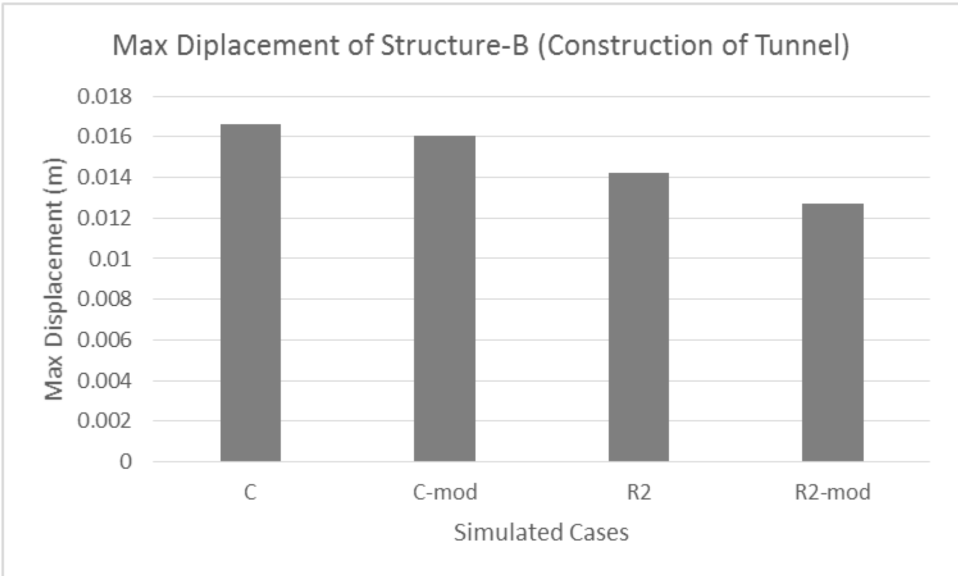

Figure 5.47 Maximum Displacement of Structure-B (construction of tunnel stage) for cases C, C-mod, R2 and R2-mod

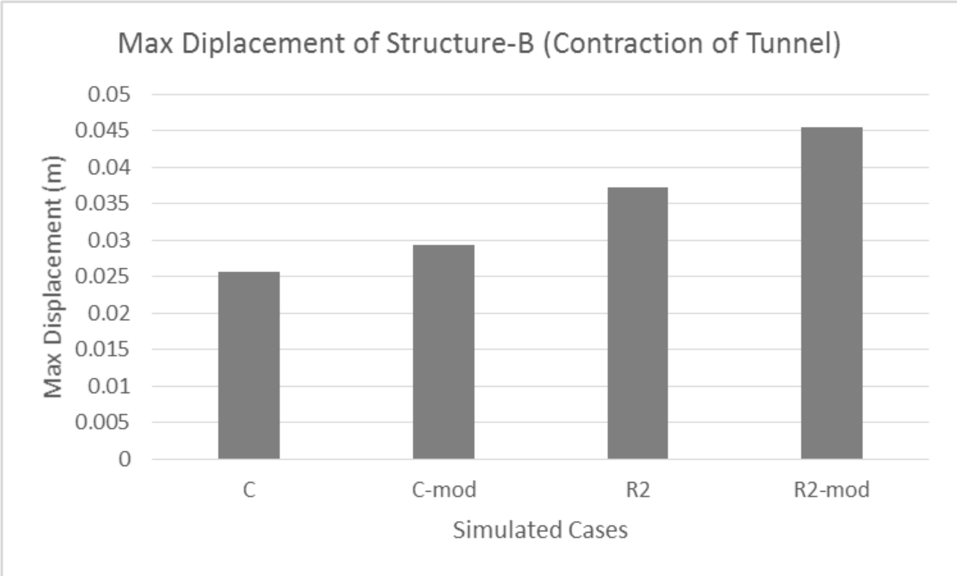

Figure 5.48 Maximum Displacement of Structure-B (contraction of tunnel stage) for cases C, C-mod, R2 and R2-mod

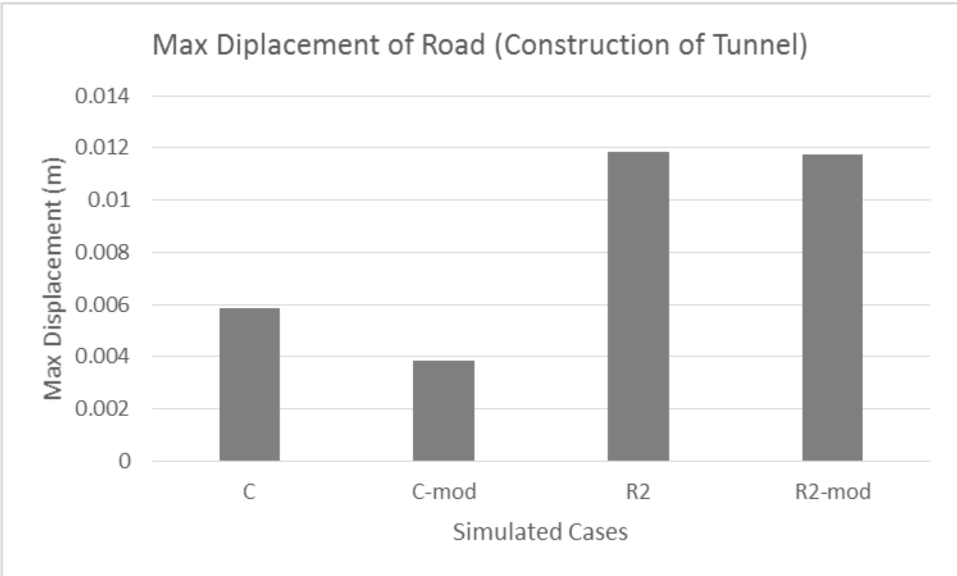

Figure 5.49 Maximum Displacement of Road (construction of tunnel stage) for cases C, C-mod, R2 and R2-mod

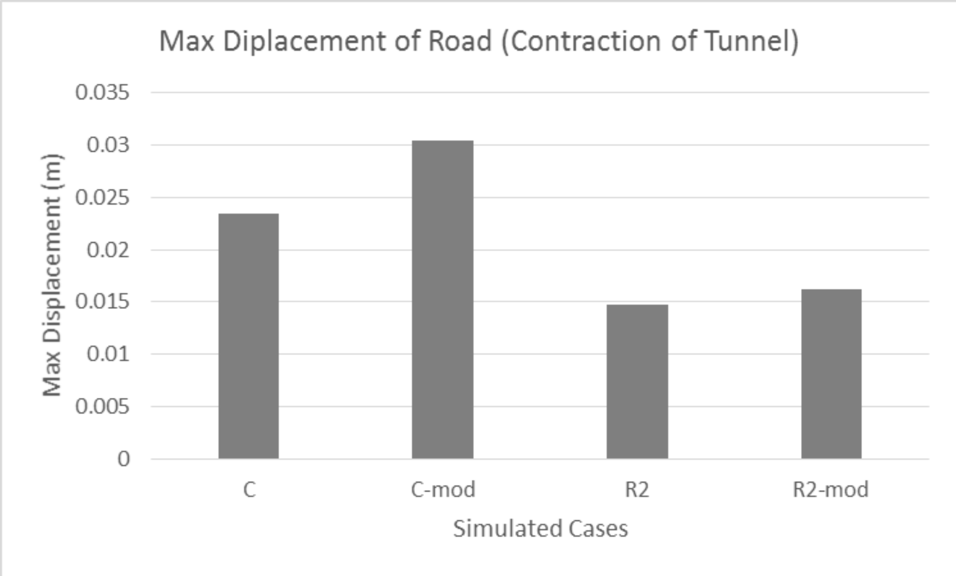

Figure 5.50 Maximum Displacement of Road (contraction of tunnel stage) for cases C, C-mod, R2 and R2-mod

Again, the same four points, point-E, point-F, point-G and point-H were considered for analysis. Total displacements of these point were plotted for different stages of simulation and were compared with previous results. In this case also, displacements of the same order were observed for all the four points.

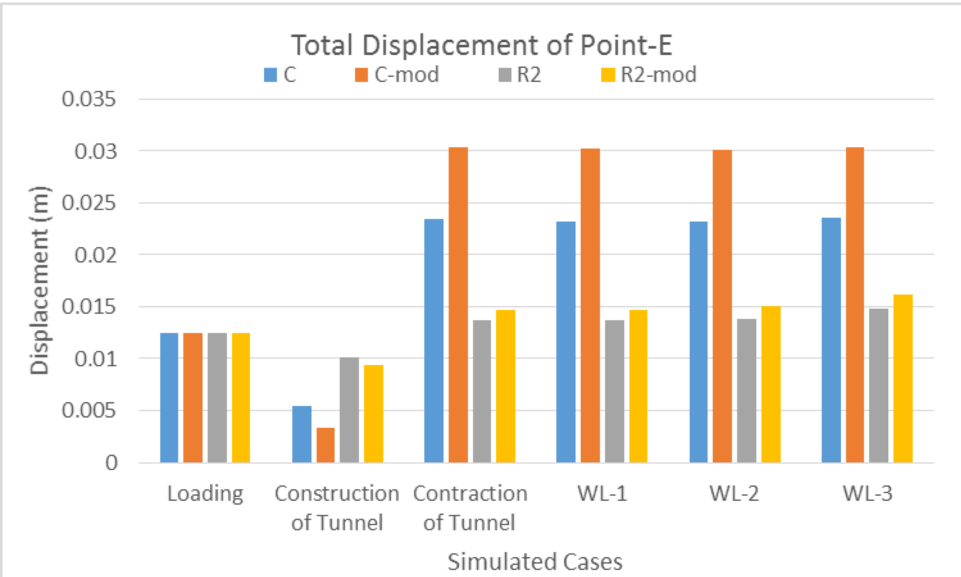

Figure 5.51 Total Displacement of Point-E for cases C, C-mod, R2 and R2-mod

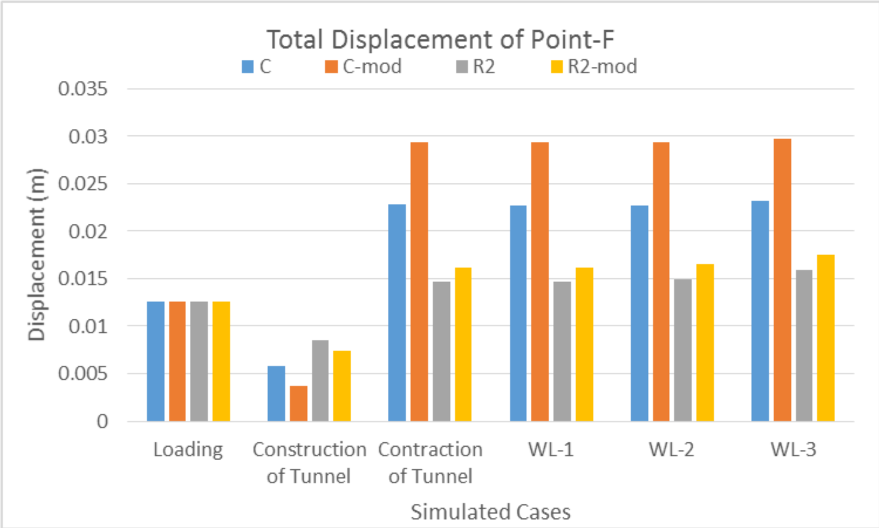

Figure 5.52 Total Displacement of Point-F for cases C, C-mod, R2 and R2-mod

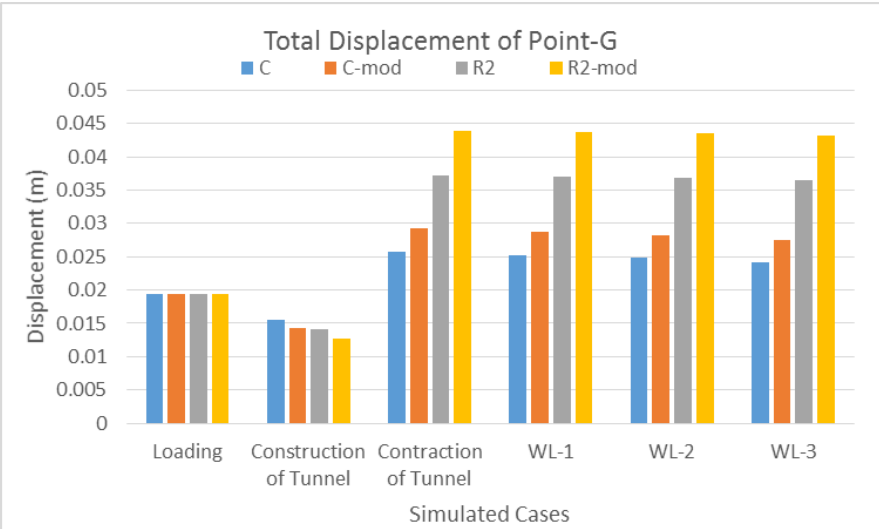

Figure 5.53 Total Displacement of Point-G for cases C, C-mod, R2 and R2-mod

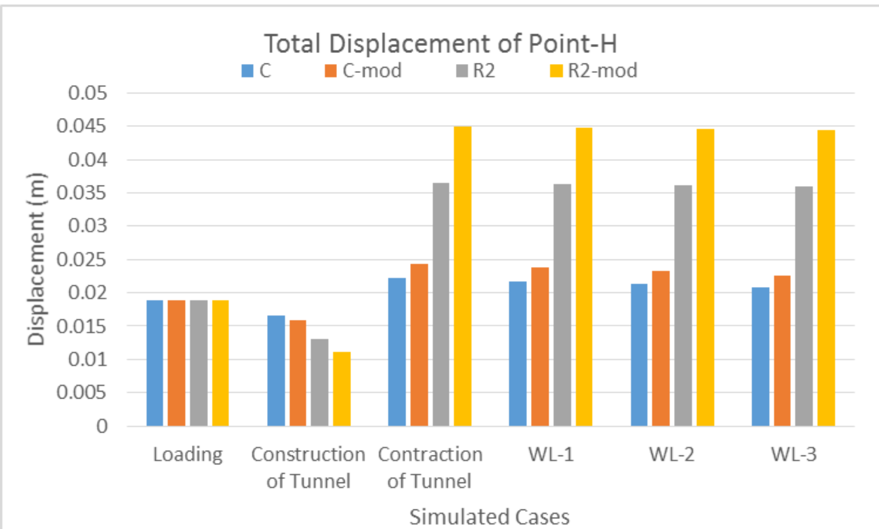

Figure 5.54 Total Displacement of Point-H for cases C, C-mod, R2 and R2-mod

Chapter 6

CONCLUSIONS AND SUMMARY OF SUGGESTIONS

6.1 Introduction

In this study, a total number of 09 (nine) 2D plain strain model was simulated to study the soil-structure interaction behavior of structures, nearby to an earthen embankment where a underground tunnel is constructed. From the obtained results and analysis done in this research, some conclusions (considering the parameters and variables of this study) and recommendations for future study can be made which are described in the following articles.

6.2 Conclusions

a) Maximum displacement at the base of any nearby structure may increase (upto 7%) with the increase in thickness of tunnel.

b) Increased depth of tunnel causes increased displacement of heavily loaded nearby structures (Structure-B). In case of lightly loaded structure (road), the increase in displacement may occur after a certain depth (around 7.5m in this case).

c) Significant increase in displacement may occur when the tunnel is constructed very near to a structure. The rate of increase in displacement has a rapid change within approximately 5.0 meter of the structure. However, this zone of influence may vary depending on the structure, loading and soil condition.

d) Although generation of high uplifting force (>10%) is expected as a result of high water level difference on both sides of the embankment, due to large overburden pressure, uplifting force at the base of any nearby structure may be significantly reduced near its center. This increase in uplifting pressure varies along the length of the base of any nearby structure, mostly depending on the point of interest for analysis.

e) Increase or decrease of displacement, bending moment and shear force of the tunnel is not only dependent on lining thickness, but also largely dependent on horizontal and vertical position of tunnel. Effects of these parameters are clearly visible in the figures provided in **Chapter 5.0**.

f) Generalized bending moment and shear force curves shown in **Figure 5.12**, **Figure 5.24** and **Figure 5.35** (valid for parameters mentioned in this study) can be used in design of tunnel linings by using equations provided in **Article 2.6**. In this case the primary concern is the determination of optimum thickness of tunnel lining meeting the design criteria provided in **Article 2.6**. The optimum thickness of tunnel lining can be different for different horizontal and vertical positions of the tunnel.

g) Continuous increase in water head difference may generate rapid high uplifting force (>10%) on the tunnel and nearby structure at a certain point (WL-3 in this case produces sudden increase in uplifting force). Considerations should be given to this factor while design and construction of tunnel and nearby structures.

h) Least displacement of 0.026m is generated on the nearby structures for a tunnel lining thickness of 0.380m which is also found to be adequate in resisting developed tension and compression in the lining.

i) In all the cases simulated in this research, a tunnel lining thickness of 0.380m has been found to be adequate considering displacements generated in nearby structures due to tunneling. Besides, two different positions of the tunnel, one below middle of the road, another below center of Structure-B, both below 6.5m from ground level, are found most suitable for tunnel construction. Any position in between the road and the Structure-B, creates skewness which increases the displacement (>0.025m) in nearby structures.

6.3 Summary of Suggestions

From the findings in this research, some recommendations can be made for future study which are as follows:

a) This research was carried out considering a 2D plain strain soil-structure interaction model. However, results of 3D soil-structure models can vary to some extent with that of 2D models. So, for better understanding the complex soil-structure interaction behavior, use of a 3D model can prove to be more useful.

b) Depending on practical conditions, actual soil-structure interaction behavior may differ from that of considered in the model where the data is idealized to a certain extent so as to represent the actual condition. This solely depends on the existing conditions of soil, method of construction of the tunnel and loading of nearby structures. So, when simulating the models, consideration should be given on any change in the variables mentioned above.

c) Simulation of models done in this research assuming static loading condition. Presence of any dynamic load such as vehicle load over the embankment, may induce significant change in the results obtained in this study. So, for future study, some dynamic load cases may be considered to have an idea about the behavior of soil-structure interaction model as compared to the present study.

d) In this study, to incorporate the long term behavior of soil, the soil condition was assumed to be drained. The short term behavior of soil may produce significant variation of results from that obtained in this research. For a comparative future study, short term soil-structure interaction behavior may be analyzed by considering the soil as undrained.

e) In this research, a total number of 09 (nine) cases were simulated to study the impact of tunneling on nearby structures and finding the best suitable location and thickness of tunnel. Considering the economy and duration of the project and suitability of the surroundings, more cases can be simulated with less variation in thickness, horizontal and vertical position of tunnel in each case to identify the best tunnel section in a best suitable position.

Chapter 7

REFERENCES

Arunkumar, S. and Ayothiraman, R. (2010), Effect of Vertically Loaded Pile on Existing Urban Tunnel in Clay, *Indian Geotechnical Conference, Bombay*, p.751 – 754.

Atwa, Mr., Magnan, J.P. and Leca, E. (2001), Analysis of the consolidation of the grounds around the tunnels dug in clay, *Laboratory Power Station of Bridges and Chausses, Paris*.

Augarde, C.E. (1997). Numerical modeling of tunneling processes for assessment of ramming to buildings, *Doctoral Thesis*, *University of Oxford, The United Kingdom*.

Aydinoglu, M.N., Cakiroglu, A. (1977), Dynamic Interaction Between Soil and A Group of Buildings, *Sixth world conference on earthquake engineering, New Dehli, India,* p.1596–601.

Ayothiraman, R. and Arunkumar, S. (2011), Influence of vertical pile loading on existing tunnel lining in soft clay, *14th Australasian Tunnelling Conference, Auckland, New Zealand*, p.1-13.

Benton, L.J. and Phillips, A. (1991), The Behaviour Of Two Tunnels Beneath A Building on Build Foundation, *Deformation of Soils and Displacements of Structures, Florence*, 2: 665-668.

Beskos DE (1993), Applications of the boundary element method in dynamic soil-structure interaction In Development in Dynamic Soil–Structure Interaction, *Dordrecht: Kluwer Academic*, p. 61–90.

Bielak J. (1976), Modal analysis for building-soil interaction, *Engineering Mechanics Division,* ASCE 771–86.

Bloodworth, A.G. (2002), Three-dimensional analysis of tunneling effects on structures to develop design methods, *Doctoral Thesis, University of Oxford, the United Kingdom*.

Chopra, A.K. and Gutierrez, J.A. (1974), Earthquake response analysis of multistory buildings including foundation interaction, *Earthquake Engineering Structure Dynamics*, 3:65–77.

Dias, D. (1999), Reinforcement of the coal face of the tunnels by bolting, Numerical study and application with a real case in urban sites, *Doctoral Thesis. INSA of Lyon, France*.

Dolzhenko, N. (2002), Experimental and numerical two dimensional modeling of urban underground works. Realization of biaxial tests and oedometrics on the analogical ground of Taylor-Schneebeli, *Doctoral Thesis, INSA of Lyon, France*.

Gonzalez JJ. (1977), Dynamic interaction between adjacent structures, in R77-30, *Department of Civil Engineering, Massachusetts Institute of Technology, Cambridge*.

Houari, N.El., Allal, M.A. and Abou Bekr, N., (2011), Numerical Simulation of the Mechanical Response of the Tunnels in the Saturated Soils by PLAXIS, *Jordan Journal of Civil Engineering*, 5(1).

Iguchi M. (1978), Dynamic interaction of soil–structure with elastic rectangular foundation, *Fifth Japanese earthquake engineering symposium, Tokoyo, Japan*, p. 457–64.

Kasper, T. and Meschke, G. (2006), A numerical study of the effects of soil and grout material properties and cover depth on shield tunneling, *Computers and Geotechnics*, 33: 234-247.

Laing,VC (1974), Dynamic Response of Structures in Layered Soils, *Department of Civil Engineering, Massachusetts Institute of Technology, Cambridge MA*, R74-10.

Liu, G. (1997), Numerical modeling of ramming of masonry buildings to tunneling, *Doctoral Thesis, University of Oxford, The United Kingdom*.

Lou Menglin et. Al. (2011), Structure–soil–structure interaction: Literature review, *Soil Dynamics and Earthquake Engineering*, 31:1724–1731.

Lysmer J et al. (1975), Efficient Finite Element Analysis of Seismic Soil Structure Interaction, *Earthquake Engineering Research Center, University of California, Berkeley, C.A*. EERC-75-34.

Magnan, J.P. and Serratrice, J.F. (2002), Analysis and prevision of settlements of surface during the digging of the northern tunnel of the underground traverse of Toulon, *Bulletin of the Laboratories of Bridges and Chausses*-238- ref. 4412, 5-36.

Manolis, G.D., Beskos, D.E. (1988), Boundary Element Methods in Elastodynamics, *London, Unwin Hyman*.

N. El Houari, M. A. Allal, N. Abou Bekr, (2011), Numerical Simulation of the Mechanical Response of the Tunnels in the Saturated Soils by Plaxis, *Jordan Journal of Civil Engineering*, 5(1).

Ollier, S. (1997), Experimental study of the interaction ground-machine during the digging of a not very deep tunnel by tunneller with mud pressure, *Thesis: Civil Engineering, Lyon: INSA of Lyon, 323*.

Peck, R.B. (1969), Deep excavations and tunnelling in soft ground, *7th int. Conference on Soil Mechanics and Foundation Engineering, Societal Mexican de Mechanical de Solos*, 225-290.

Poulos H.G., Davis E.H. (1980), “Pile Foundation Analysis and Design”, *The University of Sydney*, Rainbow-Bridge Book Co.

Roesset, J.M. and Gonzalez, J.J. (1978), Dynamic interaction between adjacent structures, D*ynamic mechanical soil and rock mechanics, Karlsruhe, Balkema*. p. 127–66.

Sato, T., Kawase, H. and Yoshida, K. (1983), Dynamic response analysis of rigid foundations subjected to seismic waves by boundary element method, F*ifth international conference on boundary elements, Hiroshima, Japan: Springer-Verlag,* p. 765–74.

Sesharao, P. (2014), Influence of Basement Raft Loading on Existing Tunnels, *M. Tech Thesis, Indian Institute of Technology, Delhi, India*.

Shabna, P.S. and Sankar, N. (2016), “Numerical Analysis Of Shallow Tunnels In Soft Ground Using Plaxis2D”, *International Journal of Scientific & Engineering Research*, 7(4).

Solari, G., Stura, D. and Vardanega, C. (1980), On the accuracy of numerical models in 3-D soil–structure interaction, S*eventh World Conference on Earthquake Engineering, Istanbul, Turkey,* p. 237–44.

Sumeet Mahajan et. al. (2016), Numerical Analysis on Effect of Basement Raft Loading on Existing Urban Tunnel in Soil, *Indian Geotechnical Conference (IGC).*

Technical Manual for Design and Construction of Road Tunnels- Civil Elements, FHWA-NHI-10-034, December 2009.

Wong, H.L. (1977), The coupled translations and rotations caused by the weight distribution of nearby buildings, *The symposium on applications of computer methods in engineering. University of Southern California, Los Angeles*.

Wong, H.L. and Luco, J,E. (1986), Dynamic structure-to-structure interaction for closely spaced building, *Third U.S national conference on earthquake engineering. Columbia, South Carotina*, p. 553–64.

Yahyai M, et al. (2008), Soil structure interaction between two adjacent buildings under earthquake load, *American Journal of Engineering and Applied Sciences*, 1(2):121–5.

Yoshida K, Sato T., Kawase H. (1984), Dynamic response of rigid foundations subjected to various types of seismic waves, *Eight World conference on earthquake engineering. San Francisco, California, USA,* p. 745–52.